# CHARACTERISTICS OF COMPRESSED STABILIZED EARTHEN BLOCK FABRICATED WITH SAWDUST ASH BASED GEOPOLYMER

**JOYA RANI MALLICK**

**M. SC. ENGG. (CIVIL & GEOTECHNICAL)**

**DEPARTMENT OF CIVIL ENGINEERING**

**BANGLADESH UNIVERSITY OF ENGINEERING AND TECHNOLOGY (BUET)**

**DHAKA, BANGLADESH**

**November 2022**

# CHARACTERISTICS OF COMPRESSED STABILIZED EARTHEN BLOCK FABRICATED WITH SAWDUST ASH BASED GEOPOLYMER

by

**JOYA RANI MALLICK**

A thesis submitted to the Department of Civil Engineering,
Bangladesh University of Engineering and Technology, Dhaka,
in partial fulfillment of the degree of
M. Sc. Engg. (Civil & Geotechnical)

DEPARTMENT OF CIVIL ENGINEERING

BANGLADESH UNIVERSITY OF ENGINEERING AND TECHNOLOGY

**November 2022**

The thesis titled "Characteristics of Compressed Stabilized Earthen Block Fabricated with Sawdust Ash Based Geopolymer", submitted by Joya Rani Mallick (Roll No. 1018042138, Session: October, 2018) has been accepted as satisfactory in partial fulfillment of the requirement for the degree of M. Sc. Engg. (Civil & Geotechnical) on November 23, 2022.

## BOARD OF EXAMINERS

Dr. Mohammad Shariful Islam
Professor
Department of Civil Engineering
BUET, Dhaka-1000

Chairman
(Supervisor)

Dr. Md. Delwar Hossain
Professor and Head
Department of Civil Engineering
BUET, Dhaka-1000

Member
(Ex-Officio)

Dr. Mohammed Kabirul Islam
Professor
Department of Civil Engineering
BUET, Dhaka-1000

Member

Dr. Faria Fahim Badhon
Sub-divisional Engineer
Bangladesh Water Development Board (BWDB),
BWCSRP 72, Green Road, Dhaka-1205

Member
(External)

## DECLARATION

It is thereby declared that except for the contents where specific references have been made to the work of others, the study contained in this thesis is the result of investigations carried out by the author under the supervision of Dr. Mohammad Shariful Islam, Professor, Department of Civil Engineering, Bangladesh University of Engineering and Technology.

No part of this thesis has been submitted to any other university or educational establishment for a degree, diploma, or other qualification (except for publication).

JRMallick

**Joya Rani Mallick**

# ACKNOWLEDGEMENT

All praises to Lord Sri Krishna the most beneficial and merciful. By the grace and proper guidance of Almighty God the author has been able to complete the thesis work after a journey of nearly four years.

The author would like to express her utmost gratitude towards Dr. Mohammad Shariful Islam, Professor, Department of Civil Engineering, BUET for his earnest supervision, prudent guidance, inclusive and important comments, timely and efficient discussion sessions. It was my honor and pleasure to work under his constant guidance. I shall always be indebted to him for making me familiar with an environment conducive to research. It would not have been possible for me to complete the thesis within this amount of time except his encouragement. His devotion towards research has always galvanized me to strive for better outcomes. His expertise and valuable knowledge sharing throughout the research work have provided immense assistance to me.

The author would like to express her heartfelt thanks to Dr. Md. Delwar Hossain, Professor and Head, Department of Civil Engineering, BUET, for the valuable time he has provided as member of the board of examiners. The author is indebted to Dr. Mohammed Kabirul Islam, Professor, Department of Civil Engineering, BUET, for sharing his knowledge and experience and thus enlightening me. The author would also like to take the opportunity to express genuine admiration towards Dr. Faria Fahim Badhon, Sub-divisional Engineer, Bangladesh Water Development Board (BWDB), for her kind consent to be a member of my advisory committee. Her co-operation and essential suggestions helped me to understand the importance of research.

And finally, the author would like to express her heartiest gratitude towards her parents and family members for their continuous support and cooperation without which this path would never have reached its destination.

# ABSTRACT

Expansive soil has always been a major concern for civil engineers. The problematic swell-shrink behavior of this soil due to seasonal fluctuation of water content can be mitigated through mechanical, physical, chemical, or biological stabilization. Among chemical stabilization processes, geopolymerization has recently achieved better efficacy due to its lower carbon footprint. This study explores investigating the strength and durability characteristics of Compressed Stabilized Earthern Blocks (CSEBs) fabricated with Sawdust Ash (SDA) based geopolymer. An expansive soil of high swell index (Free Swell Index, FSI = 83.3%) was reconstituted with a mixture of NaOH (10M), $Na_2SiO_3.9H_2O$ (70%/30% w/w), and a variety of SDA content ranging from 0% to 20% at different compaction effort based on the workability. By varying the Alkaline Solution (A) to Binder (B) ratio (A:B) from 0.3 to 0.5, optimum A:B ratio was obtained at various amounts of SDA percentage indicating an increase in A:B ratio with increasing SDA content.

Uniaxial compression tests of the samples cured at room temperature at 7 day and 28 day bulk condition showed that, the highest compressive strength (0.82 and 1.78 MPa) is obtained for the composition having 20% SDA and A:B ratio of 0.5 which also satisfies minimum strength requirements of several codes and standards. From durability perspective, around half of the samples showed efflorescence which can be mitigated thourgh moist curing. The improvement of compressive strength due to water submersion also emphasizes on the application of moist curing for enhanced strength and reduced efflorescence.

The maximum flexure (0.35 MPa) and tensile strength (0.31 MPa) were obtained for the same composition (20% SDA and A:B ratio of 0.5) which is around 180% and 400% greater than unstabilized soil respectively. The microstructural analysis by Scanning Electron Microscope (SEM), Energy Dispersive X-ray Analysis (EDXA), and Fourier Transformed Infrared Spectroscopy (FTIR) supported the formation of geopolymer as well as improved mechanical strength. Overall, the experimental results obtained in the present study corroborate the successful application of SDA based geopolymer in the fabrication of CSEBs from expansive soil.

# TABLE OF CONTENTS

# LIST OF TABLES

# LIST OF FIGURES

# NOTATIONS AND ABBREVIATIONS

| Symbols | Description |
|---|---|
| A | Alkaline Solution |
| B | Binder |
| BD | Bulk Density |
| BWA | Biomass Wood Ash |
| BFA | Biomass Fly Ash |
| C | Compaction |
| CA | Coarse Aggregate |
| CAGR | Compound Annual Growth Rate |
| CSEB | Compressed Stabilized Earth Blocks |
| DM | Dynamic Modulus |
| DS | Drying Shrinkage |
| DST | Direct Shear Test |
| E | Efflorescence |
| EDXA | Energy Dispersive X-ray Analysis |
| FA | Fly Ash |
| FAgg | Fine Aggregate |
| FS | Flexure Strength |
| FSI | Free Swell Index |
| FTIR | Fourier Transformed Infrared Spectroscopy |
| $G_s$ | Specific Gravity |
| GGBS or GBFS | Ground Granulated Blust Furnace Slag |
| GP | Geopolymer |
| HCWA | High Calcium Wood Ash |
| LL | Liquid Limit |
| MK | Metakaolin |

| Symbols | Description |
|---|---|
| OMC | Optimum Moisture Content |
| OPC | Ordinary Portland Cement |
| P | Porosity |
| PFA | Pulverized Fuel Ash |
| PL | Plastic Limit |
| PI | Plasticity Index |
| RHA | Rice Husk Ash |
| $R_H$ | Relative Humidity |
| S | Slump |
| SB | Submersion |
| ST | Setting Time |
| SDA | Sawdust Ash |
| SEM | Scanning Electron Microscope |
| SL | Shrinkage Limit |
| STS | Split Tensile Strength |
| SH | Sodium Hydroxide |
| SS | Sodium Silicate |
| TGA | Thermogravimetric Analysis |
| USCS | Unified Soil Classification System |
| UCS or CS | Unconfined Compressive Strength |
| W | Water |
| WA | Water Absorption |
| XRD | X – Ray Diffraction |
| XRF | X – Ray Fluroscence |

# Chapter 1
# INTRODUCTION

## 1.1 General

The world is leading towards sustainability which has instigated engineers to discover smart, durable, and environment friendly building materials. Traditional building materials, Fired Clay Brick, and concrete blocks are not suitable due to high energy consumption and carbon footprint. In this context, earthen block is gaining popularity for its availability of raw materials, easier fabrication process, and low energy consumption. However, low tensile and flexure strength, high shrinkage, and durability issues are major concerns for earthen materials (Islam and Iwashita 2010). To overcome these deficiencies, proper type and amount of stabilizers are added with raw earth and compacted which is then called Compressed Stabilized Earthen Block (CSEB). Among stabilizers, industrial wastes like – fly ash, slag, sawdust ash, etc. are recently being used as partial replacement of traditional stabilizer – Ordinary Portland Cement (OPC) instead of full replacement to achieve sufficient strength (Mumtaz 2019, Sekhar and Nayak 2018, Elahi et al. 2020, Ayodele et al. 2019, Fadele and Ata 2018, Elahi et al. 2021). Thus, the application of cement still remains and so do the concerns associated with cement production. In recent years, the Geopolymerization process has emerged as a viable alternative for the hydration process of cement that imparts higher strength in aggregate-binder matrix (Davidovits 1994). Geopolymers (GP), materials thus formed in this process are amorphous or semi-crystalline materials obtained by low-temperature reaction of aluminosilicates and alkaline activators (Davidovits 2008). When compared to OPC, Geopolymer has a low carbon footprint, is four times stronger, and has high chemical resistance to acids, and temperature. Among various industrial waste products used as a source of aluminosilicate, successful use of sawdust ash (SDA) in Geopolymer Concrete preparation has been reported in various studies (Arunkumar et al. 2020, Arunkumar et al. 2021, Alabduljabbar et al. 2020, Pereira et al. 2019, Kong et al. 2018). However, significant study has not been reported on the use of Sawdust Ash based geopolymer in fabrication of CSEB. Therefore, it was deemed necessary to address the research gap in the present state-of-the-art considering the enormous potential of this material as a sustainable construction unit.

## 1.2 Motivation

Although earth is an abundant material, suitable earth type for fabricatioin of building block is not always available. Hence, researchers are trying to utilize various types of earth for fabricating building blocks that has not been deployed before, ranging from river dredged sand (Xu et al. 2014, Mumtaz 2019) to problematic soil (Seco et al. 2011), contaminated marine sediments (Agostini et al. 2007, Wei et al. 2008, Wang et al. 2015), dried sludge (Tay and Show 1997, Weng et al. 2003, Cusidó and Cremades 2012) and so on. The motivation of this study originated from this very concept of utilizing unconventional earth which is in this case, expansive soil for fabrication of building blocks. In summary, the motivation lies in –

i. Stabilization of problematic soil (expansive soil)
ii. Through stabilizers having Low Carbon Footprint
iii. Using the stabilized soil for the fabrication of building blocks

## 1.3 Objectives of The Research

The present study aims to achieve the following objectives:

i. To determine the effect of sawdust ash and amount of alkaline solutions on mechanical properties of Soil-SDA based GP mixtures.
ii. To suggest an optimum mix combination for making strong and durable CSEBs from Sawdust Ash based geopolymer comparing their strength and durability properties with existing standards and codes.
iii. To analyze the microstructural behavior of CSEBs to ascertain the microscopic changes that occur at various sawdust ash and alkalinity contents.

## 1.4 Organization of The Thesis

The present study has been divided into five sequential chapters to present the development of research framework, methodology of execution and findings from the study.

Chapter 1 contains introduction, background and present state of the problem, motivation and objective of the research and finally the organization of the thesis.

Chapter 2 contains literature review. This chapter states the current practices of earthen construction in Bangladesh and around the world. The characteristics of expansive soil and different types of stabilization methods used for it's strength improvement has also been reported while specially focusing on sawdust ash and geopolymerization. Finally, a summary of the previous studies and research gap about CSEBs made from geopolymerization are presented.

Chapter 3 contains the experimental methodology for execution of the current study. Index properties of soil, properties of sawdust ash and chemical properties of alkaline solution are discussed in this chapter. Detailed method of sample preparation, curing and performing laboratory experiments have also been presented in this chapter.

Chapter 4 contains the finding of this study along with relevant discussions and explanations. Strength properties such as – compressive, flexure, tensile and durability properties such as – water absorption, wet compressive strength, effloresecene has been reported while identifying the effect of sawdust addition and alkaline solution conetent on these properties. Moreover, findings from microstructural investigation and infrared spectra has also been reported to investigate chemical changes within matrix.

Finally, Chapter 5 presents salient conclusion of the study based on the findings from experiments and provides suggestions for future studies on this topic.

# Chapter 2
# LITERATURE REVIEW

## 2.1 Introduction

Since the dawn of civilization, people have been using earth for the construction of their abode which is evident from the archeological records and earthen construction present throughout the world. Earth being cheap and most importantly easily available became the first choice for construction and gained much popularity over time. However, raw earth has some inherent limitations that restrict its use in several aspects. These limitations can be overcome with stabilization by proper means that include physical, mechanical, chemical, and biological stabilization.

This chapter describes the history and current scenario of earthen construction around the world. The limitations of raw earth and methods for improving them have also been discussed in detail. Moreover, previous studies on various traditional and recently emerged stabilization techniques have been reviewed and summarized. Finally, based on the detailed review, the literature gap has been identified that will be addressed through the present research work articulated in the further chapters.

## 2.2 Earth as a Construction Material

Since the beginning of time, mankind has been bonded to the earth. It is one of the most plentiful and resourceful raw materials to have established a solid basis in the world of architecture and construction, appearing in both modern homes and old archaeological sites. Mud as a building material has improved over time, and various construction methods have advanced in various parts of the world as a result of its development. Simply said, construction using earth has a remarkable history and a bright future.

The construction of the world's oldest earthen building, Ramasseum, located on the left shore of the Nile can be dated back to the $13^{th}$ century BC. The existence of other earthen construction around the world (Figure 2.1) can be seen in a positive perspective that puts emphasis on the environmental friendliness of this construction. However, due to some shortcomings of raw earth especially the durability issue, the focus shifted towards "concrete" as a construction material after the emergence of cement that took place in

1824 when Joseph Aspdin of Leeds, Yorkshire, England took out a patent for "Portland Cement". Since then, global production and market demand for cement have been on a drastic rise The global cement market is projected to grow from $340.61 billion in 2022 to $481.73 billion by 2029, at a Compound Annual Growth Rate (CAGR) of 5.1% in the forecast period, 2022-2029 (Fortune Business Insights, April 2022). However, due to the enormous amount of $CO_2$ emission associated with cement production which entails approximately 0.47 ton of $CO_2$ emission due to 1 ton of cement production (Baxter and Walton 1970), the concern of climate change and the greenhouse effect is gradually emerging resulting in a shifting focus towards earthen construction again.

### 2.3 Construction Techniques in Earthen Architecture

There are several techniques for the construction of earthen structures that include – Cut blocks, poured earth, adobe, super adobe, cob, rammed earth, CSEB (Compressed Stabilised Earth Blocks), Wattle and Daub, Shaped Earth, etc. Figure 2.2 illustrates some of these earthen construction techniques.

Among all these techniques, construction using adobe bricks can be considered as the most widely used form of earthen construction (Trujilo 2016). Adobe bricks are basically sun-dried mud or clay bricks with sufficient consistency that can be shaped by hand or in wooden molds. The adobe mixture is utilized as a bonding material that makes the assembling process simple. This type of construction is very durable but vulnerable to seismic damage. Superadobe is another technique that uses short and long sandbags filled with moistened earth and arranged in layers or coils. Barbed wires are placed between each layer that serves as both reinforcements as well as mortar. The structures built using this technique employ vaults, corbelled arches, and domes to create sturdy shells. The use of compressed earthen blocks originated in the early days of $19^{th}$ century Europe. In this technique, raw soil is moistened and compressed by manual or mechanical means. Sometimes the raw earth is stabilized using traditional stabilizers such as cement and lime. The blocks made from the stabilized soil are then called Compressed Syabilized Eartehen Blocks (CSEBs). These stabilizers provide improved mechanical strength and higher durability allowing construction of higher and thinner walls.

(a)

(b)

(c)

**Figure 2.1:** Earthen construction around the world (a) Great Mosque of Djenné (Africa, 1907), (b) Auroville Visitors Centre (1988) and (c) METI Handmade School (Bangladesh) (source: webpage - Rethinking The Future)

(a) (b)

(c) (d)

(e) (f)

**Figure 2.2:** Common Earthern Construction Techniques (a) Cut Blocks, (b) Superadobe, (c) Cob, (d) Compressed Earthen Block, (e) Adobe, and (f) Rammed Earth (source: webpage - Rethinking The Future)

Wattle and Daub can be characterized as an infill wall technique that has been used for 6,000 years at least. In this techinique dried thin timber parts are arranged in a wooden lattice and plastered with earth mixture that usually consists clay, sand, animal manure, and straw. Cob is another traditional building method that includes placing a mixture of clay and straw in a layered form by means of hand or foot without using any special formwork. This type of formation leads to the shapes such as curved walls, arches, and niches. The porous nature of the cob structure allows it to withstand weathering action. The rammed earthen structure incorporates application of manual or pneumatic rammers that compresses moistened raw earth in between formworks.

### 2.4 Major Drawbacks of Earthen Construction

The major limitations of earthen construction that are hindering its widespread use can be listed as follows:

i) Low compressive strength
ii) Below-par tensile and flexure strength
iii) Low impact and abrasion resistance
iv) Shrinkage and durability issues
v) Poor response under seismic loading
vi) Lack of standards and guidelines for proper construction
vii) Lack of skilled craftsmanship
viii) Aesthetic issues

To overcome these limitations, researchers are continuously trying to find out better solutions in terms of material refinement at the particle level as well as improving the efficiency of construction techniques. The current study mainly focuses on reviewing the literature that addresses material refinement by means of stabilization for achieving improved strength and durability characteristics.

### 2.5 Compressed Stabilized Earthen Block

Compressed Stabilized Earthen Block (CSEB) is a comparatively recently emerged construction material that is gaining much popularity in recent years due to its eco-friendliness. Although the use of stabilized earthen block can be dated back to a very early age, it can be considered a recent innovation due to dynamic research breakthroughs

in recent years. Compressed earthen blocks are fabricated with the appropriate mixture of soil, water, and stabilizers through the application of compaction energy which can be imparted either by manual or mechanical means. The most important factor in the fabrication of earthen block is the choice of an appropriate type of stabilizer as well as stabilization technique based on the available soil type. It often becomes necessary to modify either the soil type (by changing the gradation) or the type of stabilizers to make an appropriate mixture that can result in a desirable construction material. According to Auroville Earth Institute which is a leading institution promoting earthen construction around the world has suggested the following compositions to determine the applicability of soil for producing CSEBs: 45-65% gravel-sand, 20% silt, and 15-35% clay. However, this specific type of soil may not always be available (Islam et al. 2020). For this reason, research is being conducted to apply stabilization technique on different types of soil.

### 2.6 Different Methods of Soil Stabilization

To date, there are four types of stabilization methods – mechanical, physical, chemical, and biological with biological stabilization being the newest edition in this group. Figure 2.3 summarizes the basic methodology or materials used in these stabilizations.

Mechanical stabilization mainly indicates increasing soil density by compaction that results in increased mechanical strength, water resistance, and reduced permeability, porosity. Physical stabilization indicates the alteration of soil texture by - adding or removing soil particles or adding inert materials such as fiber reinforcement with can be either natural or artificial in nature. Among natural fibers - jute, coconut, hemp, straw, sisal, barley straw, wool, palm, sugarcane bagasse, banana and among artificial fibers – Polystyrene, Polypropylene, Plastic, Polyester, Polyethylene, Glass Fiber Reinforced Polymer, basalt fiber are currently in use (Paul et al. 2022). Chemical stabilization can be done either by adding cementing and/or pozzolanic materials or by geopolymerization. The cementing agent/pozzolona/precursor commonly used in chemical stabilization include – Lime, Cement, Metakaolin, Volcanic Ash, Fly Ash, Coal Ash, Sawdust Ash, Steel Slag, Rice Husk Ash etc. On the other hand, Biological stabilization is done by incorporating living organism or adding substances that have been derived from living organism such as plants and microbes.

The present study will mainly focus on chemical stabilization by using geopolymer that has been discussed in detail in the following articles.

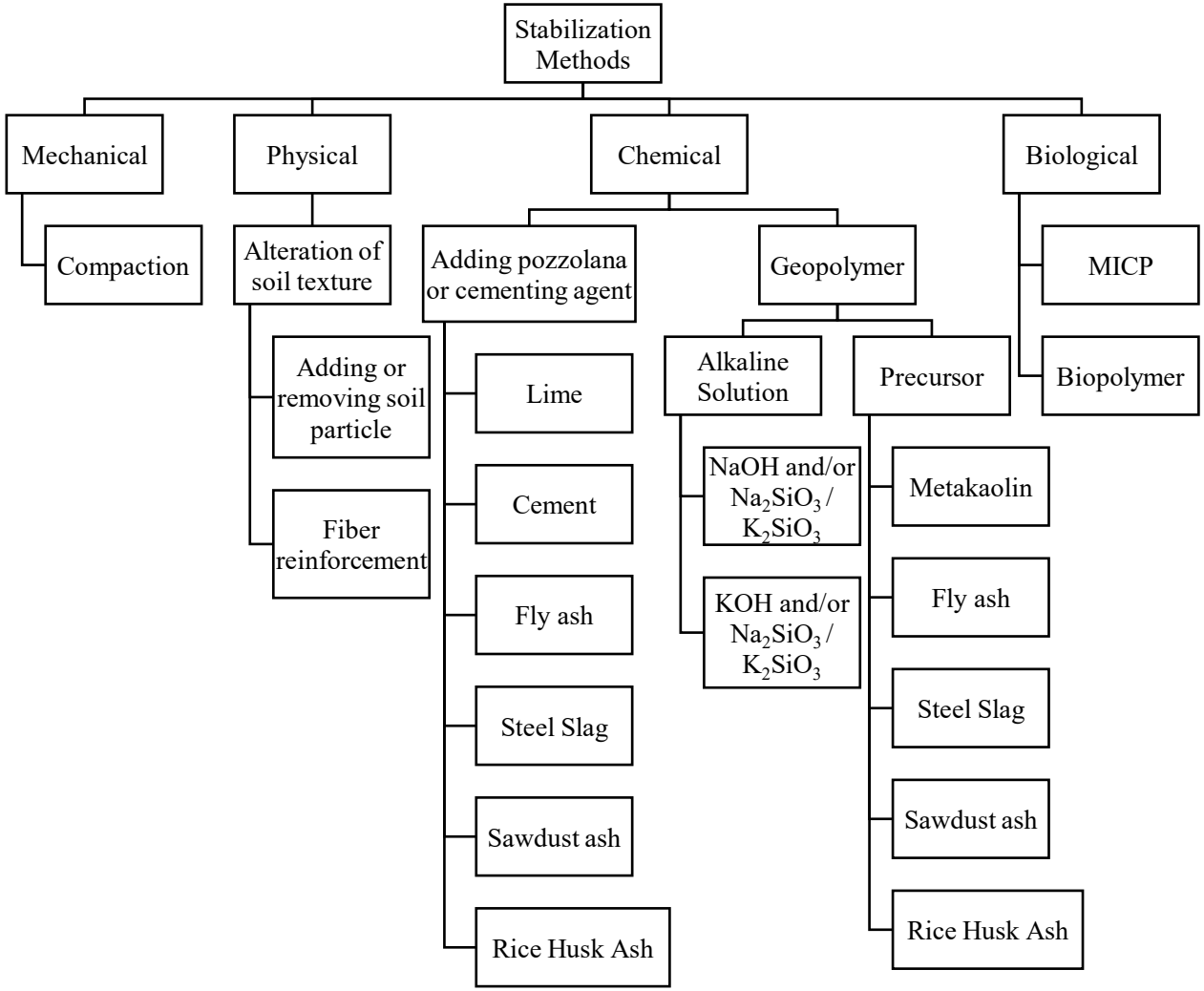


**Figure 2.3:** Different Methods of Soil Stabilization

## 2.7 Geopolymer

In 1978, Joseph Davidovits developed and patented binder obtained from the alkalination of Metakaolin (anhydrous calcined form of the clay mineral kaolinite) and named it after "Geopolymer". The term "Geopolymer" has been derived from "Geo" and "Polymer". "Geo" represents earth material that incorporates the use of Metakaolin derived from clay minearal kaoline calcined at a very high temperature which is at about 500˚C or greater. On the other hand "Polymer" represents the polymeric nature of the derived product. The constituents of geopolymer include – binder, alkaline solution as major elements and aggregates, water as optional elements. Figure 2.4 provides a representation of these constituents.

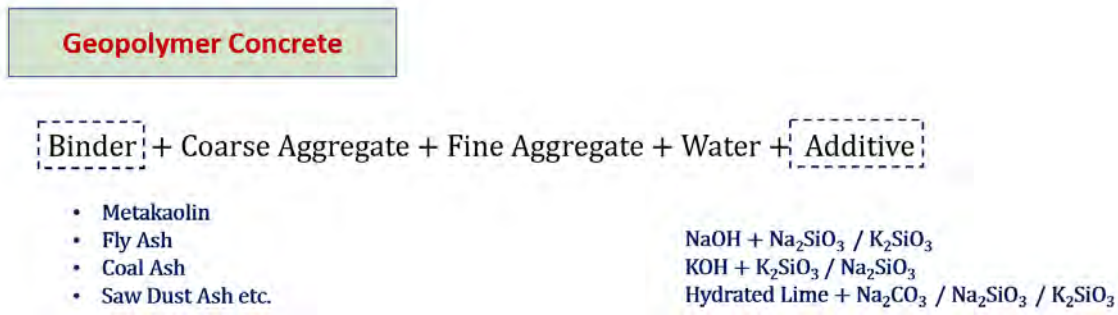


**Figure 2.4:** Constituents of geopolymer (Author 2022)

The alkalination is done by using an alkaline solution with a high concentration that provides greater amount of $OH^-$ ions. The typical alkali materials used are – NaOH, KOH, $Ca(OH)_2$, $Na_2SiO_3$, $K_2SiO_3$, etc. These are usually used either individually or in a combination with other alkali materials. Although in the beginning geopolymer was made with Metakaolin binder which is highly reactive due to its smaller particle size and is a rich alumino-silicate source, later it has been replaced by various types of binders that possess similar characteristics.

### 2.7.1 Geopolymer Formation

The process of Geopolymer formation is referred to as Geopolymerization. The complexity of various factors affecting geopolymerization during synthesis makes it difficult to fully understand the setting and hardening mechanism of geopolymer (Pacheco-Torgal et al. 2008a). However, according to Pacheco-Torgal et al. (2008a) the mechanism consists of a three-stage model which includes –

i) Destruction
ii) Reorientation
iii) Hardening/Solidification

At the very first stage, the internal bonding of aluminosilicate source or precursor is destructed by means of dissolution by alkaline solution which results in reactive silica and alumina species. After that the dissolved species are reoriented and reorganized facilitating the formation of gel or oligomer which is a complex three dimensional cross-network. These cross-linked network incorporates silicon and aluminium tetrahedral when the negative charge on $Al^{3+}$ ion is balanced with positive charge of alkaline ion ($Na^{+}$, $K^{+}$). In the later stages polycondensation takes place resulting in the formation of amorphous to semi-crystalline structure (Suwan 2016). Figure 2.5 provides a representation of geopolymerization mechanism as developed by Ryu et al. (2013).

The developed cross-linked structure (Figure 2.6) comprises several molecular unit with the major units being (Davidovids 2017) –

i) Si-O-Si-O- siloxo, poly(siloxo)
ii) Si-O-Al-O- sialate, poly(sialate)
iii) Si-O-Al-O-Si-O- sialate -siloxo, poly(sialate -siloxo)
iv) Si-O-Al-O-Si-O-Si-O- sialate - disiloxo, poly(sialate - disiloxo)

The empirical formula of geopolymer resultant products can be written as follows as suggested by Davidovids (2005) –

$$M_n [– (SiO_2)_z – AlO_2 –]_n \cdot wH_2O \quad (2.1)$$

where,

M = alkaline element such as potassium (K+), calcium (Ca+) or sodium (Na+)

n = degree of polymerization

z = Si/Al ratio which varies from 1, 2, 3 or higher

"–" indicates the presence of bonding

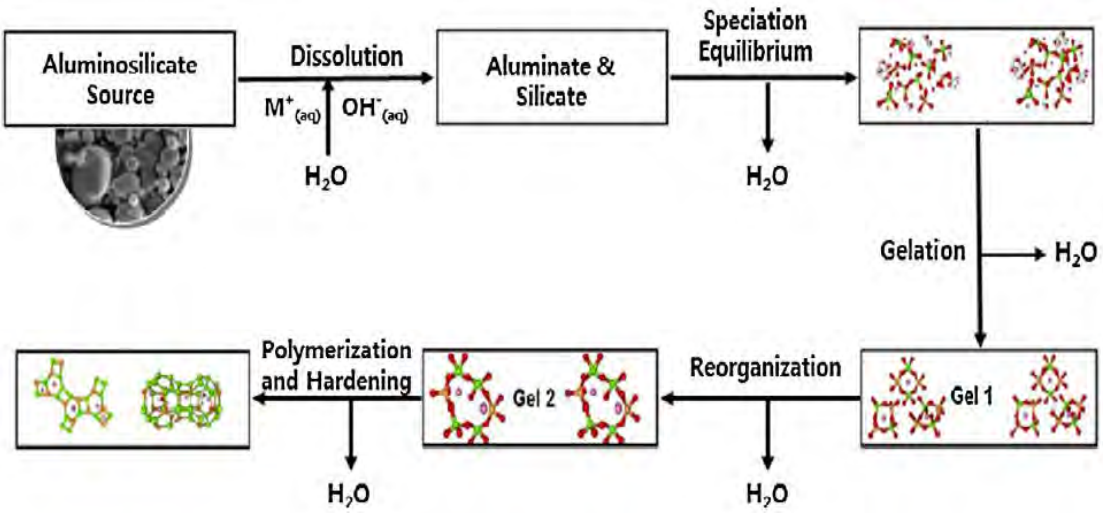


**Figure 2.5:** Mechanism of geopolymerization (Ryu et al., 2013)

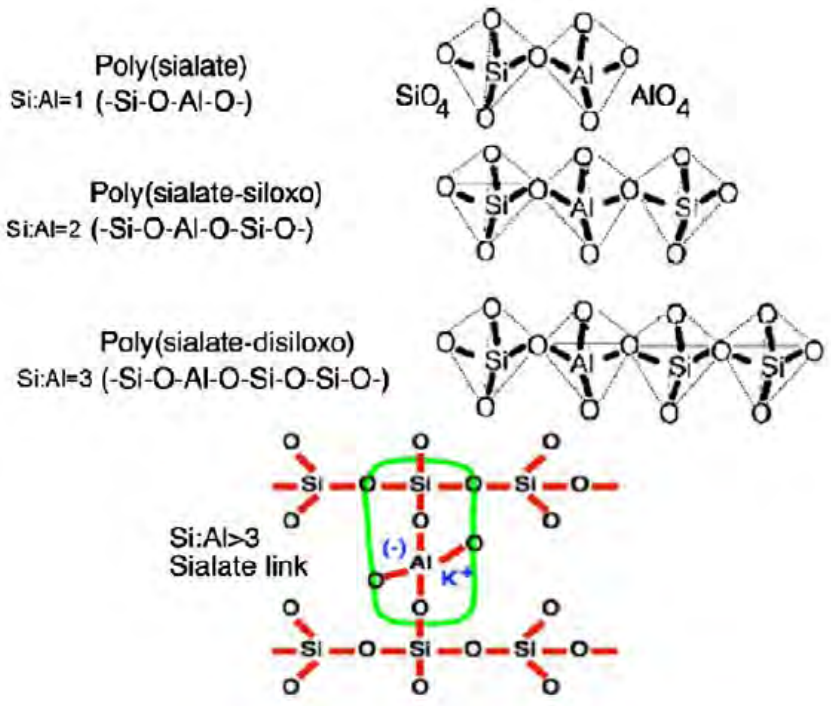


**Figure 2.6:** Poly(sialates) structures according to Davidovits (2005)

The variation in the ratio of Si/Al causes different properties in obtained geopolymer. However, for cements and ceramics, the low ratio of Si/Al (≤ 3) is widely used (Davidovids 2005). With the increase in Si/Al ratio, fire resistance property of the product increases (Davidovids 2002) .

### 2.7.2 Characteristics of Geopolymer

In recent years geopolymer is gaining much popularity as a viable alternative construction material for traditional cement-concrete due to its low carbon footprint. Moreover, it has some excellent properties which have made it beneficial to use it in a variety of sectors. The advantages of geopolymer include –

i) This is four times stronger and more durable than regular cement concrete. Hence, for high-performance concrete and off-shore construction, geopolymer is being used.
ii) Significantly less $CO_2$ emission associated with its production compared to traditional cement.
iii) The binders or precursors used in it are mostly derived from waste products which allow recycling and rreduceenvironmental burden.
iv) Geopolymer can bind specific hazardous material within its matrix facilitating toxic material immobilization.
v) It has excellent thermal insulation properties resulting in improved indoor environment.

### 2.7.3 Geopolymerization vs. Cement Hydration vs. Pozzolanic Reaction

The traditional cement (Portland) mainly acquires its strength through hydration reaction. The major minerals within Portland Cement include – Tri Calcium Silicate ($C_3S$), Di Calcium Silicate ($C_2S$), Tri Calcium Aluminate ($C_3A$) and Tetra Calcium Aluminoferrite ($C_4AF$). With the addition of water hydration reaction takes place resulting in Calcium Silicate Hydrate gel (C-S-H) as the main product. The equation can be expressed as follows:

$$\text{Portland Cement} + \text{Water} \rightarrow \text{C-S-H gel} + Ca(OH)_2 + \text{Heat} \qquad (2.2)$$

This C-S-H gel imparts the maximum strength which can be about 80%. The rest of the strength comes from the secondary C-S-H gels formed by interaction between $Ca(OH)_2$ and excess silica species which is actually Pozzolanic Reaction.

The pozzolanic reaction takes place in presence of silica and alumina-rich compound that reacts with the available Ca species and form secondary C-S-H gels in the later stages of hydration reaction. These secondary gels provide pore refinement resulting in reduced

permeability and enhanced resistance to chemical attack. The pozzolanic reaction can be expressed as follows:

$$\text{Binder } (SiO_2, Al_2O_3) + \text{Water} + Ca(OH)_2 \rightarrow \text{ Secondary C-S-H gel} \qquad (2.3)$$

In comparison, strength development due to hydration reaction is much higher than pozzolanic reaction. Moreover, pozzolanic reaction provides strength development at later ages while hydration reaction results in early strength improvement.

When geopolymerization is compared with these two types of reactions, the major difference evident is the end product. Hydration or pozzolanic reaction results in gel formation that does not have any definite shape. On the contrary, geopolymerization results in a polymeric structure that has definite shape. The resultant polymer also has more condensed structure proving improved mechanical strength in comparison with the other products derived from those two reactions.

### 2.7.4 Application of Geopolymer

The enhanced mechanical performance of Geopolymer products has facilitated their widespread use in various construction sectors including soil stabilization as well as cement-concrete production. Based on the properties of precursor and alkaline products used in the synthesis of geopolymer, the resultant product can exhibit a variety of response and engineering characteristics which have been extensively studied by various researchers over the past two decades. Till now, past studies included the application of different types of binder/precursor in geopolymer such as – Fly Ash (FA), Saw Dust Ash (SDA), Blast Furnace Slag, Rice Husk Ash (RHA), Metakaolin (MK), Volcanic Ash etc.

Wang et al. (2005) studied the effect of concentration of NaOH solution on the mechanical and chemical properties of the geopolymer systhesized from metakaolin. Heat curing was applied on the geopolymer at 65℃ in oven for 10 h. The test results showed that with the increase in the concentration of NaOH from 4 to 12 mol/L, flexural strength, compressive strength and apparent density of the geopolymer increased. The maximum value of these properties were obtained for NaOH concentration of 12 mol/L and the highest value being 70 MPa and 55 MPa for compressive and flexure strength respectively. Chemical property analysis of the geopolymer by means of XRD, SEM and FTIR spectra showed amorphous and semi-crystalline phase in the formed geopolymer.

Based on the obtained data, the study also reported that geopolymeric reaction mainly occurred at the surface of the of metakaolinite particulates.

Guo et al. (2010) studied the strength and microstructural characteristics of a class C Fly Ash based geopolymer. In this study they mixed Sodium hydroxide (99.2% NaOH) and sodium silicate (9.1% $Na_2O$, 29.2% $SiO_2$, and 61.7% $H_2O$) in 1.0, 1.5, and 2.0 M ratios of $SiO_2/Na_2O$. Two different types of curing condition was incorporated, one at ambient temperature (23˚C) and another one at elevated temperature (60-90˚C). The highest compressive strength (63.4 MPa) was achieved at $SiO_2/Na_2O$ ratio of 1.5. the microstructural investigation by XRD, FTIR and SEM-EDXA supported the formation of geopolymeric bonds.

Chen et al. (2016) studied the properties of alkali activated metakaolin based geopolymer by changing the molar ratio $SiO_2$:$Al_2O_3$:$Na_2O$:NaOH:$H_2O$. Curing duration (24h, 72h and 168h) and temperature (20℃, 40℃, 60℃, 80℃ and 100℃) were also varied in the study to determine its effect on the compressive strength, microsctural and thermal insulation properties. The study reported that the optimal geopolymer was prepared with metakaolin, sodium hydroxide, sodium silicate and water, with the molar ratio of $SiO_2$:$Al_2O_3$:$Na_2O$:NaOH:$H_2O$ being 3.4:1.1:0.5:1.0:11.8. The microstructural investigation by XRD and FTIR provided in depth insight into the influence of curing conditions on the microstructures of the geopolymers. The maximum compressive strength obtained at the aforementioned molar ratio composition and at a curing of 60℃ for 168h was 52.26 MPa.

Djobo et al. (2016) studied the mechanical and durability properties of volcanic ash based geopolymer mortars synthesized at two different temperature - 27℃ and 80℃ and the properties were evaluated after 7, 28, 90, 120 and 180 days of curing. The maximum compressive strength was reported 37.9 MPa that was found after 90 days of curing and at a systhesis temperature of 80℃. The lower temperature resulted in a lower compressive strength which was 20.5 MPa after 28 days and did not change that much after prolonged curing duration. The water absorption and apparent porosity increased up to 28 days, then become almost constant with time as reported by the study.

Luukkonen et al. (2018) studied the development of one-part geopolymer mortar that uses alternate silica source (rice husk ash and microsilica) as a replacement of sodium silicate in a blast furnace slag based geopolymer mortar. Comprerssive strength, fresh

and hardened property of mortar, microstructural investigation and durability in terms of freeze-thaw cycle were investigated. The highest compressive strength was obtained at 28 days was 107 MPa. The results demonstrated the effect of available silica content on the compressive strength which varies with time. The mix composition also showed excellent durability properties.

### 2.8 Sawdust Ash as a Construction Material

Sawdust ash is derived from the burning of the wooden biomass of trees. The burning can be done in several ways including controlled burning in a furnace, or open/uncontrolled burning. Based on the type of tree and wood content, the derived ash can have different types of elemental composition that play an important role in the strength development mechanism in the soil or cement composites, wherever it is used. Each year a tremendous amount of waste sawdust is produced from sawing in timber mills that posses a health hazard for human and animals. Hence, attempts are being made in rescent years to valorize this waste product and incorporate it within ever-growing construction sector.

Due to its tremendous application potential, sawdust ash is being used in soil stabilization, cement-concrete, and geopolymer production. Sawdust ash used in these sectors serve as either a “filler” material providing physical stabilization or a “binder” material providing chemical stabilization. In either case, application of sawdust ash has been proven to be beneficial as supported by various past and recent literatures. The broad region of the sawdust ash’s application can be classified into several spectra which is illustrated in Figure 2.7. In the following articles, the present state-of-the-art in the application of sawdust ash in construction industry has been reported briefly.

#### 2.8.1 Application of Sawdust Ash in Cement Concrete

Elinwa and Mahmood (2002) used sawdust ash as a cement replacement with the replacement levels - 5%, 10%, 15%, 20%, 25%, and 30% by mass of ash. The study found that, sawdust ash has good pozzolanic properties with a pozzolanic index value of 75.9%. Setting time, workability and compressive strength of the cement-sawdust ash mixtures were determined and and the study concluded that 10% sawdust ash replacement showed the desired workability and strength. They also reported that sawdust ash has comperatively low $Al_2O_3$ and $Fe_2O_3$.

Elinwa et al. (2008) assessed fresh concrete properties and self-compactness of a concrete mixture containing sawdust ash with the presence of two types of super-plasticizers-melamine sulphonate and naphthalene sulphonate. For determining fresh concrete properties flow and T5 determination were done and V funnel, U-box and L-box tests were conducted. The segregation resistance and the placeability of the concrete were found to be within the specified limit set by EFNARC Standard (2002). The best performance was achieved at 10 wt% replacement od sawdust ash. The study also reported that, sawdust ash can reduce the reaction rate of cement hydration and increase the setting time.

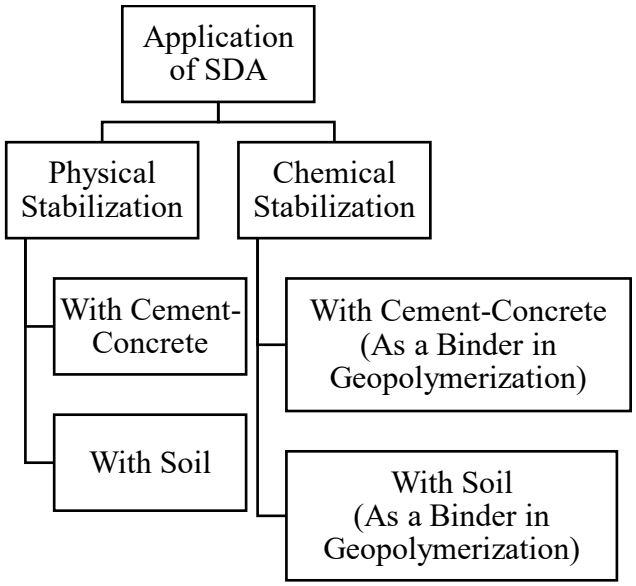


**Figure 2.7:** Application of sawdust ash in various sectors

Mageswari and Vidivelli (2009) studied the effect of using sawdust ash as a fine aggregate replacement in concrete. Sawdust ash was used in 5%, 10%, 15%, 20%, 25% and 30% replacement of natural sand. Compressive, tensile and flexure strength were determined at different curing periods- 28, 45, 60, 90 and 180 days. The study found that, with the increase in sawdust ash content, the amount of water required for a good workability also increases. The compressive, tensile and flexure strength were found to increase with prolonged curing time and to decrease with increasing sawdust ash content. The optimum sawdust ash content was found to be 10% replacement of natural sand.

Ukrainczyk et al. (2016) used biomass wood ash as a replacement of cement (5%, 10%, 15% and 20%) and sand (3.33%) in concrete production. Soundness, workability, compressive strength and flexure strength of the composite mortar were determined. The study found that, with the inclusion of ash, the rate of hydration, strength, and workability decreases. The optimum replacement dosage was found to be 15 % of ash, replacing 5 % of cement and 3.33 % of sand. From XRF, XRD and thermogavimateric analysis, the oxide compositions and hydration products were determined. It was found that, biomass wood ash contains cementitious materials and thus can be used as a cement replacement.

### 2.8.2 Application of Sawdust Ash in Geopolymer Concrete

Rossi et al. (2020) studied the effect of five different types of curing condition in the compressive strength, morphology and internal structure of wood biomass fly based geopolymer. The curing conditions included – thermal condition, hydrothermal condition, room condition, water-submerged condition and usual conditions. They used two different concentrations of alkali activators, sodium silicate and sodium hydroxide (1.0 and 1.5 weight ratios), and a fixed composition binder (75 wt.% wood biomass fly ash and 25 wt.% metakaolin) in the preparation of geopolymer. The study reported that the relative amount of alkaline activator (NaOH and $Na_2SiO_3$ ratio) plays an important role in mechanical strength development in geopolymer specially an increased amount of $SiO_2/Al_2O_3$ ratio positively affects the strength of geopolymer. Moreover, curing in environmental condition showed similar strength development compared to high temperature curing that requires higher energy consumption.

More studies on the application of sawdust ash in geopolymer concrete has been presented here in Table 2.1.

### 2.8.3 Application of Sawdust Ash in Soil

Manukaji (2012) studied linear shrinkage, solid density, apparent porosity and thermal conductivity of a clay soil with the inclusion of sawdaust from 0% to 40%. The obtained results showed a steady reduction of linear shrinkage and solid density values from 8.57% -8.32% and 3.18 -2.91 gm/cm$^3$ respectively. On the other hand, apparent porosity increased in value from 13- 17% with the inclusion of sawdust. The thermal conductivity results showed that with the inclusion of sawdust, conductivity decreases from 0.491 – 0.134 W/m/K resulting in a better thermal insulation property.

Hassan et al. (2014) prepared standard fireclay brick specimens with the inclusion of sawdust and rice husk in mangada clay and investigated their effect on physical properties such as bulk density, thermal shock resistance, porosity, fired shrinkage, specific gravity and refractoriness. The study concluded that the refractoriness of the clay sample is negatively affected by the addition of these two additives lowering the sintering temperature from 1300°C (unstabilizaed soil) to 1200°C (soil stabilized with rice husk and saw dust). On the contrary, shrinkage and thermal shock resistance was found to be improved due to the inclusion of these additives while sawdust having the greater impact. The apparant porosity increased with addition of the additives from 27.15% (bare soil) to 45.33% in sawdust amended soil and 36.74% in rice husk amended soil. On the other hand, bulk density was reduced due to these additives while rice husk (1.52 gm/cm$^3$) reducing the density to a greater amount compared to sawdust (1.59 gm/cm$^3$).

Halim and Baroudy (2014) studied the effect of fine (passing 1 mm sieve) pinewood sawdust in some hydro-physical properties of an expansive soil from the middle Nile Delta which include- hydraulic conductivity, liquid limit, plastic limit, plasticity index, linear shrinkage and cracking width. Sawdust was added with the soil at 0%, 1%, 2%, 5%, 10%, 15% and 20% on the dry weight basis. The results obtained in this study showed that, with the increase in sawdust content, hydraulic conductivity increased significantly from 1 cm/h for 0% sawdust to 37 cm/h for 20% sawdust. On the the other hand, plasticity index, linear shrinkage and crack width were reduced significantly due to the inclusion of sawdust indicating an improved shrinkage characteristics in expansive soil with the 20% sawdust inclusion showing the greatest improvement.

Jasim and Çetin (2016) added sawdust with a high plastic silty soil (MH) at a percentage of 1, 2, 3 and 5 and investigated the effect of sawdust addition on the Unconfined Compressive Strength, specific gravity and compation parameters. The study reported that, addition of sawdust up to 5% decreased the liquid limits and the plasticity index by 14.9% and 17.6% respectively. The undrained strength determined from Unconsolidated Undrained Triaxial Test was found to increase by 41.437% with 3% sawdust addition but further addition od sawdust (to 5%) reduced the strength. The study concluded that sawdust can be used as a good filler material in clayey silt soil.

More studies on the application of sawdust or sawdust ash in soil or CSEB has been presented here in Table 2.2.

### 2.8.4 Application of Sawdust Ash Based Geopolymer in Soil

Kong et al. (2018) studied the use of red mud and sawdust based geopolymer composites in potential application of construction material. They mixed sawdust ash and red mud at a ratio of 10:90, 20:80, 30:70, 40:60, 50:50 and 60:40. Red mud was treated with Boric Acid (1M) and sawdust ash was treated with NaOH, $H_2O_2$ and KOH. Compressive strength characteristics, FTIR spectra, Thermogravimetric Analysis and morphology determination through SEM were carried out. The study reported the formation of a dense mictrostructure with the addition of sawdust ash although with increasing sawdust ash content, microcrack and pore development were also observed. The maximum compressive strength was achieved in the composition having 10% ash and 90% red mud which was as high as 138 MPa (comparable to Portland Cement Strengths). Moreover, the sawdust ash-redmud geopolymer composite resulted in a mediocore workability due to high water absorption characteristics of sawdust ash.

From the above discussion it is evident that although several studies have investigated the behavior of SDA amended soil and used SDA based geopolymer in soil stabilization, significant study has not been reported on the use of Sawdust Ash based geopolymer in fabrication of CSEB utilizing the expansive soil. Therefore, it was deemed necessary to address the research gap in the present state-of-the-art considering the enormous potential of this material as a sustainable construction unit.

## 2.9 Summary

The evolution of earthen construction can be dated back to very early ages. Due to environmental friendliness and invention of new stabilization methods that facilitates overcoming the limitations of raw earth, earthen construction are once again gaining attention in the mass level. Geopolymer is such a form of stabilization method which guaranties improved mechanical strength as well as reduces environmental burden by utilizing waste materials for example sawdust ash. Since its application is still on the development stage, in the light of the present state-of-the-art extensive scientific research work is needed in this field to develop complete understanding of the behavior of CSEB fabricated with SDA based geopolymer.

**Table 2.1:** Summary of the previous studies on application of sawdust ash in geopolymer concrete

| * S= Slump, ST = Setting Time , P= Porosity, BD= Bulk Density, CS = Compressive Strength , FS = Flexure Strength, B= Binder, W= Water, FAgg= Fine Aggregate, CA = Coarse Aggregate, FA= Fly Ash, SDA= Sawdust Ash, HCWA= High Calcium Wood Ash, PFA= Pulverized Fuel Ash, SS= Sodium Silicate, SH= Sodium Hydroxide, $R_H$ = Relative Humidity | | | | Physical Tests | | | | | | | | | | Chemical and Microstructural Analysis | | | | |
|---|---|---|---|---|---|---|---|---|---|---|---|---|---|---|---|---|---|---|
| | | | | Physical Property | | | | Strength | | | | Durability | | | | | | |
| Author | Design and Mix Proportion | Alkaline solution | Curing Period (days) | S | ST | P | BD | CS | FS | STS | DM | WA | DS | XRD | FTIR | EDX | SEM | TGA |
| Kumar et al. (2015) | B : FAgg : CA = 1 : 1.76 : 3.28 B = FA + SDA ( 0 / 5/ 10/ 15/ 20 % by wt. FA replacement) | SH:SS= 1 : 2.5 NaOH = 8M | 7, 28 Curing at 60˚C | √ | | | | √ | √ | √ | | | | | | | | |
| Cheah et al. (2015) | Binder - HCWA:PFA hybridization ratio (weight basis) of 50:50, 60:40, 70:30 and 100:0; Binder : sand = 1 : 2.25 ; W:B = 0.3 and 0.35 | External activator not used; (HCWA) contained inherent reactive alkali activator minerals | 24h at 28˚C, $R_H$ =80% ; lime saturated water till the testing ages of 7, 28 and 90 days. | | | √ | | √ | √ | | √ | √ | | √ | | √ | √ | |

**Table 2.1:** Summary of the previous studies on application of sawdust ash in geopolymer concrete (cont.)

| * STS = Split Tensile Strength, DM = Dynamic Modulus, WA = Water Absorption DS= Drying Shrinkage, TGA = Thermogravimetric analysis, A= Alkaline Solution, B= Binder, FA= Fly Ash, SDA= Sawdust Ash, HCWA= High Calcium Wood Ash, GGBS= Ground Granulated Blust Furnace Slag, SS= Sodium Silicate, SH= Sodium Hydroxide, $R_H$ = Relative Humidity | | | | Physical Tests | | | | | | | | | | Chemical and Microstructural Analysis | | | | |
|---|---|---|---|---|---|---|---|---|---|---|---|---|---|---|---|---|---|---|
| | | | | Physical Property | | | | Strength | | | | Durability | | | | | | |
| Author | Design and Mix Proportion | Alkaline solution | Curing Period (days) | S | ST | P | BD | CS | FS | STS | DM | WA | DS | XRD | FTIR | EDX | SEM | TGA |
| Duan et al. (2016) | FA + SDA (replacing FA by 0/5/10/15/20 % by mass) + SH+ SS+ water Liquid/Solid ratio = 0.9 | SS:SH = 8:1; 10 M (NaOH) | 24h at 40˚C after demolding curing at 40˚C and $R_H$ = 90% | √ | √ | √ | √ | √ | √ | | | | √ | | | | √ | |
| Cheah et al. (2017) | GGBS:HCWA= 80:20. Fly ash + (GGBS-HCWA)- replacing FA by (0/10/20/30/40/50/60/70/80/90/100 %) + sand + water | SH = 12 M; A:B = 0.11; SS:SH = 1.2 | 24h at 28˚C then at 26˚C and $R_H$= 60 to 70% until the ages of 7, 28, 56 and 90 days. | √ | √ | | | √ | √ | | √ | | | | | √ | √ | |

**Table 2.1:** Summary of the previous studies on application of sawdust ash in geopolymer concrete (cont.)

| * S= Slump, ST = Setting Time , P= Porosity, BD= Bulk Density, CS = Compressive Strength , FS = Flexure Strength, FA= Fly Ash, BWA= Biomass Wood Ash, SS= Sodium Silicate, SH= Sodium Hydroxide | | | | Physical Tests | | | | | | | | | | Chemical and Microstructural Analysis | | | | |
|---|---|---|---|---|---|---|---|---|---|---|---|---|---|---|---|---|---|---|
| | | | | Physical Property | | | | Strength | | | | Durability | | | | | | |
| Author | Design and Mix Proportion | Alkaline solution | Curing Period (days) | S | ST | P | BD | CS | FS | STS | DM | WA | DS | XRD | FTIR | EDX | SEM | TGA |
| Abdulkareem et al. (2018) | FA replaced by BWA of 5%, 15% and 25% by binder mass ; FA + BWA (0/5/15/25 % by mass replacing the FA) + sand +SS+ SH | (SS+SH) binder: ash = 0.5; FA/binder-ash ratios 2.0; NaOH 12M | 24h at 70˚C, then 3, 7, 28 days at ambient temperature | √ | | √ | √ | √ | √ | | | √ | | | | | √ | |
| Pereira et al. (2019) | Metakaolin + Sawdust + SS+ SH + Microsilica (960) + Calcined alumina | Na2O - SiO2- Al2O3 Ratio sample 1= 22.50 -33.70- 43.80 ; Sample 2 = 21.20- 51.00 - 28.00 (wt%) | 7 to 10 days at (~25 °C) and then dried in an oven at 110 °C | | | √ | √ | √ | | | | | | √ | | | √ | |

**Table 2.1:** Summary of the previous studies on application of sawdust ash in geopolymer concrete (cont.)

| * STS = Split Tensile Strength, DM = Dynamic Modulus, WA = Water Absorption DS= Drying Shrinkage, TGA = Thermogravimetric analysis, SS= Sodium Silicate, SH= Sodium Hydroxide, $R_H$ = Relative Humidity, BFA= Biomass Fly Ash, MK= Metakaolin, FA= Fly Ash, SDA= Sawdust Ash, CA= Coarse Aggregate | | | | Physical Tests | | | | | | | | | | Chemical and Microstructural Analysis | | | | |
|---|---|---|---|---|---|---|---|---|---|---|---|---|---|---|---|---|---|---|
| | | | | Physical Property | | | | Strength | | | | Durability | | | | | | |
| Author | Design and Mix Proportion | Alkaline solution | Curing Period (days) | S | ST | P | BD | CS | FS | STS | DM | WA | DS | XRD | FTIR | EDX | SEM | TGA |
| Saeli et al. (2019) | BFA + MK + Grit - as aggregate; B = 70 wt% BFA and 30 wt% MK; Liquid/Solid = 0.78; Binder/ Aggregate = (1:1, 1:2, 1:3, 1:4) | SH:SS= 1:3; NaOH solution (10 M)<br><br>grit particle size between 12.5 and 0.5 mm | 24 hrs at (20 °C, 65% $R_H$); demoulded samples curing at ambient conditions for 28 days. | √ | | | √ | √ | | | | √ | | √ | | | √ | √ |
| Arunkumar et al. (2020) | FA+ SDA (replacing FA by 0/10/20/30/40/50 /60/70/80/90/100 %) + Sand + CA + SH+ SS + Poly Propelene Fibre (0/0.5/1/1.5/2 % of volume fraction) | SS and SH - specific gravity of 1.60 and 1.47 were used.<br><br>alkaline solution ratio of 0.61. | | | | | | √ | √ | √ | | | | | | √ | | |

**Table 2.1:** Summary of the previous studies on application of sawdust ash in geopolymer concrete (cont.)

| * S= Slump, ST = Setting Time , P= Porosity, BD= Bulk Density, CS = Compressive Strength , FS = Flexure Strength, SS= Sodium Silicate, SH= Sodium Hydroxide, $R_H$ = Relative Humidity, FA= Fly Ash, SDA= Sawdust Ash, CA= Coarse Aggregate, GBFS= Granulated Blust Furnace Slag | | | | Physical Tests | | | | | | | | | | Chemical and Microstructural Analysis | | | | |
|---|---|---|---|---|---|---|---|---|---|---|---|---|---|---|---|---|---|---|
| | | | | Physical Property | | | | Strength | | | | Durability | | | | | | |
| Author | Design and Mix Proportion | Alkaline solution | Curing Period (days) | S | ST | P | BD | CS | FS | STS | DM | WA | DS | XRD | FTIR | EDX | SEM | TGA |
| Alabduljabbar et al. (2020) | (A:B) = 0.40; FA (70%) + GBFS (30%) + saw dust (replacing natural agg by 0 / 25 / 50 / 75 / 100 % ) + Natural Agg. | SH = 2M, SS:SH= 0.7 | 24 hrs at (27 °C, 75% $R_H$) Testing period (1,3,7,28,56, 90 days) | √ | √ | | √ | √ | √ | √ | | √ | √ | √ | | | | |
| Arunkumar et al. (2021) | FA: Sand: CA= 1 : 1.05 : 1.57 with A ratio0.61. FA (70%) + SDA (30 %) + Sand + CA+ Waste Rubber Fibre (0/0.5/1/1.5/2 % by Volume) | SH = 10M, SH:SS= 1:2.5 | 3,7,28,56, 90 days, at ambient temperature | √ | √ | | | √ | √ | √ | | | | | | √ | | |

**Table 2.2:** Summary of the previous studies on application of sawdust ash in CSEB

| * C= Compaction Test, BD= Bulk Density, CS = Compressive Strength , FS = Flexure Strength, STS = Split Tensile Strength, DST= Direct Shear Test, WA = Water Absorption, S= Submersion, E = Efflorescence, LS= Linear Shrinkage, SDA= Sawdust Ash | | | | Physical Tests | | | | | | | | | | Chemical and Microstructural Analysis | | |
|---|---|---|---|---|---|---|---|---|---|---|---|---|---|---|---|---|
| | | | | Physical Property | | Strength | | | | Durability | | | | | | |
| Author | Design and Mix Proportion | Saw Dust Identity | Curing Period | C | BD | CS | FS | STS | DST | WA | SB | E | LS | XRD | FTIR | SEM |
| Elinwa (2006) | Clay + SDA (0/ 10 / 20 / 30 / 40 % by mass of clay ) + water - for desired consistency | - | air-dried and fired at 200 ◦C, 600 ◦C and 1200 ◦C. After firing cured for 1, 4 and 8 days | | | √ | | | | √ | | | √ | | | |
| Emmanuel A. Okunade (2008) | Soil = lalteritic soil (70%) + clay soil (30%) 1. soil (100%) 2. soil + SDA (0/2.5/5/7.5/10 % by v) + SDA (10/7.5/5/2.5/0 % by volume) | SDA = Iroko Hardwood, Burnt at 600 ℃ | 14 days of sun drying, then burnt at 1000 ℃ | | √ | √ | | | | √ | | | | | | |

**Table 2.2:** Summary of the previous studies on application of sawdust ash in CSEB (contd.)

| * C= Compaction Test, BD= Bulk Density, CS = Compressive Strength , FS = Flexure Strength, STS = Split Tensile Strength, DST= Direct Shear Test, WA = Water Absorption, S= Submersion, E = Efflorescence, LS= Linear Shrinkage, SDA= Sawdust Ash | | | | Physical Tests | | | | | | | | | | Chemical and Microstructural Analysis | | |
|---|---|---|---|---|---|---|---|---|---|---|---|---|---|---|---|---|
| | | | | Physical Property | | Strength | | | | Durability | | | | | | |
| Author | Design and Mix Proportion | Saw Dust Identity | Curing Period | C | BD | CS | FS | STS | DST | WA | SB | E | LS | XRD | FTIR | SEM |
| Ntamack et al. (2012) | Soil + 6 % lime; Soil + 6 % cement; Soil + 4 % cement + 2 % Saw dust ; 2 type of Soil has been used | - | 7 days under a plastic and 21 days under the free air | | √ | √ | | | | | | | | | | |
| Paudyal et al. (2018) | Soil + cement (12.5 %) + lime (5/7.7 / 9.4 %) Soil + cement (12.5 %) + Fly Ash (15/30 %) Soil + cement (12.5 %) + SDA (15/ 29.2 %) | - | cold water | | | √ | | | | | | | | | | |

**Table 2.2:** Summary of the previous studies on application of sawdust ash in CSEB (contd.)

| * C= Compaction Test, BD= Bulk Density, CS = Compressive Strength , FS = Flexure Strength, STS = Split Tensile Strength, DST= Direct Shear Test, WA = Water Absorption, S= Submersion, E = Efflorescence, LS= Linear Shrinkage, SDA= Sawdust Ash, OMC= Optimum Moisture Content | | | | Physical Tests | | | | | | | | | | Chemical and Microstructural Analysis | | |
|---|---|---|---|---|---|---|---|---|---|---|---|---|---|---|---|---|
| | | | | Physical Property | | Strength | | | | Durability | | | | | | |
| Author | Design and Mix Proportion | Saw Dust Identity | Curing Period | C | BD | CS | FS | STS | DST | WA | SB | E | LS | XRD | FTIR | SEM |
| Fadele et al. (2018) | Laterite soil (passing 2.36 mm /10 mm ) + Additive (3 types) at [ 0 /4 / 8 / 12 %] by mass of laterite + water – OMC | softwood sawdust [Ceiba Pentandra] , hardwood sawdust | Initially, 3 Day; Later, Cured upto testing day | √ | | | | | | √ | | | | √ | √ | |
| Ayodele et al. (2019) | Laterite soil + cement - (5% by mass of dry soil)<br>Laterite soil + equal amount of SDA and Egg Shell Ash - (0/2/4/8/16 % by mass of dry soil) | Saw dust was collected from saw mill, air dried and calcined at < 650 deg C. passing sieve 600 µm | cured for 14, 21, 28 and 90 days | √ | | √ | | | | | | | | | | |

**Table 2.2:** Summary of the previous studies on application of sawdust ash in CSEB (contd.)

| * C= Compaction Test, BD= Bulk Density, CS = Compressive Strength , FS = Flexure Strength, STS = Split Tensile Strength, DST= Direct Shear Test, WA = Water Absorption, S= Submersion, E = Efflorescence, LS= Linear Shrinkage | | | | Physical Tests | | | | | | | | | | Chemical and Microstructural Analysis | | |
|---|---|---|---|---|---|---|---|---|---|---|---|---|---|---|---|---|
| | | | | Physical Property | | Strength | | | | Durability | | | | | | |
| Author | Design and Mix Proportion | Saw Dust Identity | Curing Period | C | BD | CS | FS | STS | DST | WA | SB | E | LS | XRD | FTIR | SEM |
| Elahi et al. (2020) | Coarse grained soil (61 % Sand) + Cement % (4/6/8/10) + Sawdust ash % (0/2/4/6/8/10) | Shorea robusta wood ; passing through 600 micron sieve | 28 day ; Temperature 25 deg C, Rh = 96 % | √ | | √ | | | √ | √ | √ | √ | | √ | | √ |

# Chapter 3
# EXPERIMENTAL PROGRAM

## 3.1 Introduction

The experimental program was conducted according to the standard testing procedures to fulfill the research objectives. The collected soil was tested to determine the index properties and chemical and mineralogical compositions. Physical properties and chemical composition of SDA were also ascertained. Compacted geopolymer mixtures made with Soil, SDA, and Alkaline Solutions were prepared at different alkali-binder ratios and SDA percentages to evaluate the strength (unconfined compressive strength, split tensile strength, and flexure strength) and durability characteristics (wet compressive strength, efflorescence, and water absorption). Microstructural investigation was conducted by SEM to understand the microstructural changes that occurred at different SDA and Alkali content. FTIR was also performed on samples to detect various functional groups in geopolymer mixtures.

This chapter describes the properties of the materials used for fabricating geopolymer mixtures and summarizes the methodology of the sample preparation and procedures for performing relevant laboratory tests.

## 3.2 Materials

To investigate the mechanical behavior and durability characteristics of CSEBs, four types of materials have been used: soil, sawdust ash, sodium hydroxide, and sodium silicate.

### 3.2.1 Soil

The soil sample used in this study was a high swell-shrinkage soil collected from the Munshiganj district of Bangladesh. The index properties of the soil were determined from laboratory tests according to ASTM standards and are presented in Table 3.1. The gradation curve of the soil sample was generated from the sieve and hydrometer analysis test results based on ASTM D6913 and ASTM D7928 respectively and is presented in Figure 3.1.

**Table 3.1:** Properties of soil used in this study

| Soil Property | Value |
|---|---|
| Specific gravity, $G_s$ | 2.69 |
| Sand (%) | 0.7 |
| Silt (%) | 57.2 |
| Clay (%) | 42.1 |
| Liquid Limit, LL (%) | 57.6 |
| Plastic Limit, PL (%) | 19.5 |
| Plasticity Index, PI (%) | 38.1 |
| Shrinkage Limit, SL (%) | 24.2 |
| Free Swell Index, FSI (%) | 83.3 |
| Optimum moisture content, OMC (%) | 18.6 |
| Maximum dry density (kN/m$^3$) | 15.97 |
| Unified Soil Classification System (USCS) | CH |

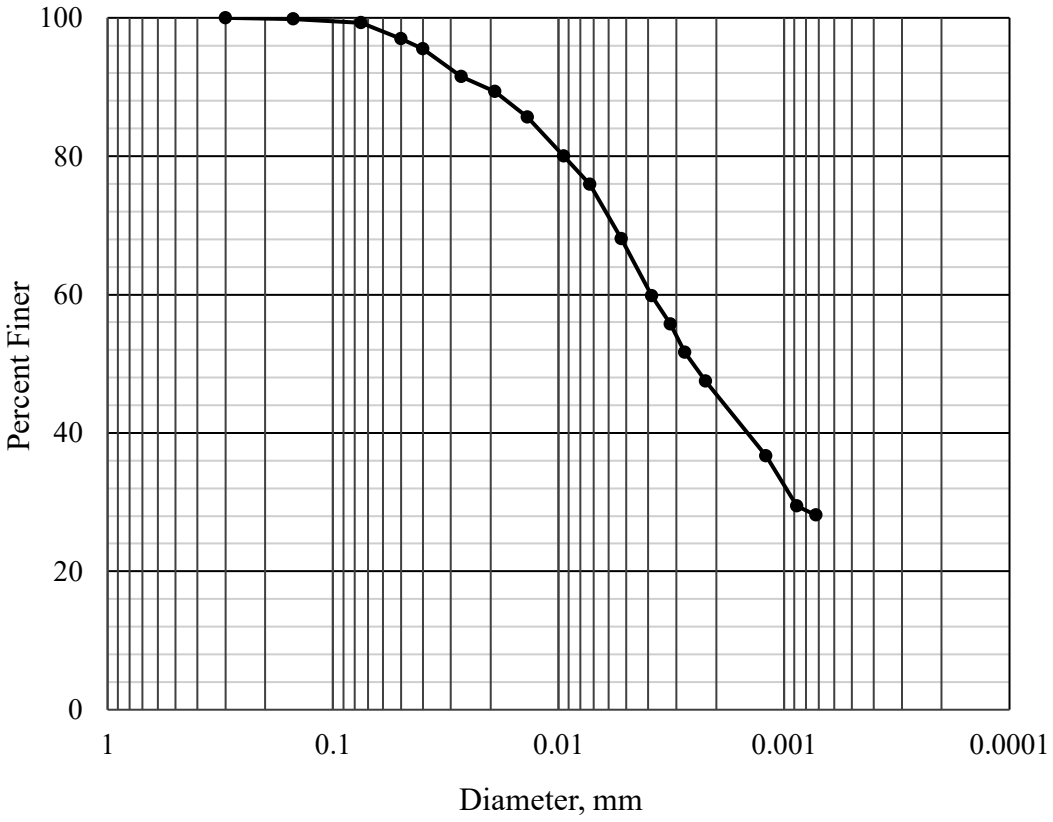


**Figure 3.1:** Gradation Curve of Soil

Atterberg limit tests were performed according to ASTM D-4318 and the LL, PL and SL was found to be 57.6%, 19.5% and 24.2% respectively. The free swell index of the soil was found 83.3% which was determined following the test procedures described in IS 2720 - 40 (1977). Standard proctor test was performed to analyze the compaction characteristics of the soil according to ASTM D698 and Optimum Moisture Content (OMC) was found 18.6% and maximum dry density was obtained 15.97 kN/m$^3$. The compaction cureve is presented here in Figure 3.2. According to the Unified Soil Classification System (USCS), the soil is classified as High Plastic Clay (CH).

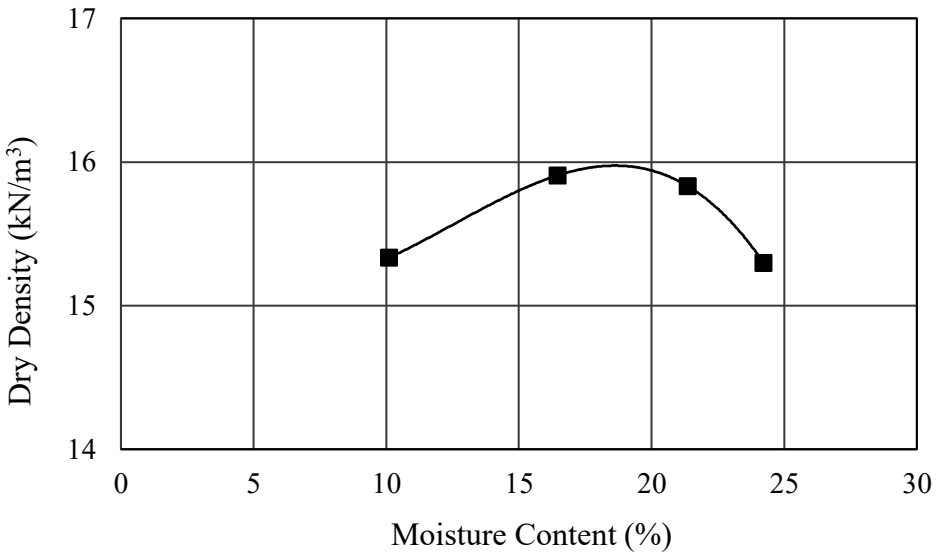


**Figure 3.2:** Variation of dry density with moisture content for soil sample

### 3.2.2 Sawdust Ash

Sawdust was collected from a local sawmill. It was a mixture of different kinds of woods including *Tectona grandis, Shorea robusta, Dipterocarpus turbinatus, Gmelina arborea, Terminalia arjuna, Swietenia mahagnoni,* etc. The collected sawdust was light brown in color. After collection, bark and organic content were removed from it and air-dried. Ash was generated from the uncontrolled burning of the air-dried sawdust. Later sawdust ash was sieved through a 75µm sieve and the ash passing through the sieve was used for the fabrication of CSEBs in this study. The specific gravity of the sawdust ash was determined following ASTM D854-14 and was found 2.75. The particle size distribution of the sawdust ash was determined using hydrometer analysis following ASTM D7928. The gradation curve of the sawdust ash is presented here in Figure 3.3.

XRF (X-ray fluorescence) technique was performed to determine the oxide compositions of soil and sawdust ash. A summary of the oxide compositions of materials used in this study has been presented in Table 3.2.

### 3.2.3 Sodium Hydroxide

The sodium hydroxide used was a technical grade sodium hydroxide in flakes form (3 mm), with a specific gravity of 2.130, 98% purity, and obtained from Merck KGaA, Germany. The concentration of sodium hydroxide (NaOH) solution used in this study was 10M. The NaOH solution was prepared by dissolving 10x40 = 400 grams of NaOH flakes in 1kg distilled water, where 40 is the molecular weight of NaOH.

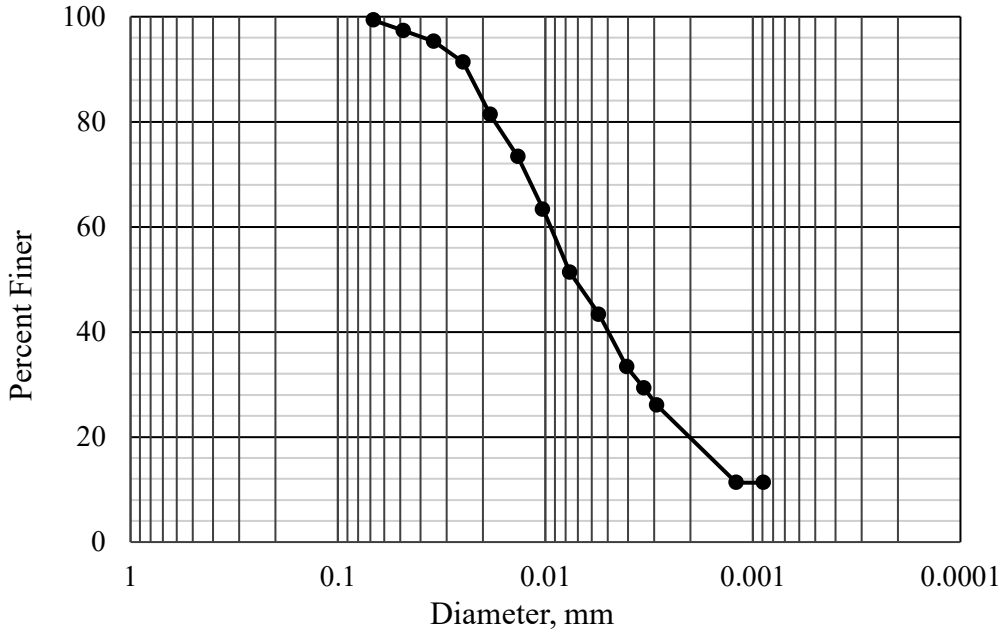


**Figure 3.3:** Gradation Curve of SDA

### 3.2.4 Sodium Silicate

The sodium silicate used was a technical grade metasilicate nonahydrate ($Na_2SiO_3.9H_2O$) in powder form, with a molecular weight of 284.2, and obtained from Loba Chemie Pvt. Ltd., India. The chemical composition of the sodium silicate powder was $Na_2O$=21.5%, $SiO_2$=21.3%, and water 57.2% by mass. A sodium silicate solution with (70%/30% w/w) concentration was used in this study which was prepared by dissolving 70 grams of silicate powder in 30 gm of distilled water. The various oxide compositions in the final silicate solution have been presented in Table 3.2.

**Table 3.2:** Chemical composition of the materials used in this study

| Compound | Chemical Composition (%) | | |
|---|---|---|---|
| | Soil | Sawdust Ash | Sodium Silicate |
| $SiO_2$ | 62.85 | 24.47 | 14.91 |
| $Al_2O_3$ | 15.42 | 2.47 | - |
| $Fe_2O_3$ | 9.36 | 4.42 | - |
| CaO | 1.71 | 30.99 | - |
| MgO | 3.47 | 8.91 | - |
| $K_2O$ | 4.67 | 16.14 | - |
| $Na_2O$ | 0.82 | 1.34 | 15.05 |
| $SO_3$ | 0.11 | 2.75 | - |
| Others | 1.59 | 8.51 | - |
| $H_2O$ | - | - | 70.04 |

### 3.3 Sample Preparation

For the preparation of samples, collected soil was air-dried and then pulverized using a wooden hammer. Thereafter, soil samples were passed through No.16 sieve and soils passing through the No.16 sieve were considered for sample preparation. Based on the test scheme (refer to Table 3.3), the required amount of sawdust ash was added to the soil and mixed homogeneously. The mixture of soil and sawdust ash is referred to here as "Binder (B)". On the other hand, NaOH (10M) and $Na_2SiO_3$ (70%/30% w/w $H_2O$) solutions are combinedly referred to here as "Alkaline Solution (A)" and were prepared 24 hours prior to mixing with the binder. The alkaline solution contained NaOH and $Na_2SiO_3$ in a ratio of 1:2. The alkaline solution was finally mixed with the binder as per the test scheme (refer to Table 3.3) to prepare the geopolymer specimens for conducting the strength and durability tests.

In order to fulfill the objective of this study, the test plan was carried out in two phases. In the first phase, the optimum amount of alkaline solution was determined based on the Unconfined Compression Test. In the second phase of the study, samples were prepared based on the optimum amount of alkaline solution, and the Flexure Test and Split Tensile Test were performed on these samples. The composition of different sample mixtures is presented here in Table 3.3. Among different compositions, one was a control mixture which was fabricated with only soil at its optimum moisture content by distilled water to

check the stabilization effect due to geopolymerization. Other than this mixture, no extra water was added to the rest of the mixtures. The only source of water was the alkaline solution.

When the alkaline solution was added to the binder (soil and SDA mix), it was mixed properly until the mixture became homogenous. Thereafter, the mixture was poured into the mold in three layers. In this study, three types of mold were used for sample preparation depending on the type of tests to be performed- i) Cylinder (38 mm × 76 mm) for Unconfined Compressive Strength Test and Split Tensile Strength Test, ii) Cylinder (38 mm × 38 mm) for Efflorescence Test and iii) Prism (40 mm × 40 mm × 160 mm) for Flexure Strength Test. Based on the alkaline solution to binder ratio as well as the percentage of SDA, the workability of different mixtures varied significantly (refer to Figure 3.4). Hence, vibration/gentle tapping or compaction by a hammer was done to remove the air void in the combined matrix.

**Table 3.3:** Composition of mixtures and tests conducted in the study

| Soil (% of total dry binder) | SDA (% of total dry binder) | A : B (by weight) | Test Plan |
|---|---|---|---|
| 100, 95, 90, 85, 80 | 0, 5, 10, 15, 20 | 0.3, 0.4, 0.5 | (1) Dry Unconfined Compression Test (7 days, 28 days)<br>(2) Wet Unconfined Compression Test (28 days)<br>(3) Dry Flexural Strength Test (28 days, selected mix)<br>(4) Dry Split Tensile Strength Test (28 days, selected mix)<br>(5) Water Absorption Test<br>(6) Efflorescence test<br>(7) Microstructural Investigation (selected mix)<br>(8) FTIR Test (selected mix) |

In case of compaction using a hammer, the mixture was poured into the mold and compacted into three layers. The amount of compaction energy applied for sample preparation was calculated using the following equation suggested by ASTM D698-12:

$$E_c = \frac{\text{No. of layers} \times \text{No. of blows per layer} \times \text{Weight of hammer (kg)} \times \text{Drop height (cm)}}{\text{Volume of mold (cm}^3\text{)}} \quad (3.1)$$

The value of applied compaction energy was 5.11 kg-cm/cm$^3$ as determined by equation (3.1) for cylindrical samples. Due to the variation in SDA percentage and A:B ratio, the bulk density of the samples were different in the various compositions. After compaction of the samples, the mold was placed in a plastic zip lock bag and kept undisturbed for 24 hours. It was done to prevent moisture loss to allow self setting. After 24 hours, the samples were removed from the mold and kept inside the plastic zip lock bag again for the rest of the period before specific testing. The plastic bags containing samples were placed in a room with temperature approximately 26℃ with a relative humidity 70%.

(a) (b) (c)

**Figure 3.4:** Workability of different mixtures (a) Low, (b) Medium and (c) High

Each sample was casted spepratiely to maintain homogeneity of mixing. 3 samples from each composition were casted for strength tests and an average strength of the 3 samples was reported as the representative strength of that particular composition.

It should be noted here that, prior to the selection of SDA percentage, concentration of sodium hydroxide and sodium silicate, and the relative amount of sodium hydroxide and sodium silicate, several trial tests of uncinfined compressive strength were performed. In one of these trials, two samples having 15% SDA and 30% SDA were prepared keeping the sodium hydroxide (10M) and sodium silicate pentahydrate (58%/42% w/w) concentration as well as their relative amount ($NaOH:Na_2SiO_3$ = 1:2) and A:B ratio (0.4) constant. The test results (refer to article 4.2.1) depicted that 15% SDA content provided maximum strength compared to 30% SDA content. Hence, for further experiments, SDA

content of 0%, 5%, 10%, 15% and, 20% was decided to use. A schematic diagram of the whole research workflow is presented in Figure 3.5. The methodology of sample preparation is also shown sequentially in Figure 3.6.

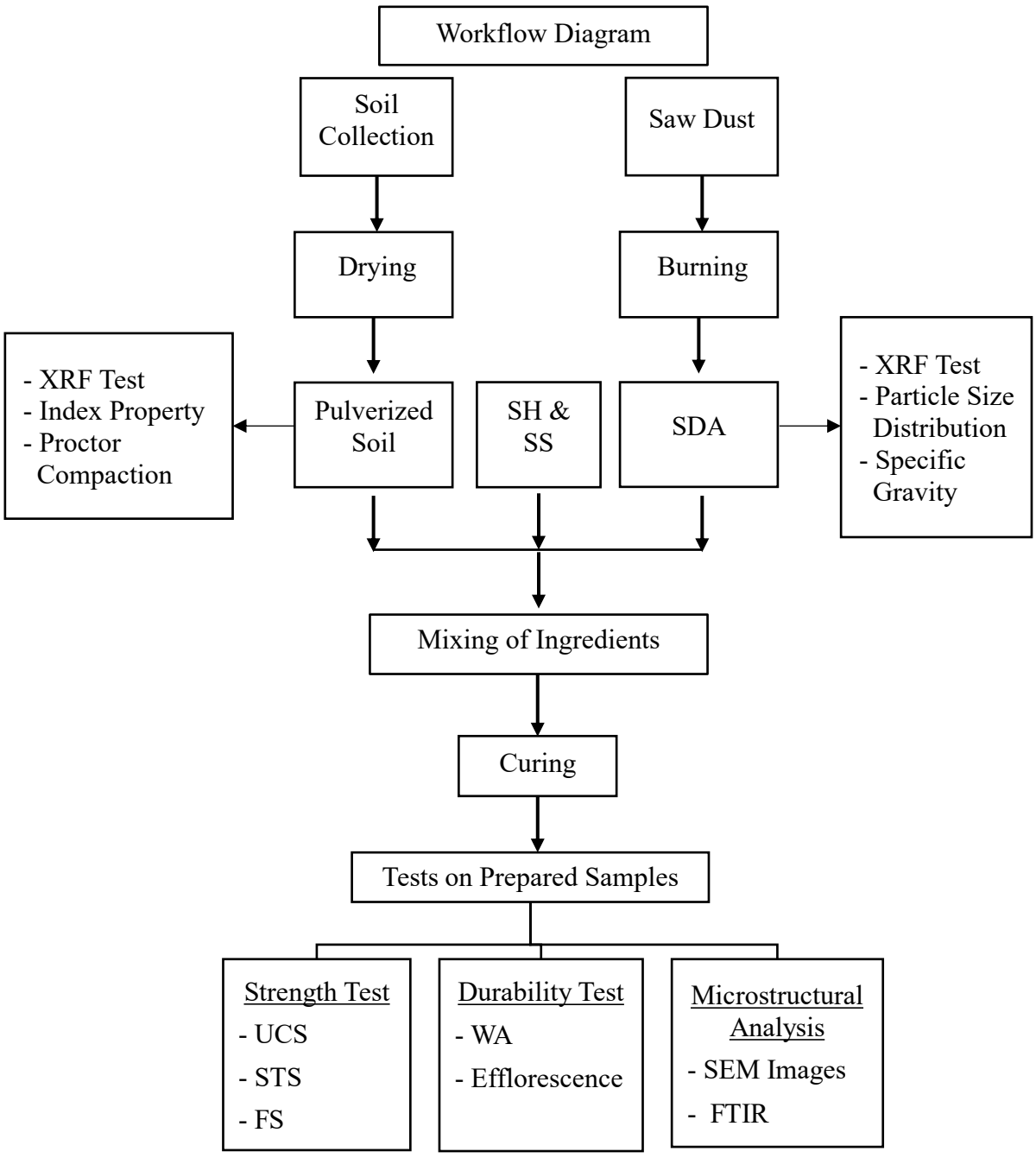


**Figure 3.5:** Research workflow diagram

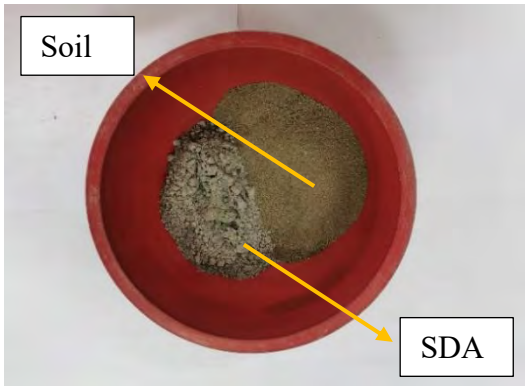


(a)

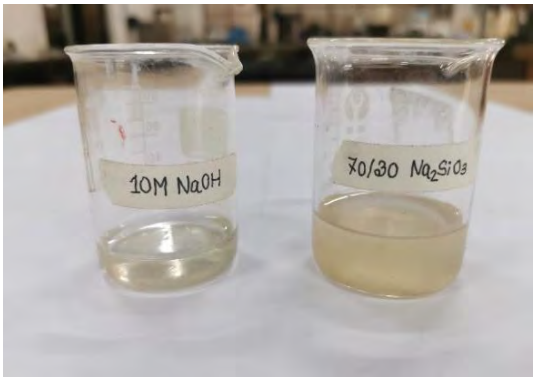


(b)

(c)

(d)

(e)

(f)

(g)

(h)

(i)

(j)

**Figure 3.6:** Different steps of sample preparation- (a) Homogenous mixing of Pulverized soil and SDA, (b) preparation of NaOH and $Na_2SiO_3$ solution, (c) homogeneous mixing of binder and alkaline solution, (d) application of oil on the inside of mold, (e) compaction of cylindrical sample, (f) removal of sample from mold, (g) storage of sample in a zip lock bag till test date, (h) prepared cylindrical samples, (i) mold for fabricating prismatic sample, and (j) prepared prismatic samples.

### 3.4 Test Scheme

#### 3.4.1 Unconfined Compression Test (Dry and Wet)

Unconfined compression test is a method to determine the compressive strength of CSEBs. Prior to the test, bedding surface was cleaned to ensure even contact and loading. Two plates were provided at the top and bottom for facilitating the loading process. The samples before testing were aligned with the center of testing machine to avoid the eccentric loading. The compressive strength of a test sample of particular mix composition was determined following the ASTM D5102-09 and using the following equation:

$$\sigma_c = \frac{P}{A} \tag{3.2}$$

Where, $\sigma_c$ is the compressive strength, P is the maximum load recorded and A is the area of the specimen upon which the load is applied.

Compressive strength test is performed for samples at two states-dry state and wet state. In case of dry compressive strength test, samples after 7 and 28 days of curing were removed from the plastic ziplock bag and test was performed. For wet strength test, samples after 28 days of curing were removed from the plastic ziplock bag and were kept under distill water for 24 hours at room temperature, thereafter test was performed. Representative samples were collected from the test specimen to measure moisture content at the time of testing. A typical test setup of compressive strength is shown in Figure 3.7.

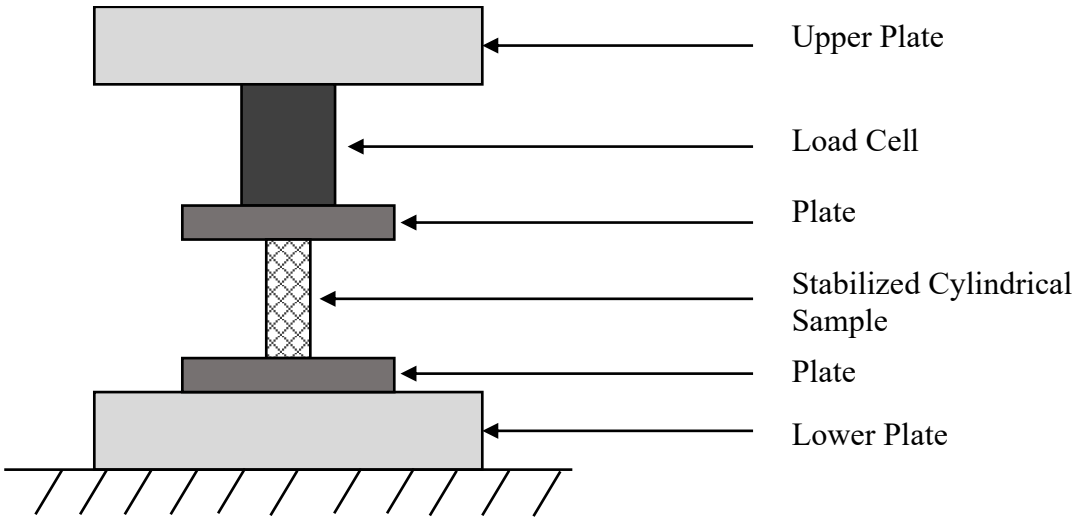


**Figure 3.7:** Test setup for unconfined compressive strength determinatiom

### 3.4.2 Split Tensile Strength Test

Split Tensile Strength (STS) of the stabilized soil was determined following the ASTM C496. Although the standard is for concrete cylindrical specimens, but various researchers have performed it for stabilized soil as well with sufficient accuracy. For this test, cylinders of diameter 38 mm and height of 76 mm were used. Cylinders were placed horizontally within the testing machine and tested at a displacement rate of 0.5 mm/min till failure. A typical test setup for determining STS, is shown in Figure 3.8 and the strength, $\sigma_T$ is calculated using the equation 3.3:

$$\sigma_T = \frac{2P}{\pi td} \tag{3.3}$$

Where, $P$ is the failure load, $t$ is the thickness or length of specimen, and $d$ is the diameter of the specimen. The test was conducted in dry condition of the specimens.

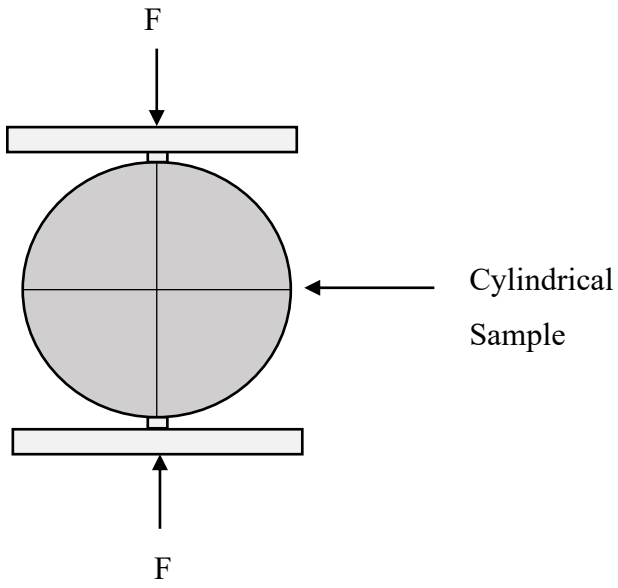


**Figure 3.8:** Test setup for split tensile strength test

### 3.4.3 Flexural Strength Test

Flexural Strength (FS) of CSEBs is defined as its capacity to resist the bending stresses coming into the blocks. For using CSEBs as a structural element in construction, determination of FS of CSEBs is important. In the present study, FS is determined based on the ASTM C 348. Center point loading method was used in this study to determine the flexural strength of the blocks. The CSEBs with dimensions 40 mm × 40 mm × 160 mm were put in a flat position on two steel cylindrical support which were placed 20 mm away from the end of CSEBs providing a span of 120 mm. Load was applied at center point (60

mm away from the end of either support). The test was conducted for dry state following the methodology described earlier and the strength was calculated using the following equation:

$$S_f = 0.0028\ P \tag{3.4}$$

Where, $S_f$ is the flexure strength in MPa and P is the total maximum load in N. It is to be noted that flexural strength of CSEBs were determined at the dry state at a rate of 0.5 mm/min. The Figure 3.9 shows the typical setup used for flexural strength of CSEBs.

**Figure 3.9:** Test setup for center-point bending test to determine flexural strength

### 3.4.4 Water Absorption Test

At first, the water absorption capacity of CSEB was evaluated using ASTM C 67. After 28 days of curing, the samples were placed in the oven for 24 hours at 105°C. However, due to high temperature, crack formation in the samples was observed (refer to Figure 3.10). This crack may allow quicker rate of absorption resulting in an erroneous water absorption value. Hence, water absorption test was later determined based on the bulk weight ($W_B$). The samples were removed from the plastic ziplock bags after 28 days and thereafter, were placed in a jar and submerged with distill water for 24 hours. Leaching of the unreacted SDA content was observed during this period (refer to Figure 3.11). After 24 hours samples were removed from the water and the surface of the blocks was wiped and weight measurement was taken

($W_W$). Based on these two weights, water absorption capacity of the blocks was determined using the equation below:

$$WA\ (\%) = \frac{W_w - W_B}{W_B} \times 100 \quad (3.5)$$

Where, WA is the water absorbed by the blocks, $W_w$ is the weight of the sample after submerging it under water for 24 hours and $W_B$ is the bulk weight of the samples.

### 3.4.5 Efflorescence Test

The efflorescence test was performed in accordance with ASTM C 67. In this test, one set of specimens from each pair is immersed in distill water to a depth of 1 inch for 7 days, while the other set of specimens is kept dry. At the end of seven days, both sets of specimens are dried in the oven for 24 hours. If a perceptible difference between the specimens is noticed when examined at 10 ft from the specimens under illumination of not less than 50 footcandle by an observer with clear vision, the rating is reported as "effloresced." Otherwise, the rating is reported as "Nil."

### 3.4.6 Microstructural Analysis

A scanning electron microscope (SEM) is a type of electron microscope that produces images of a sample by scanning the surface with a focused beam of electrons. The electrons interact with atoms in the sample, producing various signals that contain information about the surface topography and composition of the sample. The electron beam is scanned, and the position of the beam is combined with the detected signal to produce an image. In this study, microstructural analysis of five samples i) Soil at it's OMC, ii) 15% SDA with A:B 0.3, iii) 15% SDA with A:B 0.4, iv) 15% SDA with A:B 0.5 and v) 5% SDA with A:B 0.3 was performed. After oven-drying the samples for 24 hours, some small portions measuring 2 cubic inches were broken from each sample, which were mounted on a stud and placed in the chamber of a machine with SEM capabilities. Under various magnifications, a variety of images can be created.

### 3.4.7 Fourier Transform Infrared Spectroscopy

Fourier transform infrared spectroscopy (FTIR) is a technique which is used to obtain infrared spectrum of absorption, emission, and photoconductivity of solid, liquid, and gas. It is used to detect different functional groups and bonding nature present in geopolymer. The type of vibration (stretching or bending) induced by the infrared

radiation depends on the atoms in the bond. Because different bonds and functional groups absorb different frequencies, the transmittance pattern is different for different molecules.

**Figure 3.10:** Samples after 24 hour oven drying at 105℃

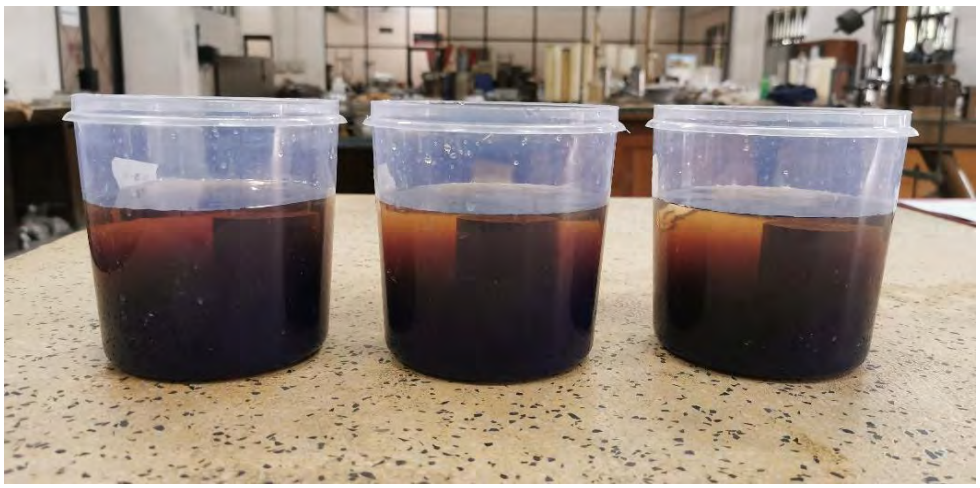

(a)

(b)

**Figure 3.11:** Samples after 24 hour water submersion (a) elevation and (b) plan view

In this study, FTIR spectroscopy was performed using a Perkin-Elmer Fourier Transform Infrared Spectrometer equipped with a diamond attenuated total reflection accessory. The spectral range was 400 – 4000 $cm^{-1}$. Three samples in powdered form (after 24 hour oven drying) with the composition - i) Soil at it's OMC, ii) 5% SDA with A:B 0.3 and iii) 15% SDA with A:B 0.3 were analyzed.

In the IR spectra, from the initial portion upto 1400 $cm^{-1}$ is called fingerprint region. In this region the most significant part lies in between 950 -1250 $cm^{-1}$ which corresponds to the asymmetric stretching of Si-O-Si and Al-O-Si representing the formation of geopolymerization. The major IR vibrational bands in this region that has been observed in several previous studies was summarized by Lee and Deventer (2003) and is presented in Table 3.4. In addition to this band spectra, there are some other peaks in the range of 3620 - 3629 $cm^{-1}$ corresponding to O-H stretching vibration (Chen et al. 2009), 3448 - 3458 $cm^{-1}$ corresponding to O-H bending vibration (Tchakouté et al. 2017), 1620 - 1683 $cm^{-1}$ corresponds to bending vibration of H-O-H (Ye et al. 2014).

### 3.5 Summary

In order to fulfill research objectives, laboratory experiment was conducted on samples made with Soil- SDA-Alklaine Solution composities. From initial trial results of 7 day unconfined compressive strength test, SDA dosage (in %) was determined which was finalized as 0%, 5%, 10%, 15% and 20%. From these trial results the concentration of NaOH (10M) and $Na_2SiO_3$ (70%/30% w/w), and their relative mixing ratio ($NaOH:Na_2SiO_3$ = 1:2) were also decided upon. The first objective was satisfied through the investigation of 7 day (bulk) and 28 day (bulk and wet) unconfined compressive strength of samples having the above mentioned SDA composition and A:B ratio of 0.3, 0.4 and 0.5. From the investigation of these strength values, the optimum amount of A:B ratio for different amount of SDA percentages were determined and based on that samples were casted for Flexure and Split Tensile Tests. The second objective was fulfilled through the compilation and analysis of all the strength (Compressive, Flexure, Tensile Strength) and durability (Water absorption, Efflorescence, Wet Comressive Strength) test results. The third objective was fulfilled through microstructural investigation by SEM images, EDXA analysis and FTIR spectra.

**Table 3.4:** Characteristic IR vibrational bands in geopolymer (Lee and Deventer, 2003)

| Wavenumber ($cm^{-1}$)[a] | Assignment[b] | References |
|---|---|---|
| 950-1250 (s) | asymmetric stretching (Si-O-Si and Al-O-Si) | Ghosh (1978), Farmer (1974), Gadsden (1975) |
| 1165 (sh) | asymmetric stretching (Si-O-Si) | Farmer (1974), Gadsden (1975), Vempati et al. (1994), Mollah et al. (1994), Uchino et al. (1991) |
| 1115-1140 (sh) | asymmetric stretching (Si-O-Si and Al-O-Si) | Gadsden (1975), Vempati et al. (1994) |
| 1077 (s) | asymmetric stretching (Si-O-Si and Al-O-Si) | Gadsden (1975), Vempati et al. (1994) |
| 950-980 (sh) | Si-O stretching ($Si-O-R^{+}$) | Uchino et al. (1991) |
| 882 (s) | Si-O stretching and OH bending (Si-OH) | Uchino et al. (1989) |
| 798 (m) | symmetric stretching (Si-O-Si) | Gadsden (1975), Mollah et al. (1994) |
| 727 (sh) | symmetric stretching (Si-O-Si and Al-O-Si) | Handke et al. (1994), Farmer (1974), Poe et al. (1992), Sitarz et al. (1997) |
| 620 (sh) | symmetric stretching (Si-O-Si and Al-O-Si) | Farmer (1974), Gadsden (1975), Poe et al. (1992) |
| 561 (s) | symmetric stretching (Al-O-Si) | Gadsden (1975), Poe et al. (1992) |
| 466 (s) | Bending (Si-O-Si and O-Si-O) | Handke et al. (1994), Ghosh (1978), Farmer (1974), Gadsden (1975), Vempati et al. (1994), Mollah et al. (1994), Uchino et al. (1991), Uchino et al. (1989), Poe et al. (1992), Sitarz et al. (1997), |

[a] The abbreviations in parentheses are as follows: s = strong, m = medium, and sh = shoulder. [b] R = Na and K

# Chapter 4
# RESULTS AND DISCUSSIONS

## 4.1 Introduction

This study intends to evaluate the strength and durability properties of CSEBs constructed with SDA based geopolymer in order to determine how effective it is for earthen construction. This chapter presents the findings from several laboratory experiments used to characterize CSEBs. The chapter includes illustrations of the effects of adding various amount of SDA and alkaline solution on the compressive, tensile, and flexural strength of stabilized soil along with necessary interpretations. In order to determine how well stabilizers perform in enhancing durability properties, which remain a significant drawback in earthen construction, the durability of stabilized earth blocks is evaluated in terms of water absorption, wet strength, and efflorescence. Results are also summarized in the present chapter.

In the subsections, the results of several tests on CSEBs constructed with various stabilizer composition will be discussed. To evaluate the performance of the stabilizer dosage, the test results will be compared to the relevant standards. Based on the comparison, the optimum mix compositions for creating CSEBs that adhere to various codes and standards will be recommended. Finally, a cost comparison was made among the produced geopolymer and traditional stabilzers – cement and lime.

## 4.2 Unconfined Compressive Strength

Unconfined Compressive Strength (UCS) of the samples were determined after 7 and 28 days of curing and at two different states- bulk and wet. Comparison of the strength with age and with testing condition were also made. Initially, some trial tests were also done to decide upon the SDA dosage (in %), concentration of NaOH and $Na_2SiO_3$ and their relative amount as well as alkaline solution to binder ratio.

### 4.2.1 Trial UCS test results for determining SDA dosage (in %)

Two samples having the following compositions were tested to determine the UCS after a curing periof of 7 days. In these two samples, all the characteristics of other components were kept constant except SDA percentage to evaluate the effect of SDA variation and

to determine the dosage of SDA that will be used in the later stages of this study. Figure 4.1 illustartes the UCS values of these 2 compositions.

Sample 1: SDA = 15% (of total binder), NaOH = 10M, $Na_2SiO_3$ = 58%/42% w/w,

NaOH : $Na_2SiO_3$ = 1:2 and A:B ratio 0.4

Sample 2: SDA = 30% (of total binder), NaOH = 10M, $Na_2SiO_3$ = 58%/42% w/w,

NaOH : $Na_2SiO_3$ = 1:2 and A:B ratio 0.4

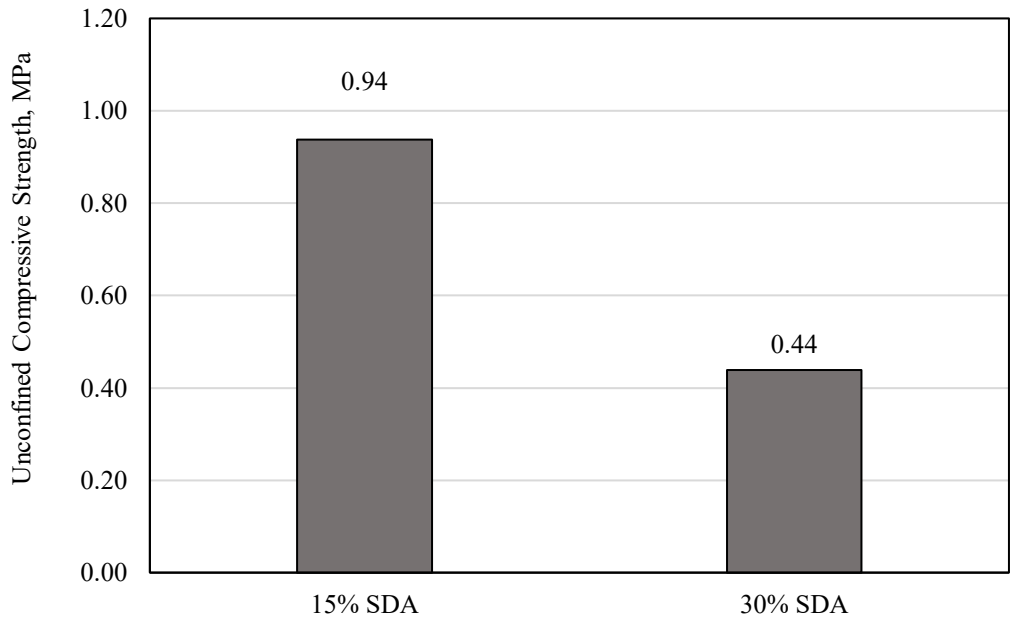


**Figure 4.1:** UCS trial test results for SDA dosage determination

From the obtained results, it was found that between these two compositions, 15% SDA provided the highest strength compared to the 30% SDA. Hence, in later stages of the study SDA was used at a percentage of 0, 5, 10, 15, 20.

### 4.2.2 Strength After 7 Days (Bulk Condition)

The variation of strength at an early age with A:B ratio and SDA percentage is presented in Figure 4.2. The figure depicts that for SDA content 0% and 5%, maximum strength is obtained at A:B ratio of 0.3. For 10% SDA content the optimum amount of alkaline solution is found 0.4, and for 15% and 20% the optimum amount is 0.5. Among all the compositions, samples with SDA 20% and A:B ratio of 0.5 exhibited the highest strength,

around 0.82 MPa. On the contrary, lowest strength was found in samples with 0% SDA content at A:B ratio of 0.5. Hence, it is evident that with the increase in SDA content, the optimum A:B ratio at which maximum strength is obtained also increases. The reason behind this occurrence is that for achieving a higher strength, complete reaction is necessary within the available SDA and alkaline solution. In case of 0% SDA content at A:B ratio of 0.5, since there were no available SDA (which acts as precursor), the alkaline solution present in the matrix may have reacted with the soil slightly or may not have reacted at all. In this situation, when alkaline solution is present in a relatively greater amount (comparing between A:B ratio 0.3 and 0.5), the strength of sample reduces due to the presence of higher amount of water that comes from the alkali solution. On the contrary, in case of 20% SDA content at A:B ratio of 0.5, since there is sufficient amount of SDA and alkaline solution present in the matrix to complete the reaction, higher strength is achieved at this composition. In this situation, when alkaline solution is present in a relatively lower amount (comparing between A:B ratio 0.3 and 0.5), the strength of sample reduces due to insufficient amount of alkali solution which is needed for completing the reaction. The stress-strain response of the samples obtained from the 7 day bulk UCS test is presented in Figure 4.3.

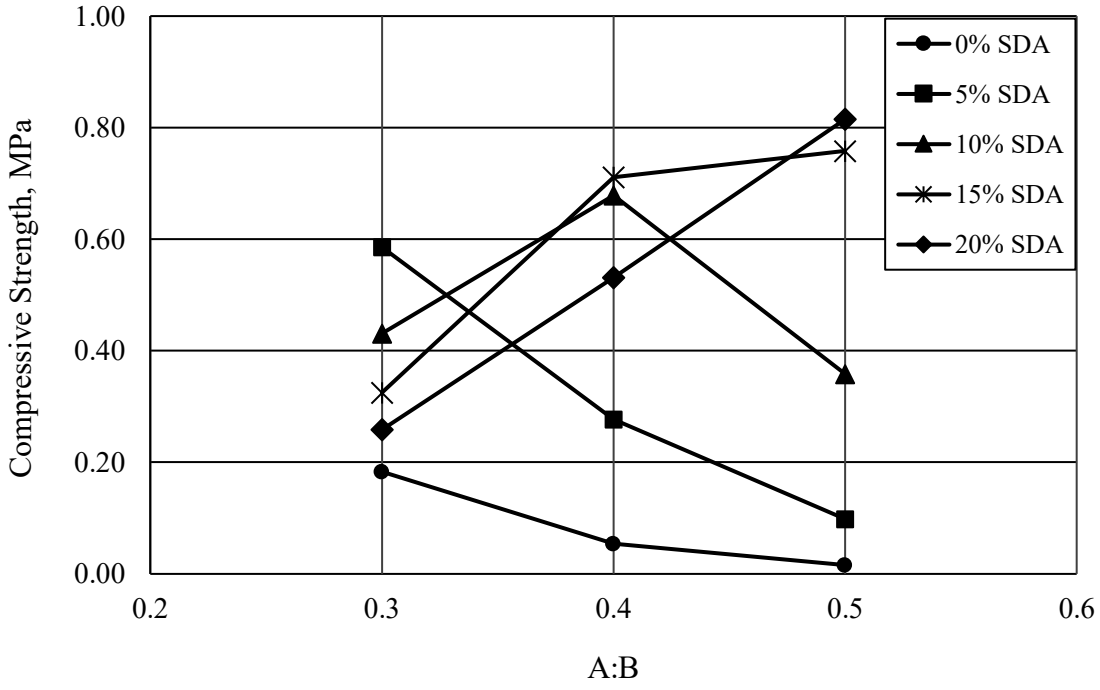


**Figure 4.2:** Relationship between the compressive strength and A:B ratio at different SDA content (7 days)

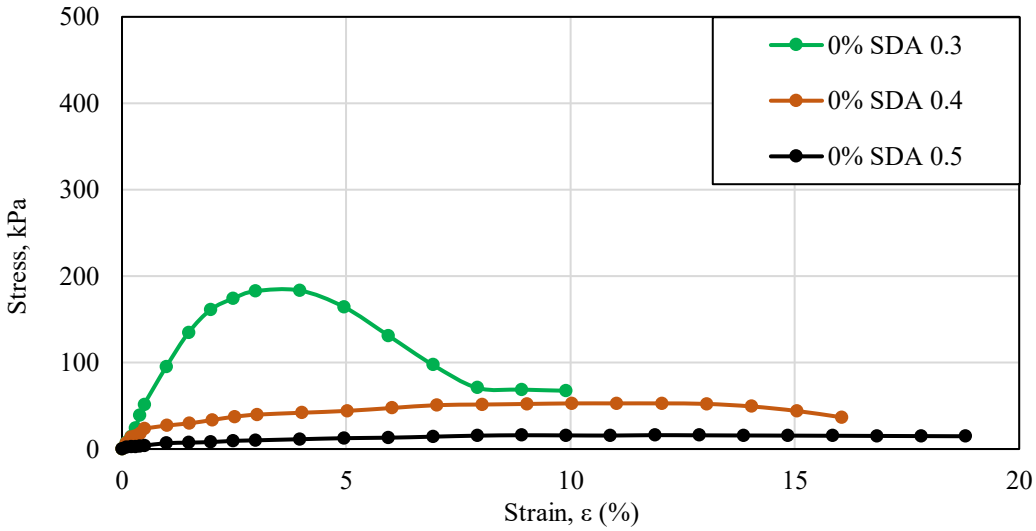
0% SDA 0.3
0% SDA 0.4
0% SDA 0.5
Stress, kPa
Strain, ε (%)
0
100
200
300
400
500
0
5
10
15
20

(a)

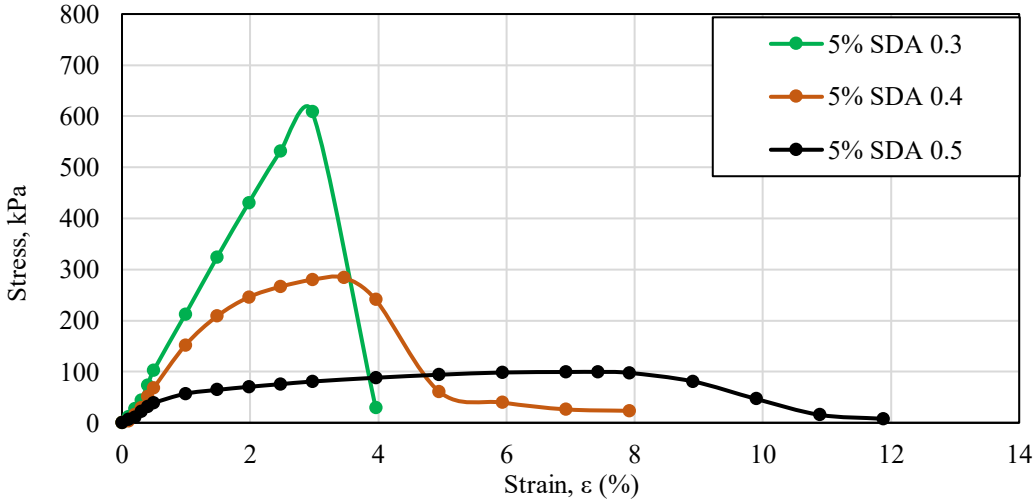
5% SDA 0.3
5% SDA 0.4
5% SDA 0.5
Stress, kPa
Strain, ε (%)
0
100
200
300
400
500
600
700
800
0
2
4
6
8
10
12
14

(b)

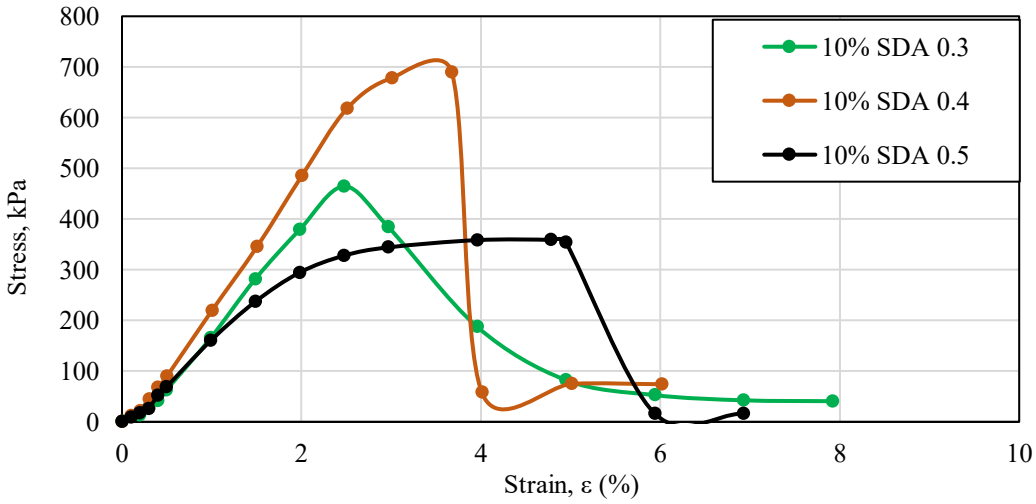
10% SDA 0.3
10% SDA 0.4
10% SDA 0.5
Stress, kPa
Strain, ε (%)
0
100
200
300
400
500
600
700
800
0
2
4
6
8
10

(c)

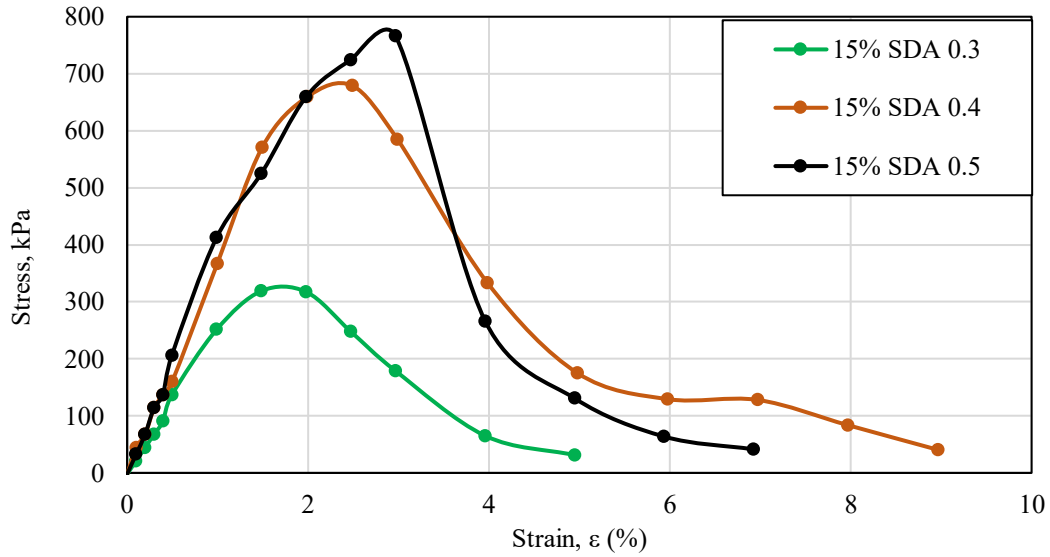


(d)

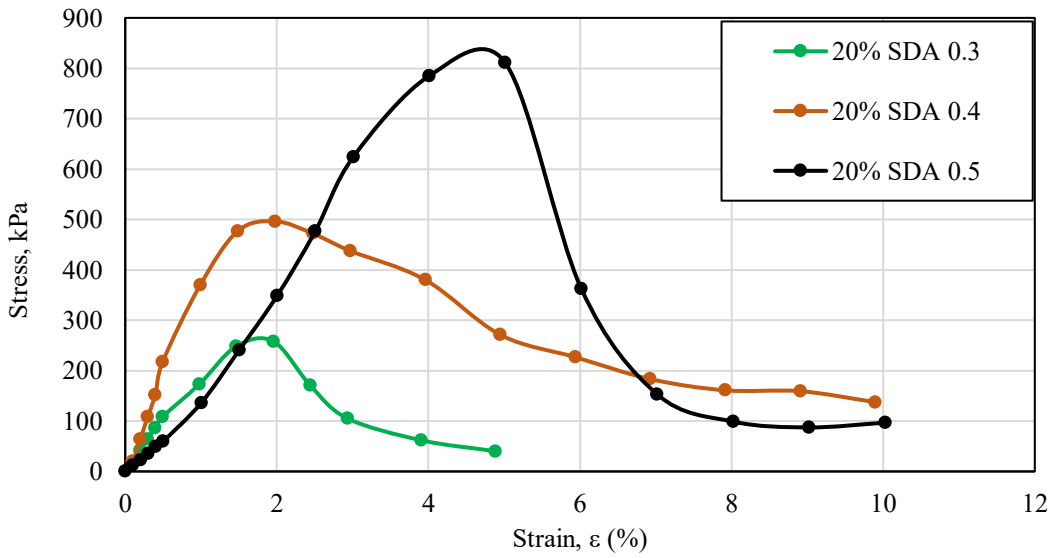


(e)

**Figure 4.3:** Stress-strain response of stabilized specimens at 7 day bulk condition with SDA (a) 0%, (b) 5%, (c) 10%, (d) 15% and (e) 20%

The stress-strain curve depicts the brittle failure nature with the inclusion of SDA. Typical peak strain ranges from 1.48 % to 12.03% with the lowest value corresponding to the most brittle failure (for 15% SDA 0.3) and the highest value corresponding to the most ductile failure (for 0% SDA 0.4). The failure strain ranges from 3.96% to 18.80% although typical maximum failure strain is considered at 15%. Initial Tangent Modulus (ITM), which is the slope of the linear portion of the stress-strain curve has been determined by following the methodology proposed by Tang et al. (2017) using the following equation:

$$E = \frac{\sigma_{1\%} - \sigma_0}{\varepsilon_{1\%} - \varepsilon_0} \quad (4.1)$$

where, E is the Initial Tangent Modulus, $\sigma_{1\%}$ corresponds to the axial stress at 1% axial strain ($\varepsilon_{1\%}$), and $\sigma_{1\%}$ and $\varepsilon_{1\%}$ are the initial stress and strain respectively. Table 4.1 lists the ITM, peak strain and failure strain of different compositions.

**Table 4.1:** Modulus of Elasticity, Peak and Failure strain of different compositions at 7 day bulk condition

| Sample Composition | Initial Tangent Modulus (ITM), MPa | Peak Strain (%) | Failure Strain (%) |
|---|---|---|---|
| 0% SDA 0.3 | 9.64 | 3.96 | 9.90 |
| 0% SDA 0.4 | 2.71 | 12.03 | 16.04 |
| 0% SDA 0.5 | 0.68 | 11.88 | 18.80 |
| 5% SDA 0.3 | 21.47 | 2.97 | 3.96 |
| 5% SDA 0.4 | 15.35 | 3.46 | 7.92 |
| 5% SDA 0.5 | 5.75 | 7.42 | 11.88 |
| 10% SDA 0.3 | 16.74 | 2.47 | 7.92 |
| 10% SDA 0.4 | 21.90 | 3.68 | 6.02 |
| 10% SDA 0.5 | 16.19 | 4.78 | 6.93 |
| 15% SDA 0.3 | 25.41 | 1.48 | 4.95 |
| 15% SDA 0.4 | 36.81 | 2.49 | 8.96 |
| 15% SDA 0.5 | 41.71 | 2.97 | 6.93 |
| 20% SDA 0.3 | 17.72 | 1.95 | 4.88 |
| 20% SDA 0.4 | 37.39 | 1.98 | 9.90 |
| 20% SDA 0.5 | 13.58 | 5.01 | 10.03 |

### 4.2.3 Strength After 28 Days (Bulk Condition)

The variation of strength with A:B ratio and SDA percentage after 28 days at bulk condition is presented in Figure 4.4. The figure depicts that, the maximum strength is achieved (1.78 MPa) in the samples with SDA 20% and A:B ratio of 0.5 which is consistent with the early (7 day) strength pettern. However, slight variation in strength

pattern with respect to early age was also observed in case of 5% and 10% SDA content at A:B ratio 0.4 and 0.5 which can be attributed to the reaction rate during this extended time period. According to New Zealand Standard (1998) and Indian Standard (1998), the minimum unconfined compressive strength of compressed stabilized earthen block is 1.3 MPa and 1.4 MPa respectively. From the figure it is evident that sample with the compositions – 15% and 20% SDA with A:B ratio 0.4 and 0.5 passes the minimum threshold of strength criteria based on these standards.

The samples casted with only soil at its OMC with the similar compaction energy showed an unconfined comprerssive strength of 0.19 MPa after 28 days of age. All compositions except 0% SDA with A:B 0.4 and 0.5, and 5% SDA with A:B 0.5 showed a higher strength than the strength of this control sample (soil at its OMC). The maximum strength that has been obtained by the composition - SDA 20% with A:B ratio of 0.5 is 1.78 MPa and it is around 800% higher than the unstabilized soil. Hence, the effect of stabilization using SDA based geopolymer is clearly evident from these strength values.

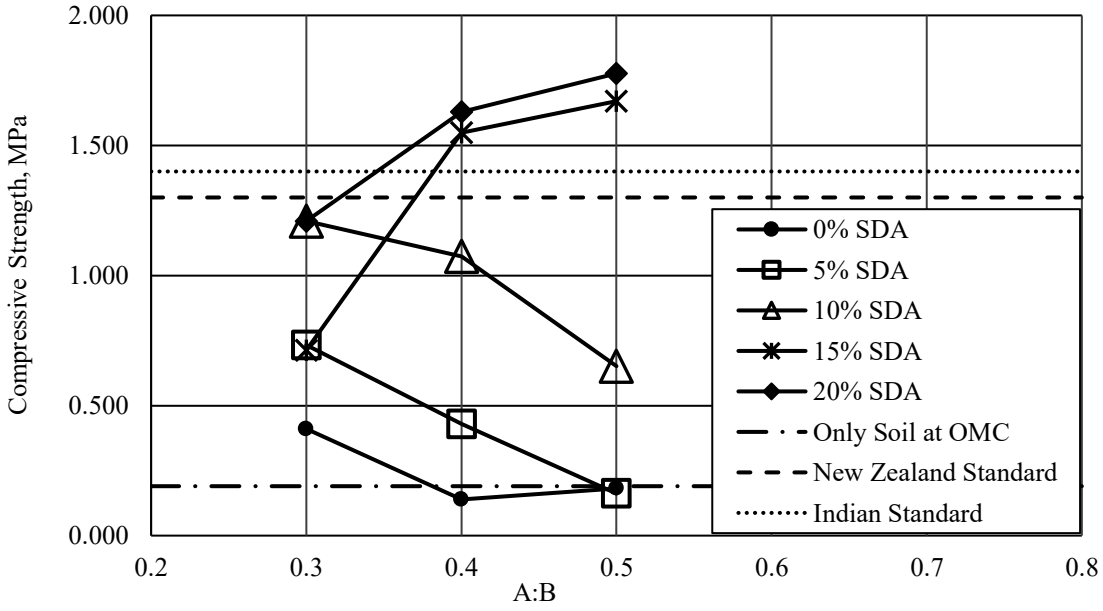


**Figure 4.4:** Relationship between the compressive strength and A:B ratio at different SDA content (28 days bulk condition)

The stress-strain response of samples with different compositions obtained from the 28 day bulk UCS test is presented in Figure 4.5. The stress-strain curve of unstabilized soil sample shows ductile deformation behavior. In absence of SDA when only soil and alkaline solution is present in the matrix, for A:B ratio 0.3 brittle type of failure is

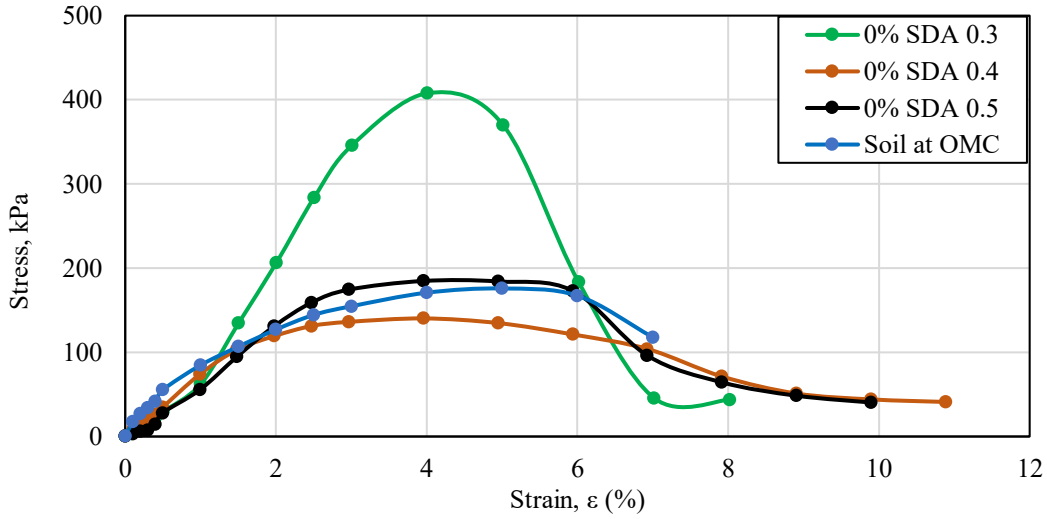
0% SDA 0.3
0% SDA 0.4
0% SDA 0.5
Soil at OMC
Stress, kPa
Strain, ε (%)
0
100
200
300
400
500
0
2
4
6
8
10
12

(a)

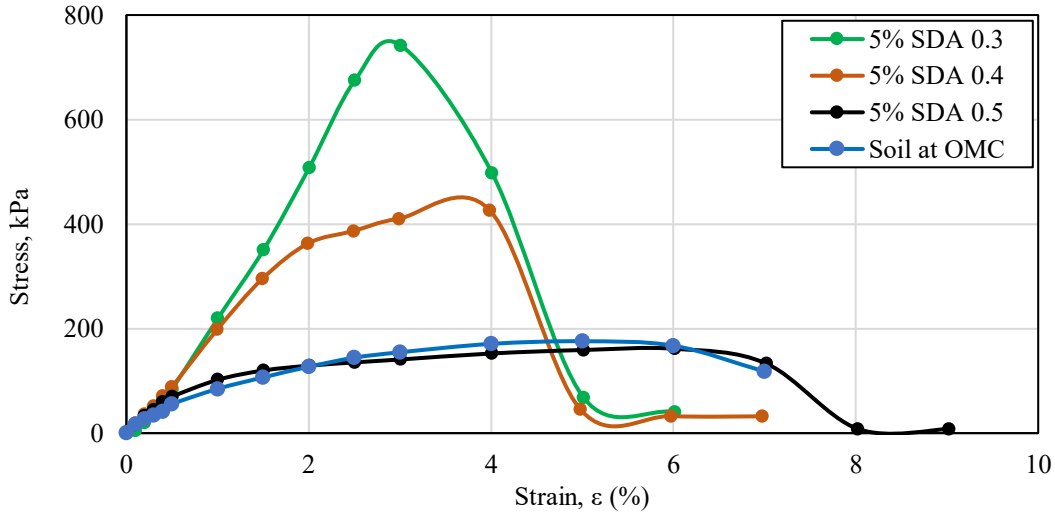
5% SDA 0.3
5% SDA 0.4
5% SDA 0.5
Soil at OMC
Stress, kPa
Strain, ε (%)
0
200
400
600
800
0
2
4
6
8
10

(b)

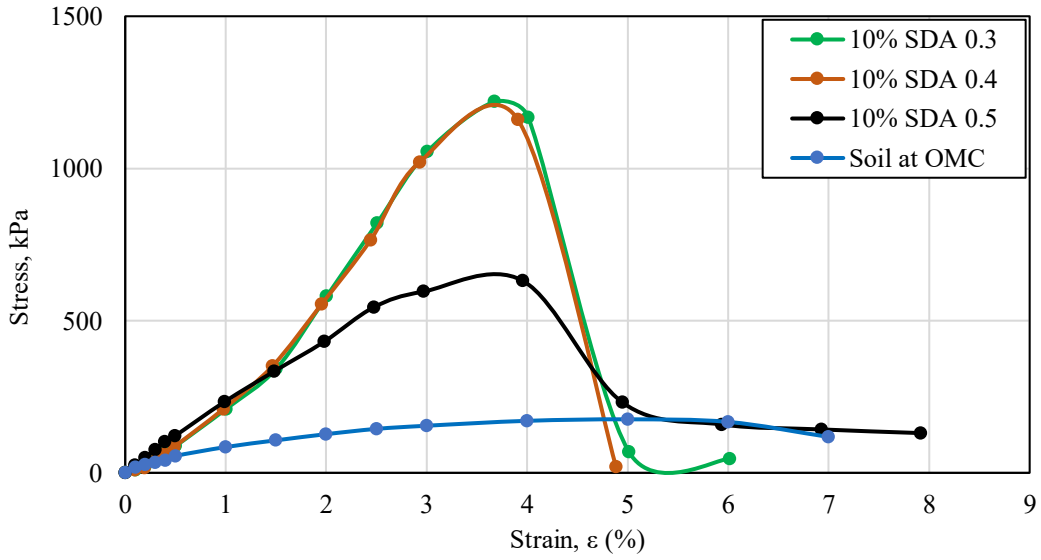
10% SDA 0.3
10% SDA 0.4
10% SDA 0.5
Soil at OMC
Stress, kPa
Strain, ε (%)
0
500
1000
1500
0
1
2
3
4
5
6
7
8
9

(c)

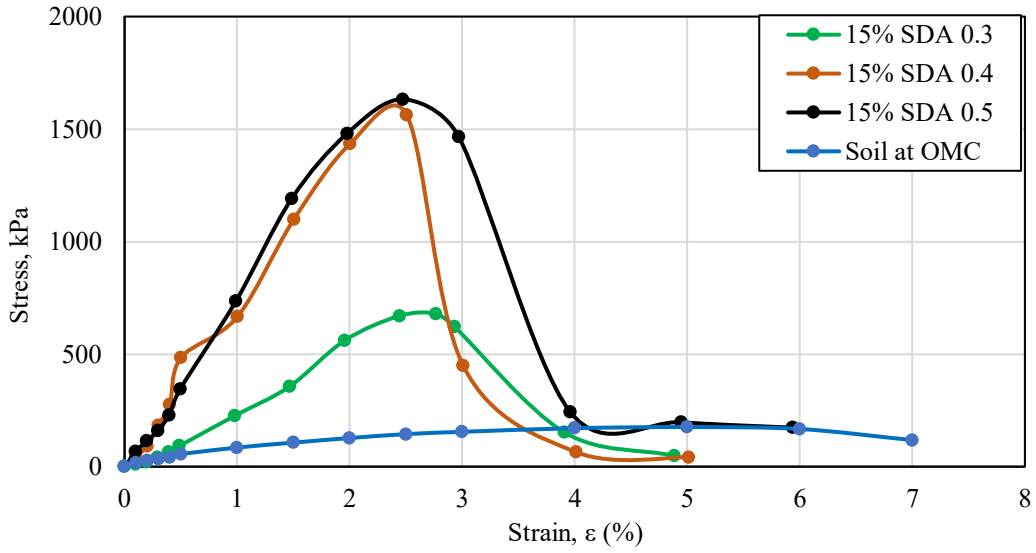


(d)

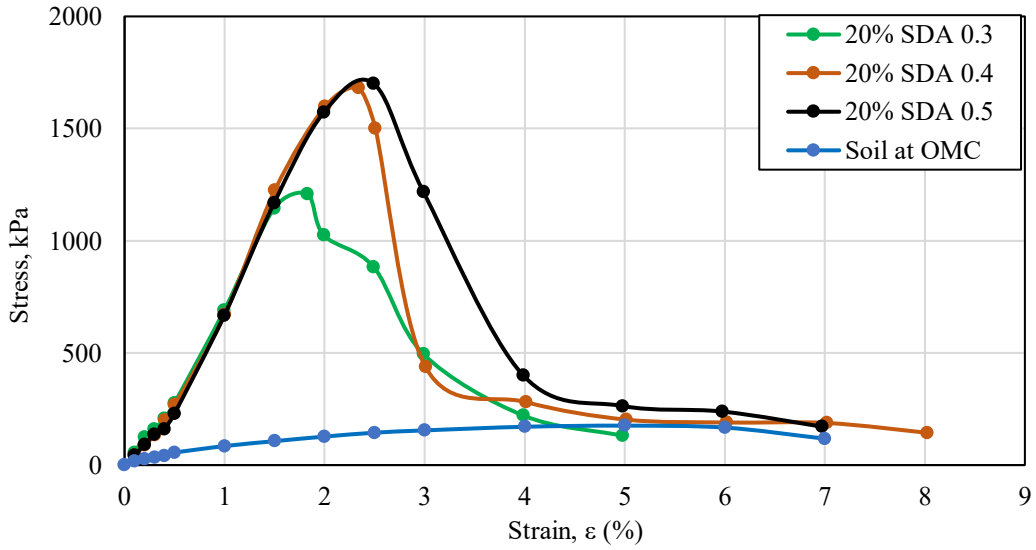


(e)

**Figure 4.5:** Stress-strain response of unstabilized and stabilized specimens at 28 day bulk condition with SDA (a) 0%, (b) 5%, (c) 10%, (d) 15% and (e) 20%

observed. On the contraty, for other A:B ratios (0.4 and 0.5) ductile failure similar to unstabilized soil is observed. However, in all these A:B ratio compostions the slope of the initial curve portion (initial modulus of elasticity) is found almost similar.

In case of 20% SDA content, for all type of A:B ratios, the stress-strain curve shows brittle failure pattern which corroborates enhanced cementation in stabilized soil samples. Point to be noted here that, samples stabilized with 20% SDA also show almost equal slope in the initial curve portion for all types of A:B ratio which is similar to the trend in stabilized samples with alkaline solutions only (0% SDA with A:B ratio 0.3-

0.5). From the figure it is also evident that, with increased amount of SDA content, the modulus of elasticity inceases and brittle failure behavior is observed.

**Table 4.2:** Modulus of Elasticity, Peak and Failure strain of different compositions at 28 day bulk condition

| Sample Composition | Initial Tangent Modulus (ITM), MPa | Peak Strain (%) | Failure Strain (%) |
|---|---|---|---|
| 0% SDA 0.3 | 6.22 | 4.01 | 8.02 |
| 0% SDA 0.4 | 7.47 | 3.96 | 10.89 |
| 0% SDA 0.5 | 5.60 | 3.96 | 9.90 |
| 5% SDA 0.3 | 21.90 | 3.01 | 6.02 |
| 5% SDA 0.4 | 19.91 | 3.98 | 6.97 |
| 5% SDA 0.5 | 10.19 | 6.02 | 9.02 |
| 10% SDA 0.3 | 20.92 | 3.68 | 6.02 |
| 10% SDA 0.4 | 21.48 | 3.91 | 4.88 |
| 10% SDA 0.5 | 23.62 | 3.96 | 7.92 |
| 15% SDA 0.3 | 23.08 | 2.77 | 4.88 |
| 15% SDA 0.4 | 66.45 | 2.51 | 5.01 |
| 15% SDA 0.5 | 74.32 | 2.47 | 5.94 |
| 20% SDA 0.3 | 69.20 | 1.83 | 5.98 |
| 20% SDA 0.4 | 66.97 | 2.34 | 8.02 |
| 20% SDA 0.5 | 66.89 | 2.49 | 6.97 |

Table 4.2 lists the ITM, peak strain and failure strain of different composiitons at 28 day bulk condition. The peak strain ranges from 1.83% to 6.02% corresponding to the brittlemost and ductilemost failure respectively. The observed trend in the ITM of the smples can be predicted as- Highest modulus of elasticity does not necessarily belongs to the composition having the highest compressive strength. The reason lies in the irregularity in the stress strain curve of the expansive soil (Kumar and Singh 2008, Li et al. 2015, Tang et al 2018).

### 4.2.4 Strength After 28 Days (Wet Condition)

The variation of strength with A:B ratio and SDA percentage after 28 days at wet condition is presented in Figure 4.6. The figure depicts that, in the wet condition, the maximum strength is achieved (1.91 MPa) in the samples with SDA 15% and A:B ratio of 0.5. According to Sri Lankan Standard (2009) and Indian Standard (1998), the minimum unconfined compressive strength of compressed stabilized earthen block in wet condition is 1.6 MPa and 0.7 MPa respectively. Since the Sri Lankan Standard has a higher threshold value than the Indian Standard, only the compositions having 15% and 20% SDA with A:B ratio of 0.5 passes this minimum strength criterion. However, considering the Indian Standard, majority of the compositions pass the minimum strength criteria of 0.7 MPa with the exceptions being 0% SDA with all types of A:B ratios, and 5% SDA with A:B ratio of 0.4 and 0.5. In general, samples with higher SDA content showed higher compressive strength in the wet condition.

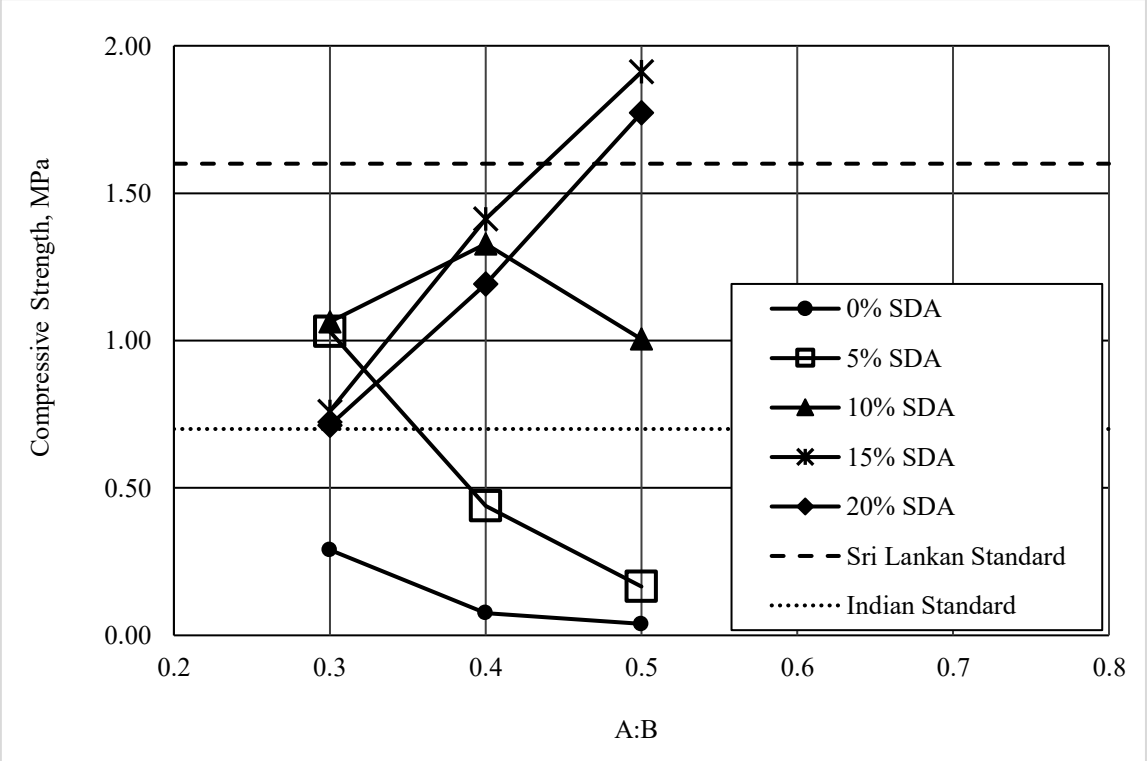


**Figure 4.6:** Relationship between the compressive strength and A:B ratio at different SDA content (28 days wet condition)

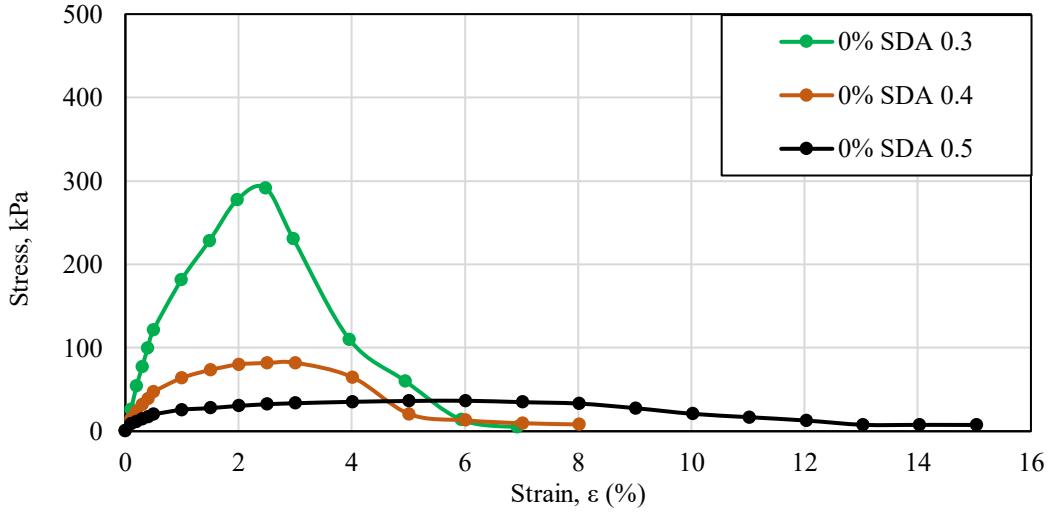
0% SDA 0.3
0% SDA 0.4
0% SDA 0.5
Stress, kPa
Strain, ε (%)
0
100
200
300
400
500
0
2
4
6
8
10
12
14
16

(a)

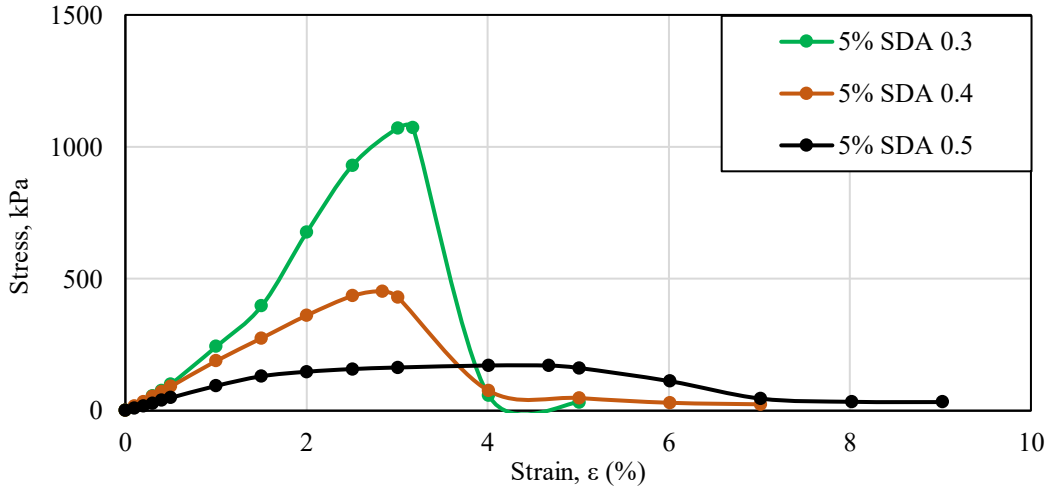
5% SDA 0.3
5% SDA 0.4
5% SDA 0.5
Stress, kPa
Strain, ε (%)
0
500
1000
1500
0
2
4
6
8
10

(b)

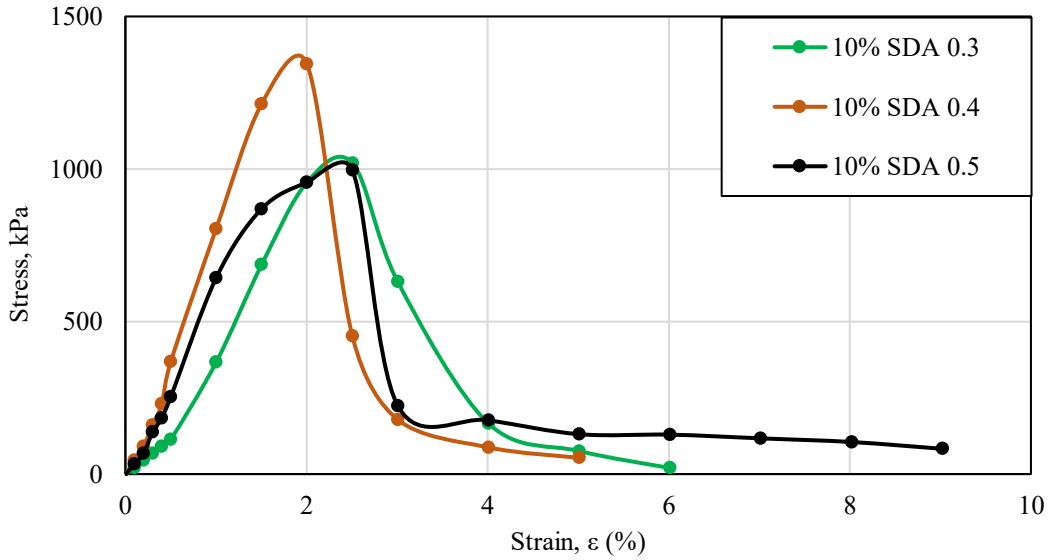
10% SDA 0.3
10% SDA 0.4
10% SDA 0.5
Stress, kPa
Strain, ε (%)
0
500
1000
1500
0
2
4
6
8
10

(c)

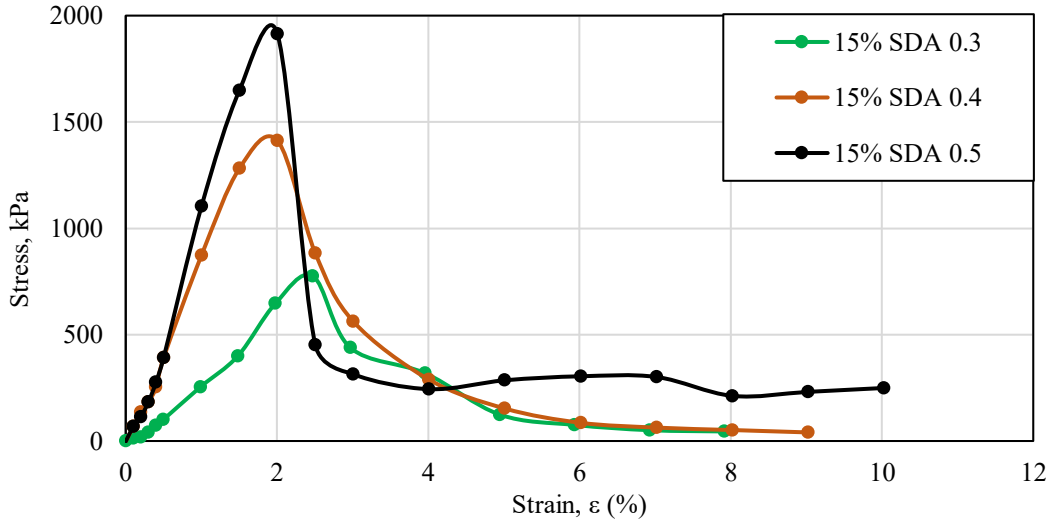


(d)

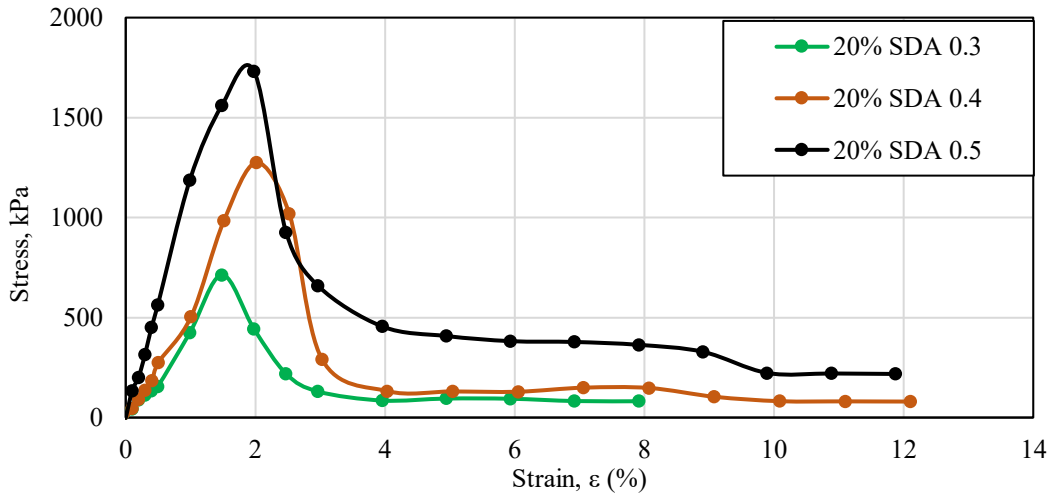


(e)

**Figure 4.7:** Stress-strain response of unstabilized and stabilized specimens at 28 day wet condition with SDA (a) 0%, (b) 5%, (c) 10%, (d) 15% and (e) 20%

Point to be noted here that, the control sample (soil at it's OMC) could not be tested under wet condition since after submersion in water, it completely losses its interparticular cohesion and bonding. On the other hand, samples fabricated with SDA and alkaline solution shows significant compressive strength even after submersion in water. Hence, it is evident that, SDA based geopolymerization can significantly improve the durability characteristics of raw soil.

The stress-strain response of samples with different compositions obtained from the 28 day wet UCS test is presented in Figure 4.7. The stress strain behavior depicts that, even after 24 hour submersion in water, the stabilized soil sample retains most of its

mechanical strength which is evident from the slope of the initial cureve portion, Initial Tangent Modulus (ITM). Table 4.3 lists the ITM, peak strain and failure strain of different composiitons at 28 day wet condition. The peak strain ranges from 1.48% to 6.02% corresponding to the brittlemost and ductilemost failure respectively. It is evident that, even after water submersion, the highest modulus is obtained in samples having maximum amount of SDA.

**Table 4.3:** Modulus of Elasticity, Peak and Failure strain of different compositions at 28 day wet condition

| Sample Composition | Initial Tangent Modulus (ITM), MPa | Peak Strain (%) | Failure Strain (%) |
|---|---|---|---|
| 0% SDA 0.3 | 18.33 | 2.47 | 6.93 |
| 0% SDA 0.4 | 6.38 | 3.01 | 8.02 |
| 0% SDA 0.5 | 2.57 | 6.02 | 15.04 |
| 5% SDA 0.3 | 24.22 | 3.18 | 5.01 |
| 5% SDA 0.4 | 18.80 | 2.84 | 7.02 |
| 5% SDA 0.5 | 9.38 | 4.01 | 9.02 |
| 10% SDA 0.3 | 36.57 | 2.51 | 6.02 |
| 10% SDA 0.4 | 80.24 | 2.01 | 5.01 |
| 10% SDA 0.5 | 64.15 | 2.51 | 9.02 |
| 15% SDA 0.3 | 25.76 | 2.47 | 7.92 |
| 15% SDA 0.4 | 87.13 | 2.01 | 9.02 |
| 15% SDA 0.5 | 110.11 | 2.01 | 10.03 |
| 20% SDA 0.3 | 42.90 | 1.48 | 7.92 |
| 20% SDA 0.4 | 50.02 | 2.02 | 12.11 |
| 20% SDA 0.5 | 120.04 | 1.98 | 11.88 |

### 4.2.5 Failure Pattern

Figure 4.8 illustrates common failure pattern associated with different sample composition. For ductile kind of failure most common failure pattern is bulging (i.e., unstabilized soil, 0% SDA at A:B ratio 0.4 and 0.5). On the other hand, for brittle type of failure the observed failure pattern is mostly shear failure and vertical crack (i.e., 20%

SDA at A:B ratio 0.3-0.5 and 0% SDA at A:B ratio 0.3). For other compositions (5%, 10% and 15% SDA content), similar trend was observed which is with the increased amount of SDA content brittleness increased leading to a higher modulus of elasticity and shear failure pattern.

(a) Bulging Failure

(b) Shear Failure

(c) Bulging, Shear Failure

(d) Bulging Failure

(e) Shear, Vertical Crack

(f) Shear Failure

(g) Shear, Vertical Crack

**Figure 4.8:** Common failure pattern of specimens (a) Only soil at OMC, (b-d) 0% SDA at A:B ratio 0.3, 0.4, 0.5, and (e-g) 20% SDA at A:B ratio 0.3, 0.4, 0.5

### 4.2.6 Strength Comparison Between 7 days and 28 days (Bulk Condition)

Early strength gaining is an important factor in the strength characteristics of CSEBs. Figure 4.9 depicts a relationship between 7 day and 28 day strength where 7 day strength has been expressed as a percentage of 28 day strength.

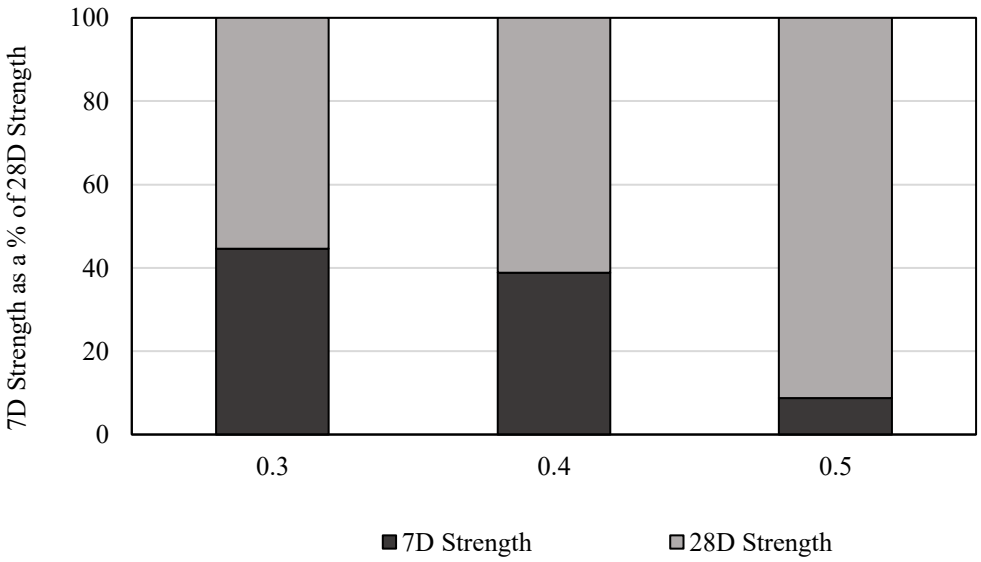


(a)

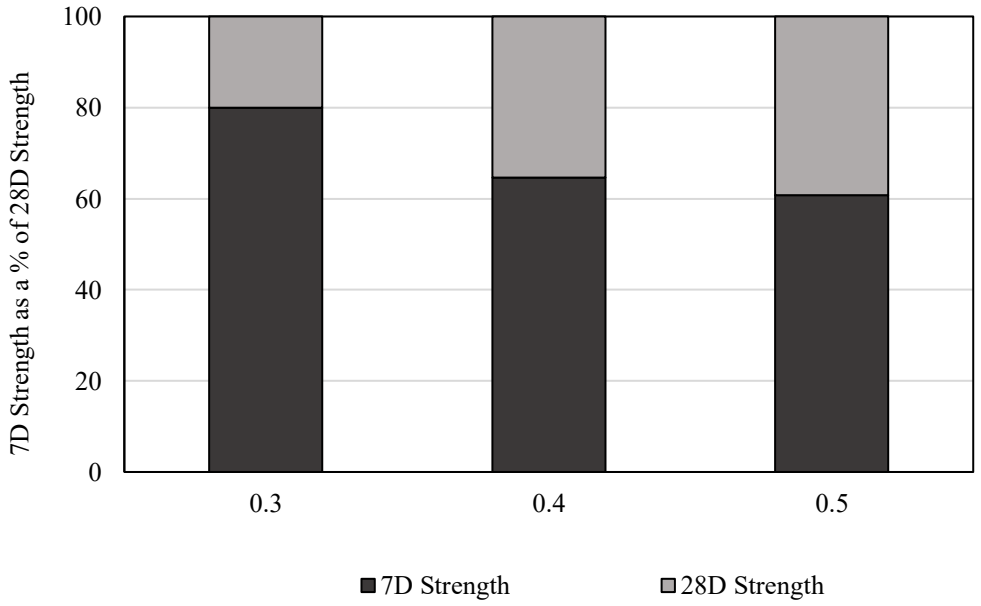


(b)

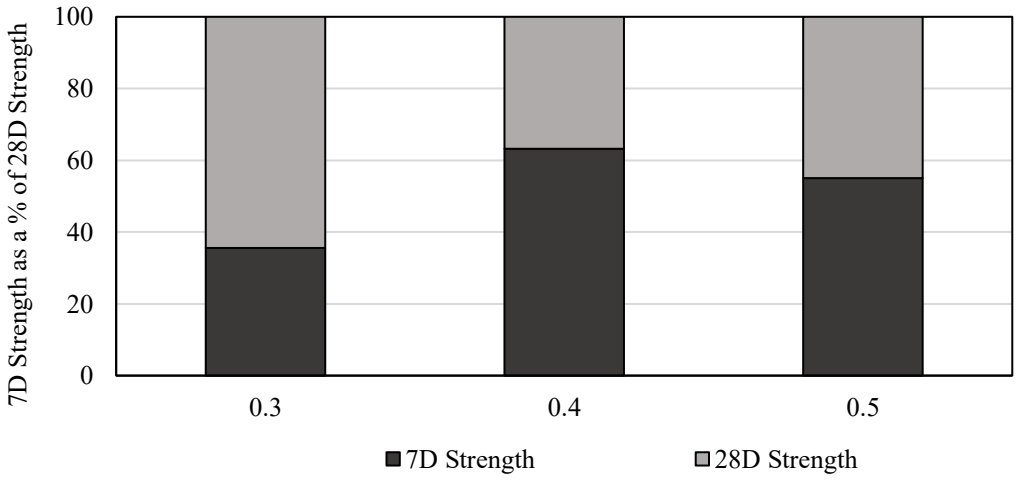


(c)

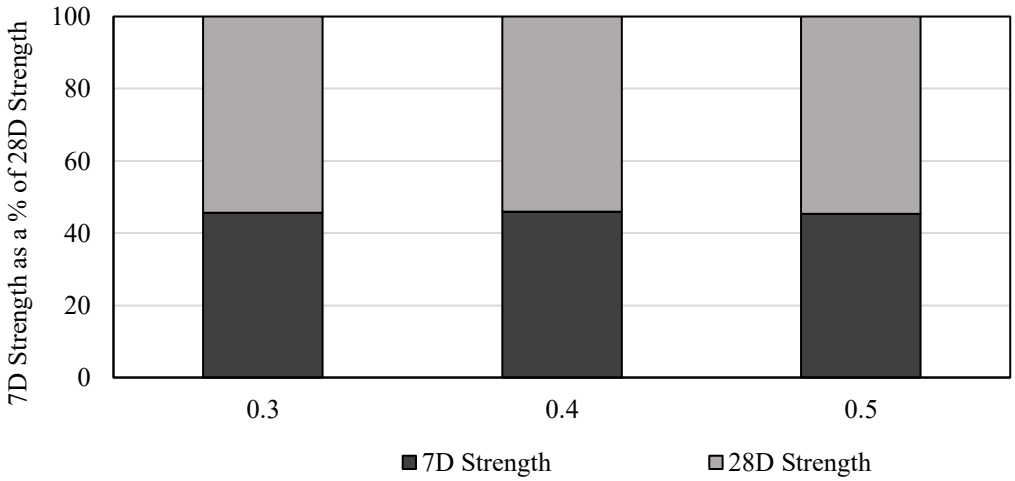


(d)

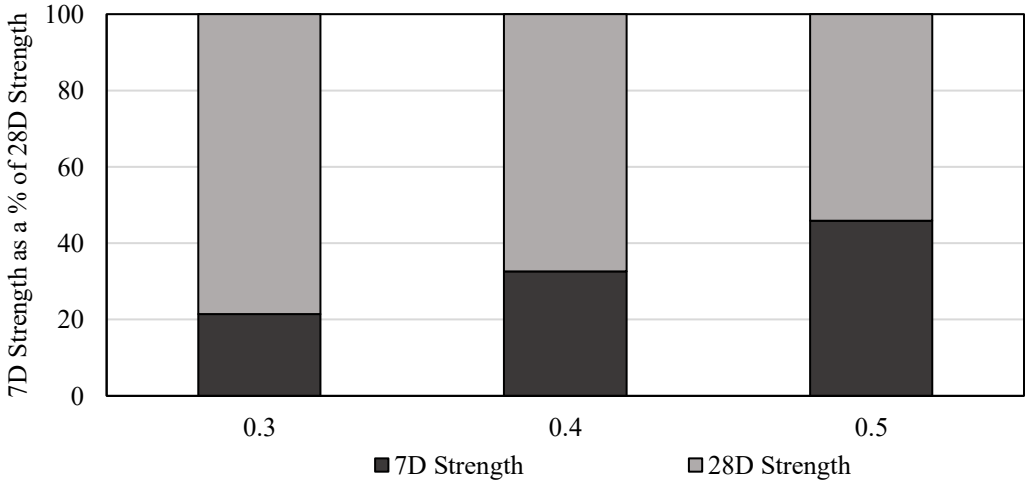


(e)

**Figure 4.9:** Relationship between 7D and 28D compressive strength at different A:B ratio and SDA- (a) 0% SDA, (b) 5% SDA, (c) 10% SDA, (d) 15% SDA, (e) 20% SDA

From the figure it is evident that, maximum early strength development is observed in samples with 5% SDA followed by 10%, 15% and 20% consequtively. This trend supports the fact that with smaller amount of SDA (precursor), majority part of the reaction is completed within this early age. On the contrary, availability of higher amount of SDA in the matrix promotes long term reaction and strength development at later ages as confirmed by various researchers (Cheah et al 2015, Cheah et al 2017, Alabduljabbar et al. 2020, Arunkumar et al. 2021) .

Curing condition and temperature plays an important role in the strength development of SDA based geopolymer (Tchakouté et al. 2017, Duan et al. 2016, Rajamma et al. 2012). In this study, the focus was given to the fabrication of green CSEBs which requires a minimum amount of energy for manufacturing. Hence, the samples were cured at room temperature without applying additional heat. As a result, on an agerage 40% early strength gaining has been observed in samples with different mix composition. Application of heat may increase this amount significantly (Davidovits 2002, Ojo et al. 2018).

Considering the effect of A:B ratio in the early strength development, it can be observed that early strength gain has a direct correlation with optimum amount of A:B ratio for a particular amount of SDA content present in the matrix. Previously (refer to article 4.2.2) it was found that for SDA content 0%, 5%, 10%, 15% and 20% the optimum A:B ratio at which maximum strength is found are 0.3, 0.3, 0.4, 0.5 and 0.5 respectively. A similar trend has been observed while compaing 7D and 28D strength. For SDA content 0% and 5%, maximum early strength with respect to 28D strength is achieved with A:B ratio 0.3 which is about 44% and 80% respectively. Moreover, for SDA content 10%, 7D strength is about 63% of 28D strength at A:B ratio 0.4. As for 15% and 20% SDA content, highest early strength gain is observed at A:B ratio 0.5 which is approximately 45% in both SDA content.

### 4.2.7 Strength Comparison Between 28 days Bulk and 28 days Wet Condition

Wet compressive strength is an indicator of durability characteristics of CSEBs. Figure 4.10 illustrates a comparison between 28 day bulk and wet strength at different SDA content. From the illustration it can be seen that, at 0% SDA content, for all A:B ratios wet compressive strength is lower than bulk compressive strength. However, for other SDA content (5%, 10%, 15% and 20%), at optimum A:B ratio for that particular

composition, wet compressive strength is found to be greater than bulk compressive strength. This signifies that, moist curing may facilitate the strength development in these particular SDA based geopolymer compositions.

This strength improvement during water submersion occurs due to hydration reaction which is facilitated with the presence of Ca ion species. Unlike geopolymerization that requires minimum amount of water for the polymerization process, hydration reation mainly takes part in the presence of water. In the present study, samples were cured at ambient temperature and moisture exchange was minimized by keeping the samples within zip lock bags. During this time, polymerization process was active.

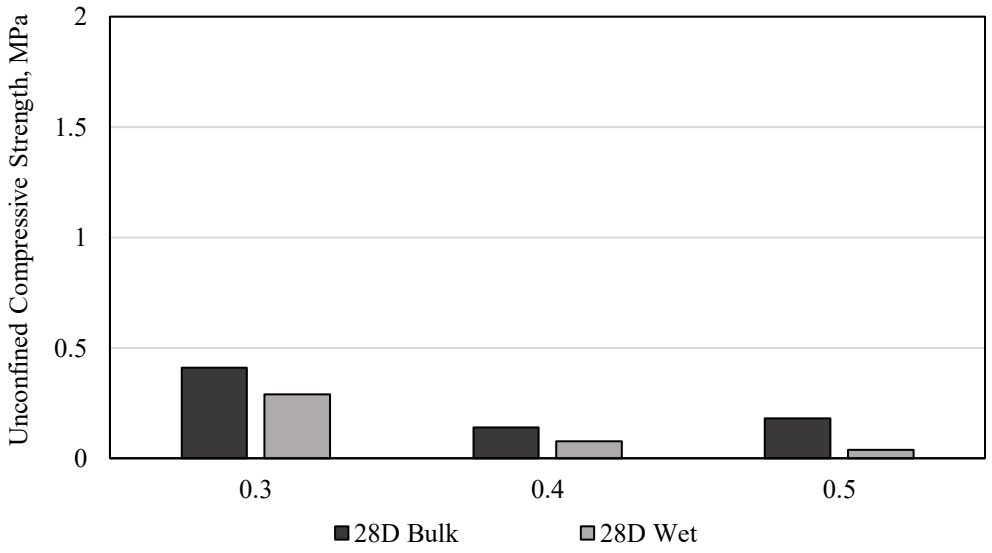


(a)

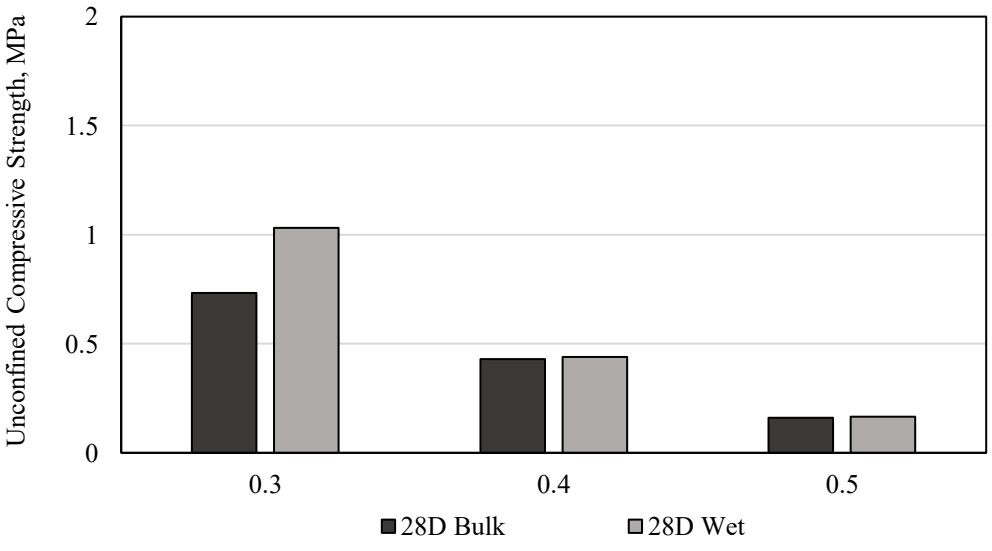


(b)

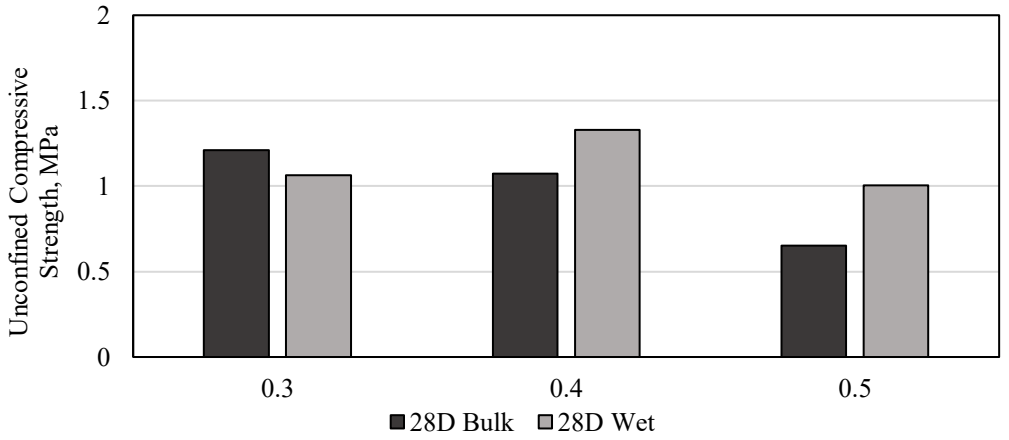


(c)

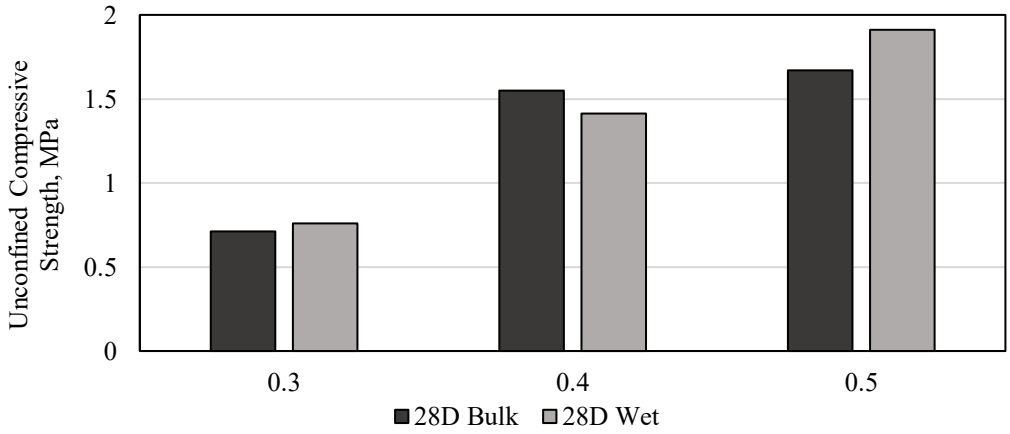


(d)

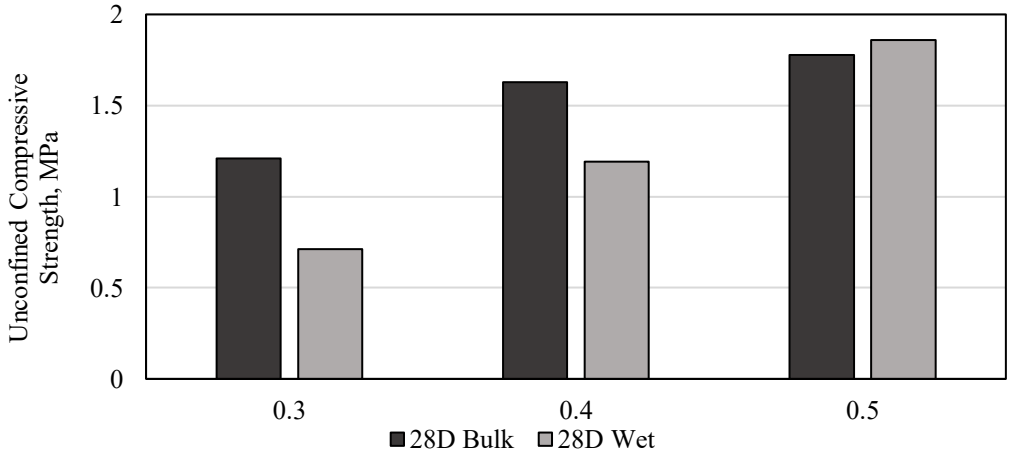


(e)

**Figure 4.10:** Comparison between 28D bulk and wet compressive strength at different A:B ratio and SDA content- (a) 0% SDA, (b) 5% SDA, (c) 10% SDA, (d) 15% SDA, (e) 20% SDA

When the samples were submerged in water, hydration reaction (due to the presence of sawdust ash which is rich in Ca) was stimulated due to abundance of water and $OH^-$ from added alkali. This initiation of hydration reaction and pozzolanic reaction resulted in improved mechanical strength. Hence, the phenomenon of strength improvement was observed for the samples having sawdust ash but this behavior could not found in samples having soil only.

### 4.2.8 Relationship Between Bulk Density and A:B ratio at Different SDA Content

Figure 4.11 (a) and (b) illustrate the relationship between bulk density and A:B ratio at different SDA content. From previous discussions, for SDA content 0% and 5% maximum UCS was found at A:B ratio 0.3. From Figure 4.11 (a) it is also evident that at this A:B ratio the samples had the highest density supporting the fact that higher strength is obtained at higher density. However, from Figure 4.11 (b) it can be seen that in case of 10%, 15% and 20% SDA content, the A:B ratio at which the samples achieved maximum strength did not have the highest density, contradicting the previous fact.

Hence, it can be said that, for higher amount of SDA content, the actual strength in the matrix comes from chemical changes in the internal bonding rather than physical changes. Thus in that case, effect of compaction energy in providing a densified structure will be negligible.

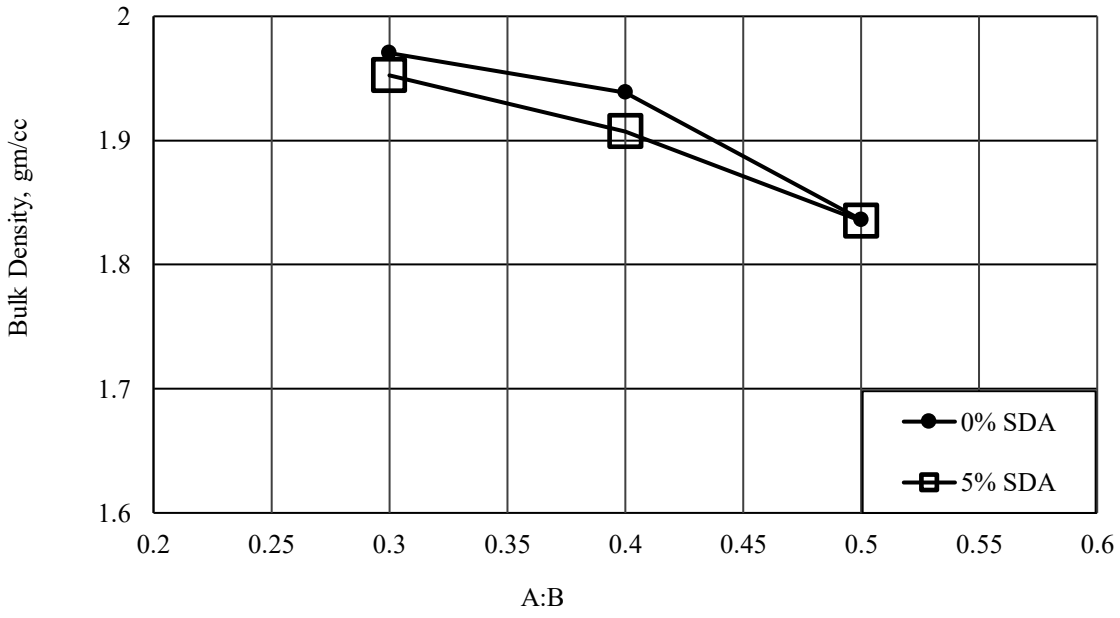


(a)

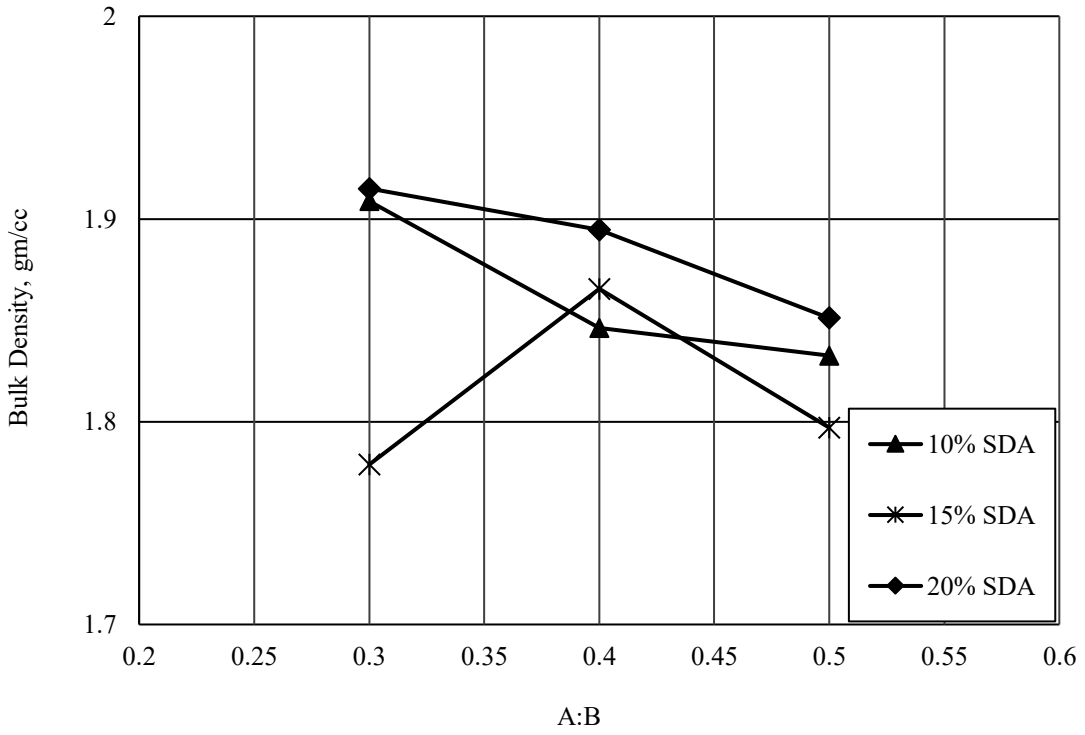


(b)

**Figure 4.11:** Variation of bulk density with A:B ratio (a) at 0% and 5% SDA and (b) at 10%, 15% and 20% SDA

### 4.2.9 28 Day Normalized Strength at Bulk Condition with respect to Bulk Density

The current study observed the fact that by increasing the SDA content, the effect of mechanical energy in densifying the matrix can be reduced. Since the previously reported 28 day strength in bulk condition was reported (refer to article 4.2.3) without considering the density effect (density variation in different compositions), in this section a normalized 28 day strength curve with respect to bulk density has been presented in Figure 4.12. The figure shows that even if we consider the density effect, the strength gaining pattern is similar to the unaltered curve, i.e., all compositions except 0% SDA with A:B ratio 0.4 and 0.5 have higher strength than unstabilized soil. Hence, the effect of density variation in strength can be considered negligible here.

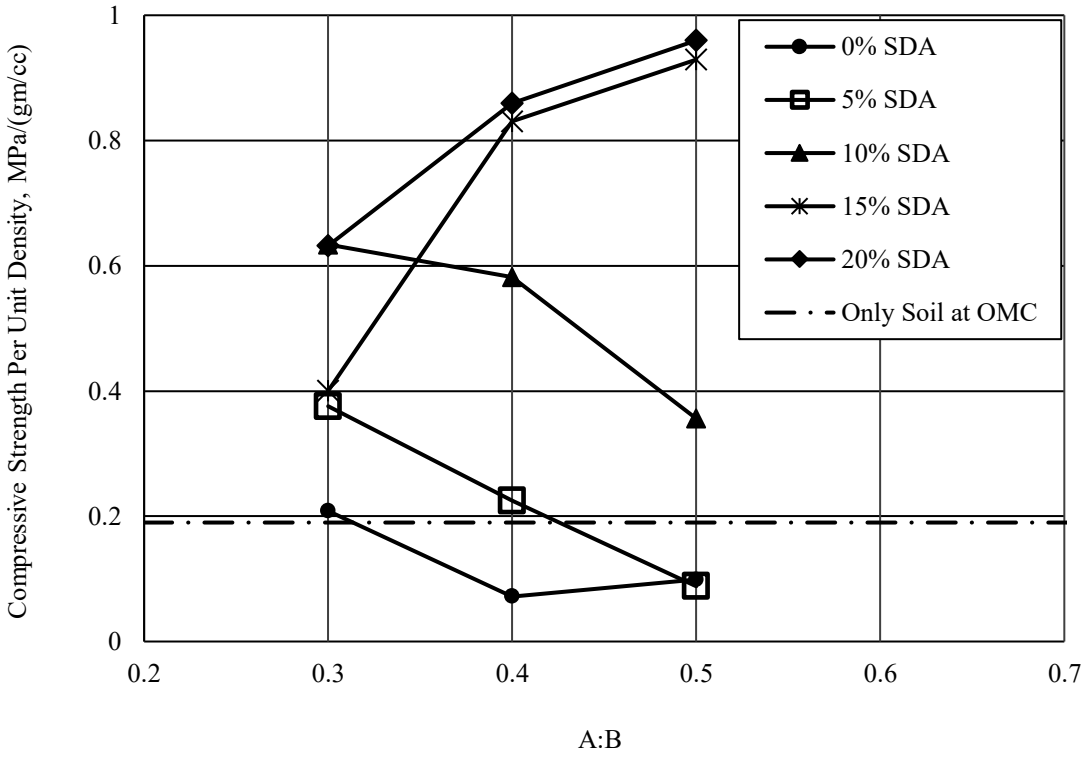


**Figure 4.12:** 28 day normalized strength curve with respect to bulk density

### 4.3 Flexure Strength

Flexure strength test was performed on samples with the compositions- soil at OMC and SDA content 0%, 5%, 10%, 15% and 20% with a A:B ratio of 0.3, 0.3, 0.4, 0.5 and 0.5 respectively. Figure 4.13 illustrates the flexure strength variation with SDA percentage. The figure depicts that maximum flexure strength is 0.35 MPa which is obtained from 20% SDA content. The unstabilized soil has a flexure strength of 0.121 MPa which is quite low when compared to soil stabilized with SDA and alkaline solution. The only composition that showed a lower flexure strength than the unstabilized soil is the samples with SDA content 0% and A:B ratio 0.3. This strength reduction trend in the absence of SDA content was also observed in case of compressive strength. From the illustration it is also evident that, the addition of SDA content increases the flexure strength significantly with the strength improvement ranging from 38% – 180%. Since the load was applied at the center point along the span, the fracture propagated from the bottom surface toward the top surface along the centre section. Figure 4.14 illustrates a typical failure mode of stabilized soil block.

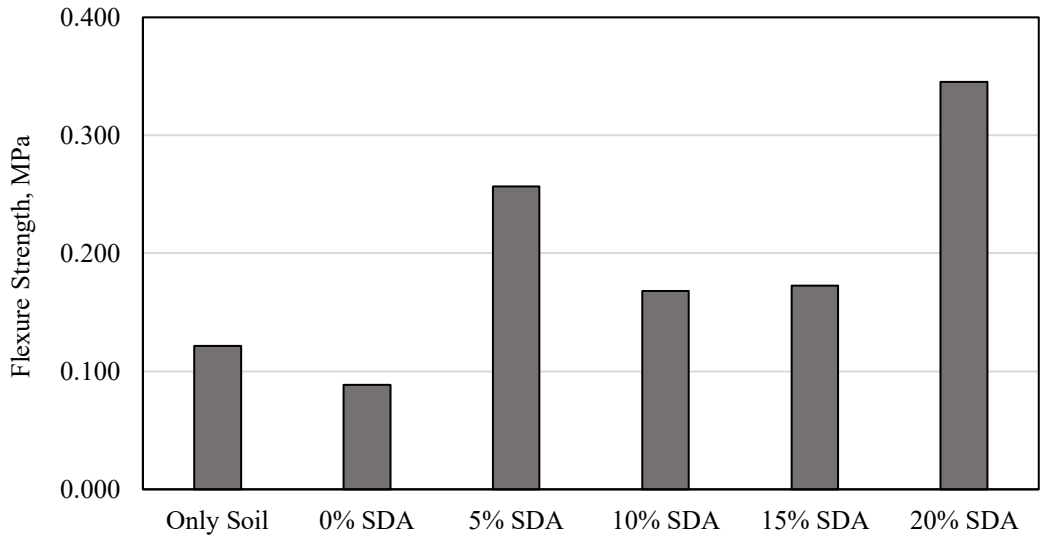


**Figure 4.13:** Variation of flexure strength with SDA percentages

**Figure 4.14:** Typical failure mode in flexure strength test

Different stnadards of earthen block construction has reported the minimum passing strength criteria for fleaxure strength. For example, New Mexico Earthen Building Materials Code (2009) suggested minimum value of flexural strength to be 0.35 MPa, whereas New Zealand Standard (1998) suggested required flexural strength to be > 0.25 MPa. Sri Lankan Standard (2009) and Indian Standard (1998) specified the required flexural strength to be > 0.5 MPa for stabilized earth blocks. Considering this minimum strength criterion only the composition having 20% SDA with A:B ratio 0.5 passes the

minimum flexure strength requirement of New Mexico Earthen Building Materials Code and New Zealand Standard. However, no compositions considered in this study passes the minimum flexure strength requirement of Sri Lankan Standard and Indian Standard. It should be noted here that, flexure strength determination in this study was done using smaller size prismatic samples instead of using full size brick. Hence, effect of scaling factor may to be studied in future to verify these strength values.

### 4.4 Split Tensile Strength

Split tensile strength test was carried out on samples with the compositions- soil at OMC and SDA content 0%, 5%, 10%, 15% and 20% with a A:B ratio of 0.3, 0.3, 0.4, 0.5 and 0.5 respectively. Figure 4.15 illustrates the split tensile strength variation with SDA percentage. The figure depicts that the maximum obtained tensile strength is 0.313 MPa which is obtained from 20% SDA content. The unstabilized soil has a tensile strength of 0.058 MPa which is quite low when compared to soil stabilized with SDA and alkaline solution. The only composition that showed a lower flexure strength than the unstabilized soil is the samples with SDA content 0% and A:B ratio 0.3. The trend of tensile strength improvement with different amount of stabilization is found consistent with the flexure strength. This trend suggests that, the maximum amount of tensile or flexure strength is obtained in samples having the composition - 20% SDA followed by 5%, 15%, 10%, Soil at OMC and 0% SDA. However, this trend is quite different for compressive strength. Hence, it can be presumed that, the strength development with the addition of SDA and alkaline solution varies along the different axes of the sample. Nevertheless, stabilization with SDA improved the tensile strength greatly, ranging from 200-400% improvement.

Figure 4.16 illustrates typical failure pattern of a test specimen. Here, failure initiated at the top surface, and then the crack further propagated towards the bottom. For samples having lower SDA content (i.e. 0% SDA), the fracture was ductile type and the sample shape deformed greatly due to the application of load. On the contrary samples with higher SDA content showed brittle failure with a straight cut fracture without any shape deformation.

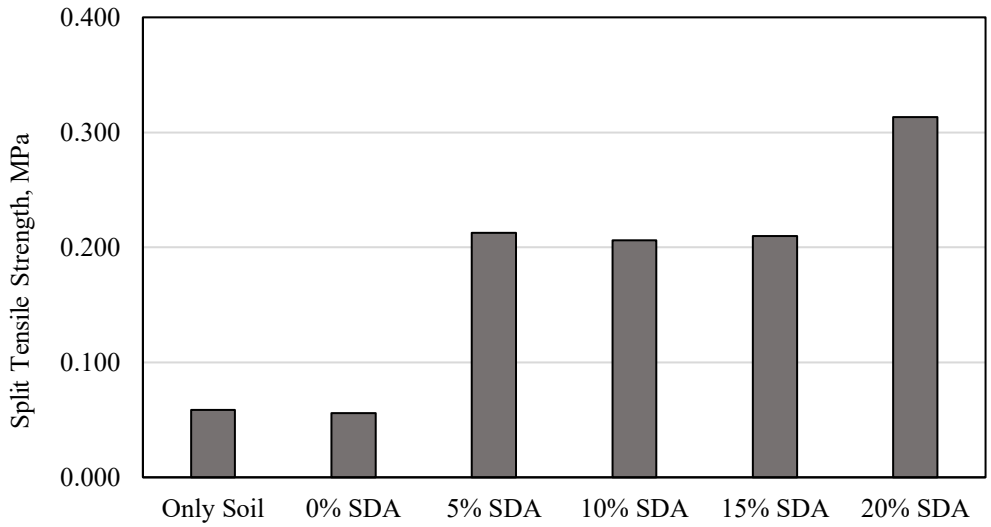


**Figure 4.15:** Variation of split tensile strength with SDA percentages

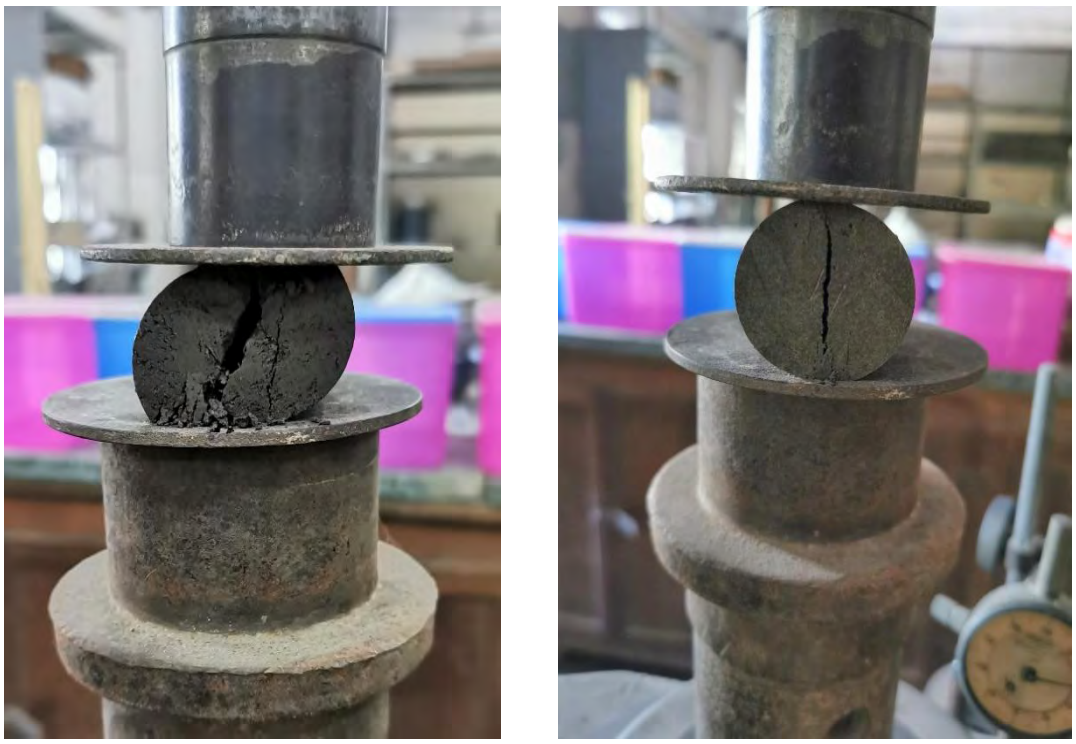

(a) 0% SDA – Ductile Failure (b) 20% SDA – Brittle Failure

**Figure 4.16:** Typical failure mode in split tensile strength test (a) 0% SDA and (b) 20% SDA

### 4.5 Water Absorption

Water absorption in this study was determined from bulk weight instead of dry weight as mentioned earlier (refer to article 3.4.4). Table 4.4 lists the water absorption values obtained in different sample compositions. Here negative sign indicates that due to 24-

hour water submersion, weight loss has occurred instead of weight gaining due to water absorption. This phenomenon is quite expected due to two reasons. First, leaching of SDA and/or Soil has occurred which may have been caused due to unfinished geopolymerization reaction resulting in weight loss. Second, the samples were fabricated with clay soil and SDA which have a very small particle size resulting in smaller void ratios, to begin with. Due to geopolymer formation, these seemingly smaller voids have refined further and formed a denser/compacted structure resulting in lower permeability or porosity. Hence, during submersion, the water did not penetrate into the matrix; even if it has penetrated and increased the weight, the effect has been curtailed by the leaching of SDA and soil due to the incomplete reaction.

**Table 4.4:** Water Absorption percentages in different sample compositions

| Sample Composition | Water Absorption (%) |
|---|---|
| 0% SDA 0.3 | -0.87617 |
| 0% SDA 0.4 | -1.38312 |
| 0% SDA 0.5 | -2.2876 |
| 5% SDA 0.3 | -0.09579 |
| 5% SDA 0.4 | -1.56707 |
| 5% SDA 0.5 | -2.02709 |
| 10% SDA 0.3 | -0.93438 |
| 10% SDA 0.4 | -1.59065 |
| 10% SDA 0.5 | -2.55962 |
| 15% SDA 0.3 | -0.97832 |
| 15% SDA 0.4 | -1.42202 |
| 15% SDA 0.5 | -1.63507 |
| 20% SDA 0.3 | -0.89822 |
| 20% SDA 0.4 | -2.40738 |
| 20% SDA 0.5 | -2.53266 |

From these data it can be depicted that, the maximum amount of leaching/mass loss is observed in samples having an A:B ratio of 0.5 among the three values for a particular SDA content. Moreover, even if the composition provided higher strength (i.e. 15% and 20% SDA at A:B ratio 0.5), mass loss was promiment for these compositions indicating that excess amount of SDA is present in the matrix that has yet to take part in reaction.

## 4.6 Efflorescence

Table 4.5 shows the results of the efflorescence tests performed on the CSEBs. It was observed that for a particular SDA content efflorescence occurred in those samples having the optimum amount of alkaline solution that results in maximum strength (i.e., 0.3 for 5% SDA, 0.4 for 10% SDA, 0.5 for 15% and 20% SDA). It was also observed that, in all the samples that showed efflorescence, the formation of visible salt occurred at the end of 6$^{th}$ day during submersion. To prevent efflorescence formation, researchers have suggested moist curing to prevent salt accumulation on the surface (Simão et al. 2021). Figure 4.17 shows typical samples during the efflorescence test.

**Table 4.5:** Results of the efflorescence test

| Sample Composition | Efflorescence |
|---|---|
| 0% SDA 0.3 | Nil |
| 0% SDA 0.4 | Nil |
| 0% SDA 0.5 | Nil |
| 5% SDA 0.3 | √ |
| 5% SDA 0.4 | Nil |
| 5% SDA 0.5 | Nil |
| 10% SDA 0.3 | √ |
| 10% SDA 0.4 | √ |
| 10% SDA 0.5 | Nil |
| 15% SDA 0.3 | Nil |
| 15% SDA 0.4 | √ |
| 15% SDA 0.5 | √ |
| 20% SDA 0.3 | Nil |
| 20% SDA 0.4 | √ |
| 20% SDA 0.5 | √ |

## 4.7 Microstructural Analysis

The microstructural investigation was carried out from SEM images in order to ascertain microscopic changes in the particle level due to geopolymer formation. The analysis was done for five samples: i) Soil at it's OMC, ii) 15% SDA with A:B 0.3, iii) 15% SDA with

A:B 0.4, iv) 15% SDA with A:B 0.5 and v) 5% SDA with A:B 0.3, to investigate the effect of SDA addition as well as different amount of alkaline solution.

### 4.7.1 Effect of SDA Addition

The effect of SDA addiotion can be investigated by comparing SEM images of 3 samples having the composition: i) Soil at it's OMC, ii) 5% SDA with A:B 0.3 and iii) 15% SDA with A:B 0.3. Figure 4.18 shows the SEM images of these compositions at different magnifications.

The figure illustrates, in the sample that has been fabricated with only soil at its OMC, no C-S-H gel has formed. But with the presence of a small amount SDA (5%), C-S-H, N-A-S-H, and K-A-S-H gel formation has been observed due to pozzolanic reaction among SDA and alkaline solution. However, when the SDA is present in a significant amount (15%), visible geopolymer formation has been observed. It should be noted here that, the C-S-H, N-A-S-H, and K-A-S-H gels have irregular shapes with no definite size. On the contrary, geopolymer has a definite size and shape (small minuscule) which is also visible in Figure 4.18 (c).

(a) No Efflorescence (b) Efflorescence

**Figure 4.17:** Typical samples during efflorescence test (a) 0% SDA A:B ratio 0.4 and (b) 10% SDA A:B ratio 0.4

### 4.7.2 Effect of Different Amounts of Alkaline Solution Addition

The effect of different amount of aklaline solution addition can be investigated by comparing SEM images of three samples having the composition: i) 15% SDA with A:B 0.3, ii) 15% SDA with A:B 0.4 and iii) 15% SDA with A:B 0.5. Figure 4.19 shows the SEM images of these compositions at different magnifications. From the images, no visible nuances can be identified among these three amounts of alkaline solution content. In all these cases, geopolymer formation has been observed but the formation extent at different alkaline solution content could not be quantified by visible means. Hence EDXA (Energy Dispursive X- Ray Analysis) was performe to identify elemental content at different surface points of these samples.

Figure 4.20 shows the elemental composition at the reactive phases of the samples. The elemental composition proves the presence of N-A-S-H and K-A-S-H gel with N-A-S-H being present in the maximum amount since the alkaline solution was Na based. Presence of K can be mainly attributed to sawdust ash which contains high amount of $K_2O$. From the elemental composition, it is evident that for A:B ratio 0.5, maximum mass percentage of Ca ion is present in the matrix, followed by A:B ratio 0.4 and 0.3 respectively. Since the strength of geopolymer structure is derived from the formation of Ca-polyalumino-sialate (Cheah et al. 2015), the presence of higher amount of Ca in samples fabricated with A:B ratio 0.5 provides support to the experimental results obtained from unconfined compressive strength test.

In geopolymer cement and concretes, the geopolymeric species (i.e., poly sialate, poly sialate-silixo) usually have Si/Al atomic ratios ranging from 1 to 3 (Davidovits 2017). For all the compositions corresponding to Figure 4.20, the Si/Al ratio falls within this limit indicating the formation of geopolymeric species. From XRF data, the calculated molar ratio of Si/Al in these three compositions were 7.6, 7.7 and 7.8 for A:B ratio 0.3, 0.4 and 0.5 respectively. Although a high amount of Si was present in the matrix with respect to Al, from EDS results it is evident that the reactive amount of Si was comperatively less than the theoretical (calculated) value which may result in an excess or unreactive silicate portion facilitating pozzolanic reaction and strength improvement in later ages.

(a)

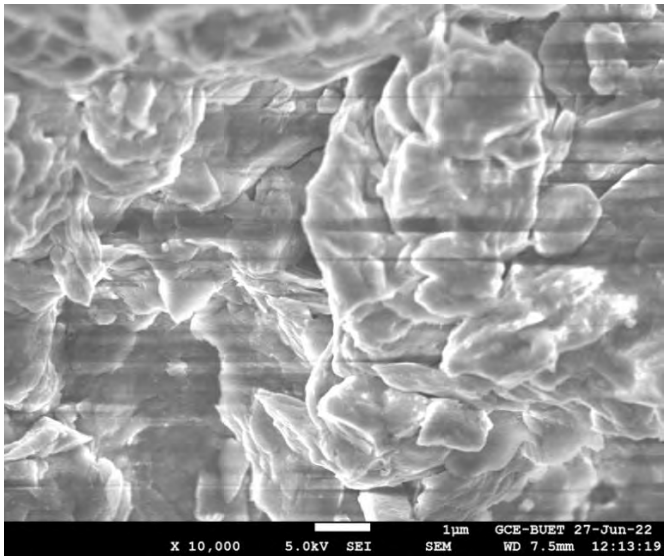


(b)

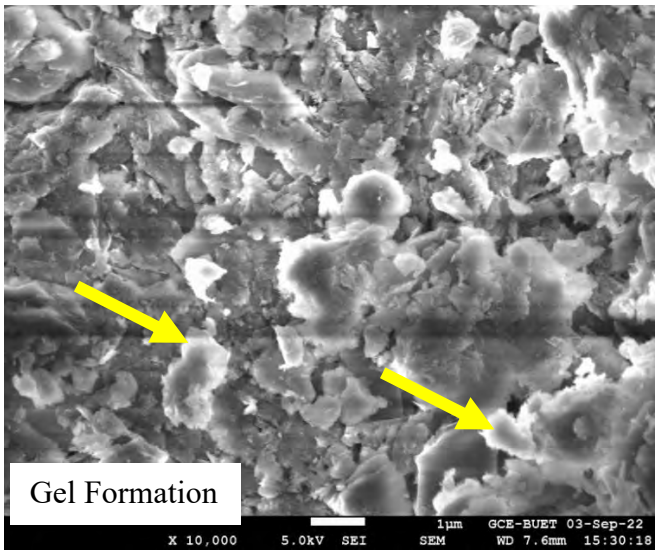


(c)

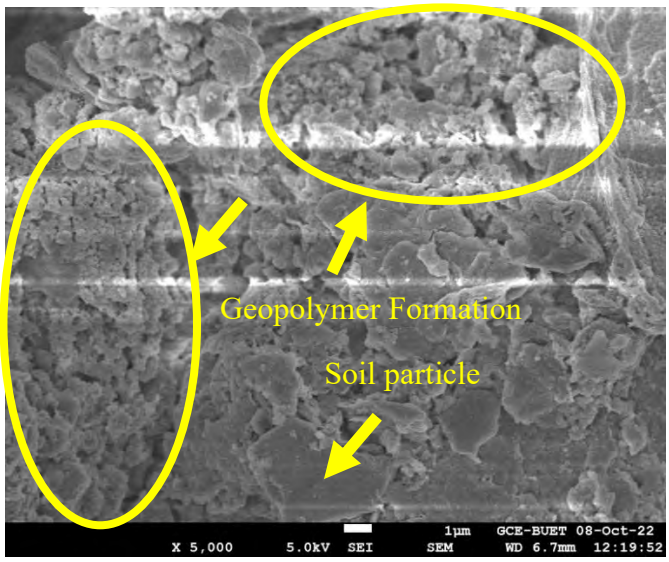


**Figure 4.18:** SEM images of samples (a) soil at OMC, (b) 5% SDA A:B 0.3, (c) 15% SDA A:B 0.3

(a)

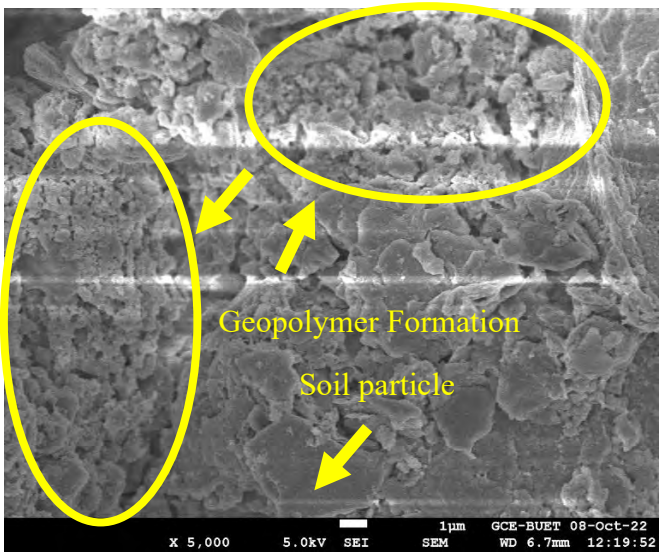


(b)

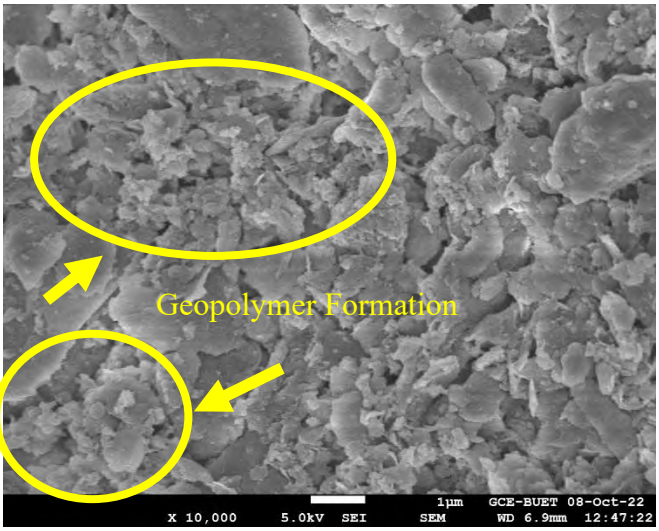


(c)

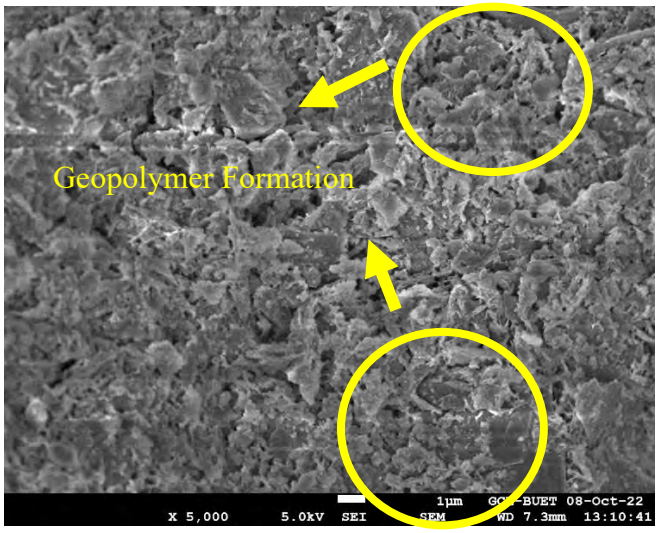


**Figure 4.19:** SEM images of samples (a) 15% SDA A:B 0.3, (b) 15% SDA A:B 0.4, (c) 15% SDA A:B 0.5

(a)

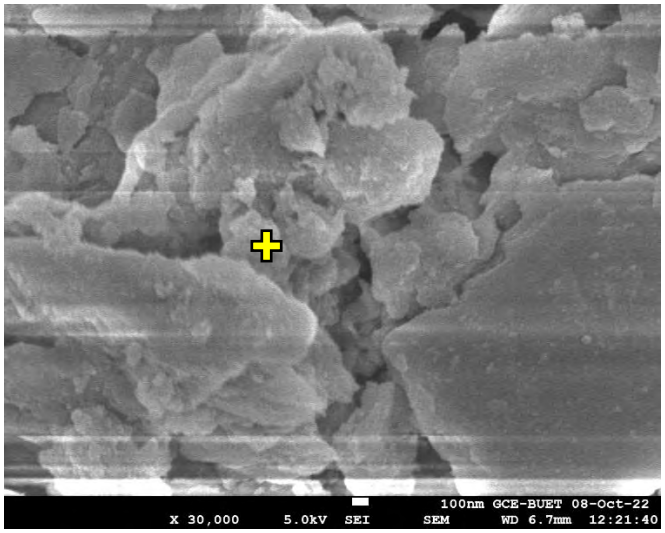


Na = 3.74

K = 3.21

Ca = 1.07

Si = 19.12

Al = 6.10

Si/Al = 3.13

*values are in mass %

(b)

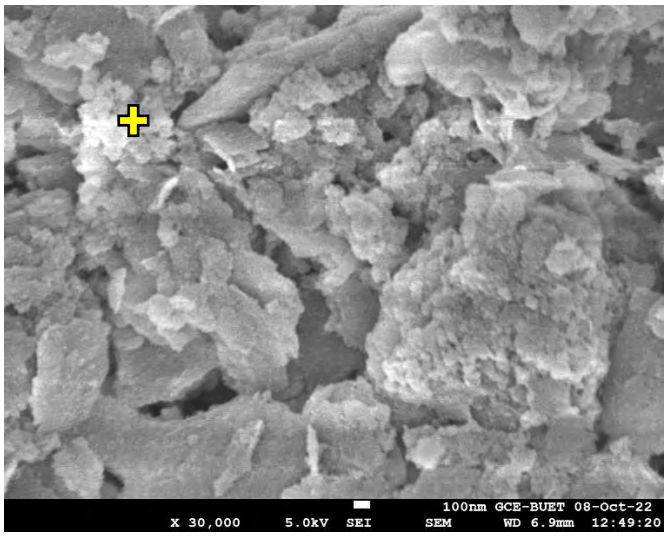


Na = 7.88

K =2.12

Ca = 6.17

Si = 15.63

Al = 4.90

Si/Al = 3.19

*values are in mass %

(c)

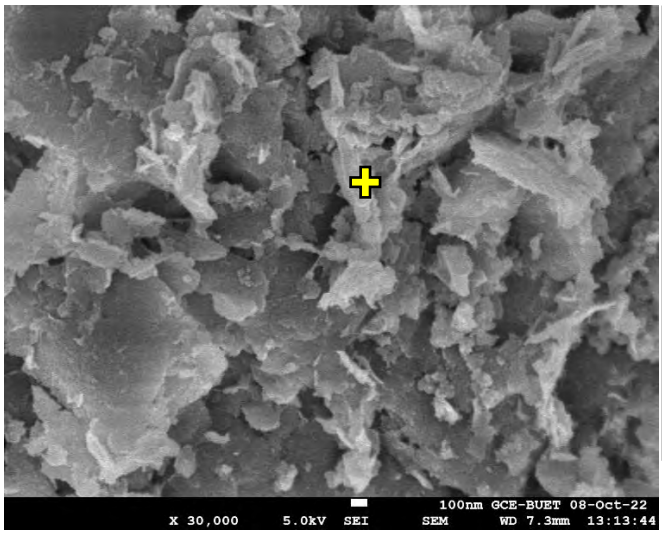


Na = 6.40

K = 3.88

Ca = 6.50

Si = 19.09

Al = 8.15

Si/Al = 2.34

*values are in mass %

**Figure 4.20:** EDX analysis of samples (a) 15% SDA A:B 0.3, (b) 15% SDA A:B 0.4, (c) 15% SDA A:B 0.5

## 4.8 Fourier Transform Infrared Spectroscopy

The FTIR spectroscopy was carried out in order to investigate the prersence of different functional groups present in the geopolymer matrix. The analysis was done for five samples: i) Soil at it's OMC, ii) 5% SDA with A:B 0.3 and iii) 15% SDA with A:B 0.3, to investigate the effect of SDA addition. Figure 4.21 shows the FTIR spectroscopy of these compositions.

The strong band in the IR spectra from 950-1250 $cm^{-1}$ refers to the presence of asymmetric stretching of (Si-O-Si and Al-O-Si) which is also indicative of geopolymerization as suggested by various researchers (Ghosh 1978, Lee and Deventer 2003). From Figure 4.21, it can be observed that, in all these samples highest peak is detected within this range though there is a significant difference in the width of these peaks among these 3 samples. For the sample having only soil, the peak band is comperatively broad. With the increase in SDA content, the peak band became narrower from 5% to 15%. Bands at 471 and 468 $cm^{-1}$ is attributed to Si–O–Si inplane bending vibration in Figure 4.21 (b) and (c). The band located at 1620 – 1683 $cm^{-1}$ range in the Figure 4.21 is related to the bending vibration of H-O-H (Ye et al. 2014). It is evident from the figure that, the intensity of this band decreases from Figure 4.21 (a) to Figure 4.21 (c) indicating the amount of free water present in the matrix is also decreasing. The band at wavenumber 3620 $cm^{-1}$ indicates the O–H stretching vibration. It is noticeable that the absorption peak of O–H stretching vibration flats gradually and steadily and vanishes almost with the increased SDA and geopolymerization.

## 4.9 Cost Comparison

A cost comparison was made among the produced geopolymer and traditional stabilizers - cement and lime. Test results from Mahedi et al. (2020) was incorporated here and used as a basis for comparison. Mahedi et al. (2020) evaluated and compared the performance of cement, lime and fly ash in expansive soil stabilization. They used three different type of expansive soil which were designated as Soil L, Soil S and Soil $L_s$ based on the sample location. Among these three type of soil, properties of Soil S are the closest to the soil properties of current study compared to the other two soil types and thus was used here for cost comparison. However, it should be noted that the amount of clay fraction and plasticity behavior is different in the two soils from the current study and the study by

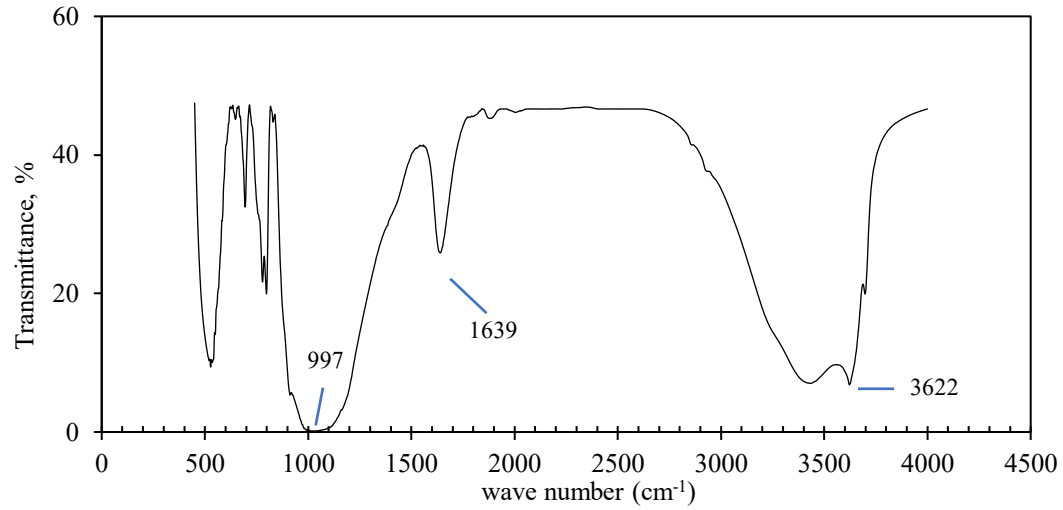


(a)

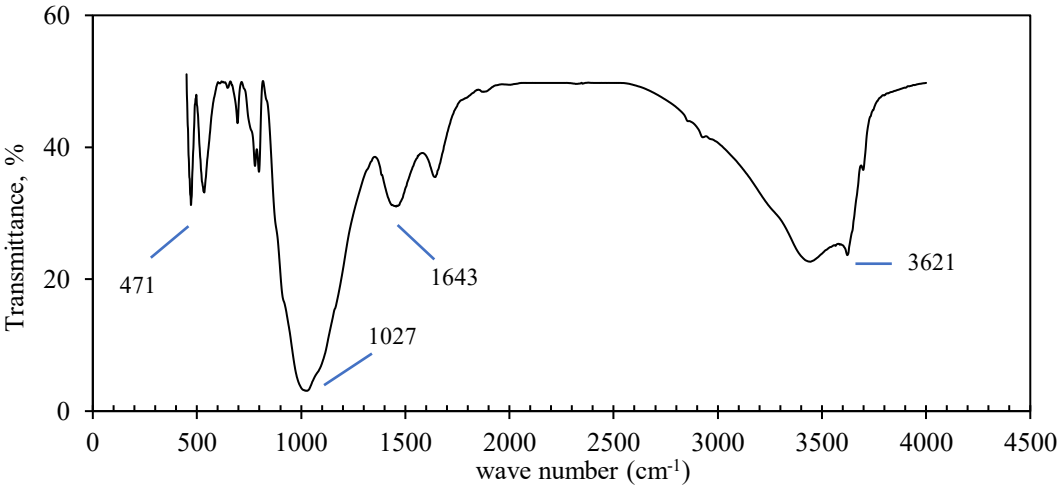


(b)

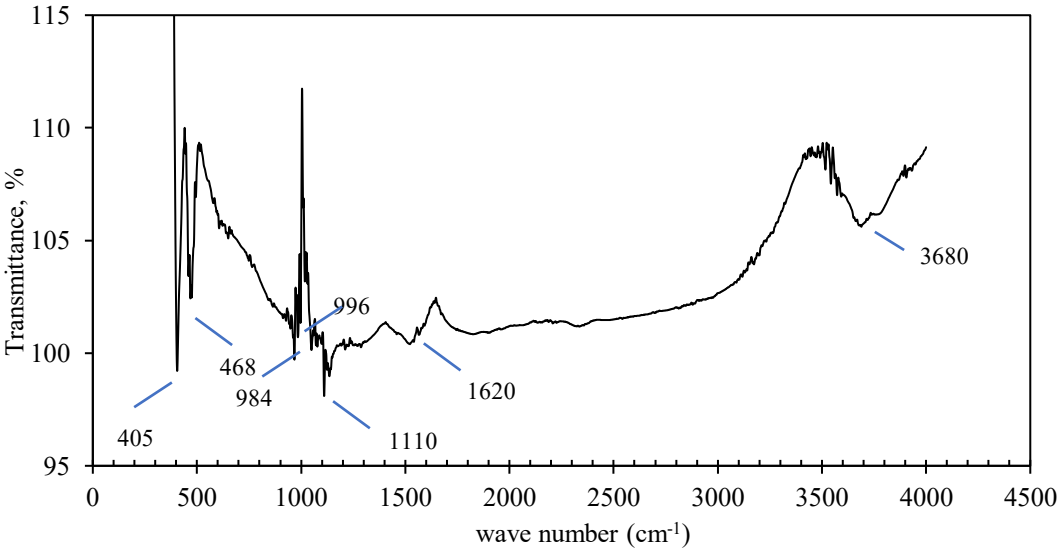


(c)

**Figure 4.21:** FTIR spectra of samples (a) soil at OMC, (b) 5% SDA A:B 0.3, (c) 15% SDA A:B 0.3

Mahedi et al. (2020). Table 4.6 illustrates a comparison of the properties of soils from these two study. Mahedi et al. (2020) reported that Soil S achieved 1300 kPa UCS with 10% cement stabilization and 1250 kPa UCS with 5% lime stabilization after 28 days curing. In the current study, a similar UCS (1275 kPa) was obtained in the composition – 20% SDA at A:B ratio 0.3. Hence, the cost comparison was done based on this composition and a detailed calculation is presented here in Table 4.7.

**Table 4.6:** Soil properties of the two studies

| Soil Property | Current Study | Mahedi et al. (2020) (Soil S) |
|---|---|---|
| Clay (%) (< 0.002 mm) | 42.1 | 40 |
| Liquid Limit, LL (%) | 57.6 | 51 |
| Plasticity Index, PI (%) | 38.1 | 31 |
| Optimum moisture content, OMC (%) | 18.6 | 17.5 |
| Maximum dry density ($kN/m^3$) | 15.97 | 17.4 |

The unit prices of NaOH, $Na_2SiO_3$, Lime and Cement are 500 Tk/kg, 600 Tk/kg, 30 Tk/kg and 10 Tk/kg respectively. All of these unit prices are based on the local market price of Bangladesh. Since, SDA is derived from waste product, the cost associated to it has been taken as zero. From the cost comparison it is evident that, for achieving a target strength, stabilization through geopolymerization has the highest cost associated with it followed by lime and then cement stabilization. However, this cost comparison can be interpretated as only an approximation and cannot be considered in a global perspective since the local market price, avaialbitly of raw materials, production cost and soil type have been highly generalized here. Moreover, lime and cement stabilization have some inherent disadvantages that may be nullified by stabilization with geopolymerization. It should be noted here that, cement industry is a much established industry compared to geoplymer and hence due to the availability of materials, the current cost compaision will always be inclined towards cement stabilization. On the contrary, geopolymerization being a recent invention, numerous studies are being conducted including material optimization to energy consumption for utilizing its enormous potential to the fullest.

**Table 4.7:** Cost comparison among different stabilizations of expansive soil

| SDA based Geopolymer | Lime Stabilization | Cement Stabilization |
|---|---|---|
| Target UCS = 1275 kPa<br>Sample Composition<br>SDA = 20% of total binder<br>A : B = 0.3 ; SH : SH = 1:2<br>NaOH = 10 M<br>(400 gm in 1000 gm water)<br>$Na_2SiO_3$ = 70/30 % w/w<br>***For total binder = 140 gm,***<br>SDA = 28 gm<br>Alklaine solution = 42 gm<br>NaOH solution = 14 gm<br>$Na_2SiO_3$ solution = 28 gm<br>NaOH solid = 4 gm<br>$Na_2SiO_3$ solid = 19.6 gm<br>***Cost of,*** SDA = 0 Tk<br>NaOH = 2 Tk<br>$Na_2SiO_3$ = 11.76 Tk<br>**Total cost = 13.76 Tk** | Target UCS = 1250 kPa<br>Sample Composition<br>Lime = 5% of total soil<br>***For total soil = 140 gm,***<br>Lime = 7 gm<br>***Cost of***, Lime = 0.21 Tk<br>**Total cost = 0.21 Tk** | Target UCS = 1300 kPa<br>Sample Composition<br>Cement = 10% of total soil<br>***For total soil = 140 gm,***<br>Cement = 14 gm<br>***Cost of,*** Cement = 0.14 Tk<br>**Total cost = 0.14 Tk** |

## 4.10 Summary

The strength and durability characteristics of sawdust ash based geopolymer samples have been investigated and results have been summarized in this chapter. From compressive, flexure and tensile test results it was found that 20% SDA with A:B ratio of 0.5 satisfies various code requirements for earthen construction. From durability consideration, the geopolymer sample with this stated composition is found satisfactory based on the wet compressive strength and water absorption results. However, this composition fails to satisfy the efflorescence criteria. Nevertheless, for rectifying this shortcoming, moist curing may be applied which was also found beneficial for strength improvement. The microstructural investigation supported the formation of geopolymer as well as improved mechanical strength.

# Chapter 5
# CONCLUSIONS AND RECOMMENDATIONS

## 5.1 General

This study aims at evaluating the effectiveness of sawdust ash based geopolymer in fabricating compressed stabilized earthern block in terms of strength and durability characteristics. Strength tests such as – compressive, flexure, tensile and durability tests such as – water absorption, wet compressive strength, effloresecene were performed to assess the effect of various amount of sawdust ash and alkaline solution addition. Microstructural investigation and Infrared Spectra were also obtained to determine the chemical changes and particulate and molecular bonding level. This chapter presents conclusions from the obtained experimental results and suggests future scope of study in this field.

## 5.2 Conclusions

The major findings and conclusions of the present study are summarized below:

1. Inclusion of sawdust ash and alkaline solution was found effective to improve the compressive strength of high swell- shrinkage soil with the composition- 20% SDA at A:B ratio of 0.5 providing the highest strength of 1.78 MPa and the composition- 5% SDA at A:B ratio of 0.4 providing the lowestest strength of 0.43 MPa after 28 days among various mix compositions. When compared with the bare soil the strength improvement is almost 800% and 120% respectively for these 2 compositions.

   The amount of alkaline solution that imparts the highest strength in the matrix is dependent on the SDA content. With the increase in SDA content, the optimum A:B ratio at which maximum strength is obtained also increases.

   The early strength development has a direct correlation with optimum amount of A:B ratio for a particular amount of SDA content present in the matrix. For a particular SDA content, the maximum early strength development (7D strength as a percent of

28D strength) was observed for the A:B ratio that provides the maximum strength at 28 days of curing.

2. Wet compressive strength was found to be greater than Bulk compressive strength with the obtained maximum value being 41% (for 5% SDA) and minimum value being 4.5% (for 20% SDA) signifying the importance of moist curing for strength improvement. This phenomenon is particularly observant in the optimum A:B ratio for a particular SDA content. With increasing SDA content, the difference between wet and bulk compressive strength also diminishes.

   Inclusion of SDA significantly improves flexure and tensile strength of the building block with the maximum obtained strength for 20% SDA content being 180% and 430% greater respectively in comparison with the unstabilized soil.

   Apparent water absorption results indicate that the stabilized blocks are seemingly impermeable supporting the formation of a dense matrix due to geopolymerization. Effloresecence was observed within some compositions that may have caused due to the migration of excess Na ion that was not bounded within the polymeric structure.

3. Microstrutural investigation supports the formation of geopolymer which was evident form the SEM images, EDX analysis and FTIR spectra.

Upon analysis of various experimental test results, it can be concluded that, the composition with 20% SDA and A:B ratio of 0.5 satisfies the minimum strength criteria of earthen building block as suggested by various codes and standards. This composition also shows excellent durability characteristics although efflorescence may occur which can be mitigated by moist curing.

### 5.3 Recommendations For Future Study

The focus of this study was valorization of waste product (sawdust ash) and a problematic soil (expansive soil) to fabricate building block. The chemical stabilization method used here is geopolymerization mechanism which is a very recent innovation in the field of “Green Construction Material” and is found to be effective in lowering the energy

consumption and carbon footprint during production. Hence, there are significant research scopes in this field and some of that can be outlined as follows:

1. The current study entails the application of a high swell-shrinkage soil in fabrication of CSEB with the help of geopolymerization. Since, clay mineralogy has a significant effect on it's internal structure and strength characteristics, the effect of geopolymerization can can be investigated in soil samples having different mineral composition. Moreover, effect of addition of coarse grained soil can also be investigated in the strength development.

2. Fibre reinforcement has always been effective in flexure strength and sometimes compressive strength improvement. The effect of various types natural or artificial fibre inclusion in the strength chacteristics may also be investigated in soil-geopolymer matrix.

3. The process of geopolymerization is largely dependent on the concentration and relative amount of alkaline solution present in the matrix as it instigates the breaking of existing Si-O-Al bonding and promotes new bonidng formation leading to polymeric structure. In the present study, the alkline solution used here has a high concentration of NaOH (10M) and the silicate solution used here was in twice the amount of NaOH. Hence, optimization of alkaline solution in terms of concentration and their relative amount may also be investigated for cost effectiveness.

4. Curing condition and duration has a significant effect in strength development of geopolymer and often dictates most of the nature of the fabricated compound. In this study focus was given on curing at ambient temperature with a duration of 7 and 28 days. For future studies effect of solar and moist curing, and with a prolonged curing duration (56 days, 90 days) upon the strength development may also be investigated.

5. Swell shrinkage behaviour is one of the important chacteistics of expansive clay soil. The swell- shrinkage (swell pressure, shrinkage percentage) behavior of the stabilized soil may also be investigated.

6. A stable geopolymer matrix formation is largely dependent on the silicate phases with the major diffenece being the bond structure among them. In order to investigate the bond and phase characteristics, MAS-NMR spectroscopy can be performed.

Moreover, the reactivity of silica and alumina content in the soil itself and in the precursor can be determined in order to get the reaction mechanism and rate in the formed geopolymer matrix.

7. The current study only focused on the static load application upon the building blocks. However, in order to evaluate complete performance of a building block, strength characteristics during dynamic load application needs to be studied.

These above mentioned research scopes may be studied further in order to gain full insight into the stabilization mechanism and address the existing research gap. The present study is expected to present a database for future researchers working on the stabilization of expansive soil using sawdust ash based geopolymer and provide the trends and exceptions that may be expected from the natural behavior. This study will also help to provide information and guideline for the civil engineers working in the construction materials field focusing on "green materials" and shifting from the traditional binder, cement. The raw materials (binders) used in this study are waste products, and the alkaline solution used are easily available and inexpensive due to wide industrial application. Hence, the CSEBs produced from the combination of these materials can be a viable alternative promoting low-cost housing option in case of resource limitation and eco-friendly material in construction sector.

# REFERENCES


Abdulkareem, O. A., Matthews, J. C., and Bakri, A. M. M. A. (2018, December). Strength and porosity characterizations of blended biomass wood ash-fly ash-based geopolymer mortar. In *AIP Conference Proceedings* (Vol. 2045, No. 1, p. 020096). AIP Publishing LLC.

Agostini, F., Skoczylas, F., and Lafhaj, Z. (2007). About a possible valorisation in cementitious materials of polluted sediments after treatment. *Cement and Concrete Composites*, 29(4), 270-278.

Alabduljabbar, H., Huseien, G. F., Sam, A. R. M., Alyouef, R., Algaifi, H. A., and Alaskar, A. (2020). Engineering properties of waste sawdust-based lightweight alkali-activated concrete: experimental assessment and numerical prediction. *Materials*, 13(23), 5490.

Arunkumar, K., Muthukannan, M., Babu, A. D., Hariharan, A. L., and Muthuramalingam, T. (2020, June). Effect on addition of polypropylene fibers in wood ash-fly ash based geopolymer concrete. In *IOP Conference Series: Materials Science and Engineering* (Vol. 872, No. 1, p. 012162). IOP Publishing.

Arunkumar, K., Muthukannan, M., and Ganesh, A. C. (2021). Mitigation of waste rubber tire and waste wood ash by the production of rubberized low calcium waste wood ash based geopolymer concrete and influence of waste rubber fibre in setting properties and mechanical behavior. *Environmental Research*, *194*, 110661.

ASTM D6913. (2009). Standard Test Methods for Particle-Size Distribution (Gradation) of Soils Using Sieve Analysis, ASTM International, West Conshohocken, PA.

ASTM D7928. (2021). Standard Test Method for Particle-Size Distribution (Gradation) of Fine-Grained Soils Using the Sedimentation (Hydrometer) Analysis, ASTM International, West Conshohocken, PA.

ASTM D4318. (2017). Standard Test Methods for Liquid Limit, Plastic Limit, and Plasticity Index of Soils, ASTM International, West Conshohocken, PA.

ASTM D698-12. (2012). Standard Test Methods for Laboratory Compaction Characteristics of Soil Using Standard Effort (12400 ft-lbf/ft$^3$ (600 kN-m/m$^3$)), ASTM International, West Conshohocken, PA.

ASTM D854-14. (2014). Standard Test Methods for Specific Gravity of Soil Solids by Water Pycnometer, ASTM International, West Conshohocken, PA.

ASTM C496/C496M-11. (2011). Standard test method for splitting tensile strength of cylindrical concrete specimens, ASTM International, West Conshohocken, PA.

ASTM C348-21. (2021). Standard Test Method for Flexural Strength of Hydraulic-Cement Mortars, ASTM International, West Conshohocken, PA.

ASTM C67-21. (2021). Standard Test Methods for Sampling and Testing Brick and Structural Clay Tile, ASTM International, West Conshohocken, PA.

ASTM D5102-09. (2009). Standard Test Method for Unconfined Compressive Strength of Compacted Soil-Lime Mixtures, ASTM International, West Conshohocken, PA.

Ayodele, A. L., Oketope, O. M., and Olatunde, O. S. (2019). Effect of sawdust ash and eggshell ash on selected engineering properties of lateralized bricks for low cost housing. *Nigerian Journal of Technology*, 38(2), 278-282.

Baxter, J. M., and Walton, A. (1970). A theoretical approach to the Suess effect. *Proceedings of the Royal Society of London. A. Mathematical and Physical Sciences*, 318(1533), 213-230.

Cheah, C. B., Part, W. K., and Ramli, M. (2015). The hybridizations of coal fly ash and wood ash for the fabrication of low alkalinity geopolymer load bearing block cured at ambient temperature. *Construction and building materials*, 88, 41-55.

Cheah, C. B., Samsudin, M. H., Ramli, M., Part, W. K., and Tan, L. E. (2017). The use of high calcium wood ash in the preparation of Ground Granulated Blast Furnace Slag and Pulverized Fly Ash geopolymers: A complete microstructural and mechanical characterization. *Journal of Cleaner Production*, 156, 114-123.

Chen, J. H., Huang, J. S., and Chang, Y. W. (2009). A preliminary study of reservoir sludge as a raw material of inorganic polymers. *Construction and Building Materials*, 23(10), 3264-3269.

Chen, L., Wang, Z., Wang, Y., and Feng, J. (2016). Preparation and properties of alkali activated metakaolin-based geopolymer. *Materials*, 9(9), 767.

Cusidó, J. A., and Cremades, L. V. (2012). Environmental effects of using clay bricks produced with sewage sludge: Leachability and toxicity studies. *Waste management*, 32(6), 1202-1208.

Davidovits, J. (1994, October). Properties of geopolymer cements. In *First international conference on alkaline cements and concretes* (Vol. 1, p. 131-149). Kiev, Ukraine: Kiev State Technical University.

Davidovits, J. (2002, October). 30 years of successes and failures in geopolymer applications. Market trends and potential breakthroughs. In *Geopolymer 2002 conference* (Vol. 28, p. 29). Saint-Quentin, France; Melbourne, Australia: Geopolymer Institute.

Davidovits, J. (2005). *Geopolymer, green chemistry and sustainable development solutions: proceedings of the world congress geopolymer 2005*. Geopolymer Institute.

Davidovits, J. (2008). *Geopolymer Chemistry and Applications.* Geopolymer Institute.

Davidovits, J. (2017). Geopolymers: Ceramic-like inorganic polymers. *Journal of Ceramic Science and Technology*, 8(3), 335-350.

Djobo, J. N. Y., Elimbi, A., Tchakouté, H. K., and Kumar, S. (2016). Mechanical properties and durability of volcanic ash based geopolymer mortars. *Construction and Building Materials*, 124, 606-614.

Duan, P., Yan, C., Zhou, W., and Luo, W. (2016). Fresh properties, mechanical strength and microstructure of fly ash geopolymer paste reinforced with sawdust. *Construction and Building Materials*, 111, 600-610.

EFNARC, S. (2002). Guidelines for self-compacting concrete. *London, UK: Association House*, 32, 34.

Elahi, T. E., Shahriar, A. R., Alam, M. K., and Abedin, M. Z. (2020). Effectiveness of saw dust ash and cement for fabrication of compressed stabilized earth blocks. *Construction and Building Materials*, 259, 120568.

Elahi, T. E., Shahriar, A. R., and Islam, M. S. (2021). Engineering characteristics of compressed earth blocks stabilized with cement and fly ash. *Construction and Building Materials*, 277, 122367.

Elinwa, A. U., and Mahmood, Y. A. (2002). Ash from timber waste as cement replacement material. *Cement and Concrete Composites*, 24(2), 219-222.

Elinwa, A. (2006). Effect of addition of sawdust ash to clay bricks. *Civil engineering and environmental systems*, 23(4), 263-270.

Elinwa, A. U., Ejeh, S. P., and Mamuda, A. M. (2008). Assessing of the fresh concrete properties of self-compacting concrete containing sawdust ash. *Construction and building materials*, 22(6), 1178-1182.

Fadele, O. A., and Ata, O. (2018). Water absorption properties of sawdust lignin stabilised compressed laterite bricks. *Case Studies in Construction Materials*, 9, e00187.

Farmer, V. C. (1974). The infrared spectra of minerals: Mineralogical Society. *London, Monograph*, 4, 539.

Gadsden, J. A. (1975). *Infrared spectra of minerals and related inorganic compounds*.

Ghosh, S. N. (1978). Infra-red spectra of some selected minerals, rocks and products. *Journal of Materials Science*, 13(9), 1877-1886.

Guo, X., Shi, H., and Dick, W. A. (2010). Compressive strength and microstructural characteristics of class C fly ash geopolymer. *Cement and Concrete Composites*, 32(2), 142-147.

Halim, A. A. E., and Baroudy, A. A. E. (2014). Influence addition of fine sawdust on the physical properties of expansive soil in the Middle Nile Delta, Egypt. *Journal of soil science and plant nutrition*, 14(2), 483-490.

Handke, M., Mozgawa, W., and Nocuń, M. (1994). Specific features of the IR spectra of silicate glasses. *Journal of molecular structure*, 325, 129-136.

https://www.fortunebusinessinsights.com/industry-reports/cement-market-101825.

https://www.re-thinkingthefuture.com/rtf-fresh-perspectives/a1704-10-construction-techniques-used-in-eartharchitecture.

Hassan, M. A., Yami, A. M., Raji, A., and Ngala, M. J. (2014). Effects of sawdust and rice husk additives on properties of local refractory clay. *The International Journal of Engineering and Science*, 3(8), 40-44.

IS (Indian Standard). (1998). Code of practice for in-situ construction of walls in buildings with soil-cement. *IS 2110*, New Delhi, India.

Islam, M. S., and Iwashita, K. (2010). Earthquake resistance of adobe reinforced by low cost traditional materials. *Journal of Natural Disaster Science*, 32(1), 1-21.

Islam, M. S., Elahi, T. E., Shahriar, A. R., Nahar, K., and Hossain, T. R. (2020). Strength and durability characteristics of cement-sand stabilized earth blocks. *Journal of Materials in Civil Engineering*, 32(5), 04020087.

Jasim, O. H., and Çetin, D. (2016). Effect of sawdust usage on the shear strength behavior of clayey silt soil. *Sigma Journal of Engineering and Natural Sciences*, 34(1), 31-41.

Kong, I., Khoo, K. M., Buddrick, O., Baharuddin, A. A., and Khalili, P. (2018). Synthesis and characterization of red mud and sawdust based geopolymer composites as potential construction material. In *Materials science forum* (Vol. 923, pp. 130-134). Trans Tech Publications Ltd.

Kumar, P., and Singh, S. P. (2008). Fiber-reinforced fly ash subbases in rural roads. *Journal of transportation engineering*, 134(4), 171-180.

Kumar, T. R. P., Sudheesh, C., and Kumar, S. (2015). Strength Characteristics of Saw Dust Ash Based Geo polymer Concrete. *International Journal of ChemTech Research*, 8(2), 738-745.

Lee, W. K. W., and Van Deventer, J. S. J. (2003). Use of infrared spectroscopy to study geopolymerization of heterogeneous amorphous aluminosilicates. *Langmuir*, 19(21), 8726-8734.

Li, L., Shao, W., Li, Y., and Cetin, B. (2015). Effects of climatic factors on mechanical properties of cement and fiber reinforced clays. *Geotechnical and Geological Engineering*, 33(3), 537-548.

Luukkonen, T., Abdollahnejad, Z., Yliniemi, J., Kinnunen, P., and Illikainen, M. (2018). Comparison of alkali and silica sources in one-part alkali-activated blast furnace slag mortar. *Journal of cleaner production*, 187, 171-179.

Mageswari, M., and Vidivelli, B. (2009). The use of sawdust ash as fine aggregate replacement in concrete. *Journal of Environmental Research and Development*, 3(3), 720-726.

Mahedi, M., Cetin, B., and White, D. J. (2020). Cement, lime, and fly ashes in stabilizing expansive soils: performance evaluation and comparison. *Journal of Materials in Civil Engineering*, 32(7), 04020177.

Manukaji, J. U. (2012). The effects of sawdust addition on the insulating characteristics of clays from the federal capital territory of Abuja. *International Journal of Enginnering Research and Applications*, 3(2), 6-9.

Mollah, M. Y. A., Hess, T. R., and Cocke, D. L. (1994). Surface and bulk studies of leached and unleached fly ash using XPS, SEM, EDS and FTIR techniques. *Cement and concrete research*, 24(1), 109-118.

Mumtaz, N. (2019). Construction of disaster resilient rural houses using CSEB made with riverbed sand. *M.Sc. Engg. thesis*, Department of Civil Engineering, Bangladesh University of Engineering and Technology, Dhaka-1000.

NMAC. (2009). New Mexico Earthen Building Materials Code. Title 14. Chapter 7. Part 4. Section 23.

Ntamack, G.E., Degho, T., Beda, T. and D'ouazzane, S.C. (2012). Determination of mechanical characteristics of compressed and stabilized earth blocks by cement, by the mixture cement and sawdust, and by the lime through the elasticity-damaging coupling model. *International Journal of Science and Technology*, 2(9), 668-674.

NZS (New Zealand Standard). (1998). Materials and workmanship for earth buildings. *NZS4298*, Wellington, New Zealand.

Ojo, E. B., Isah, A. K., Teixeira, R. S., Matawal, D. S., and Savastano, H. (2018, June). Geopolymer Stabilisation of Earth Building Materials for Sustainable Construction. In *NBRRI International Conference: Emerging Materials and Technologies for Sustainable Building and Road Infrastructure* (pp. 20-21).

Okunade, E. A. (2008). The effect of wood ash and sawdust admixtures on the engineering properties of a burnt laterite-clay brick. *Journal of applied sciences*, 8(6), 1042-1048.

Pacheco-Torgal, F., Castro-Gomes, J., and Jalali, S. (2008). Alkali-activated binders: A review: Part 1. Historical background, terminology, reaction mechanisms and hydration products. *Construction and building Materials*, 22(7), 1305-1314.

Paudyal, A., Dhapakhel, N., Puri, R., Tuladhar, A. M., Chhetri, R., Dhapkhel, N., and Rai, O. B. (2018, September). Study on Alternative Materials Used for Interlocking Compressed Stabilized Earth Blocks (ICSEB). In *1st KEC Conference Proceedings* (Vol. I, pp. 109-113). Kantipur Engineering College, Dhapakhel, Lalitpur, India.

Paul, S., Islam, M. S., and Elahi, T. E. (2022). Comparative effectiveness of fibers in enhancing engineering properties of Earth as a building Material: A review. *Construction and Building Materials*, 332, 127366.

Pereira, D. D. C., Amaral-Labat, G., and Silva, G. F. B. (2019). Effect of sawdust as porosity agent on final properties of geopolymers. *Cerâmica*, 65, 104-109.

Poe, B. T., McMillan, P. F., Angell, C. A., and Sato, R. K. (1992). Al and Si coordination in $SiO_2$-$Al_2O_3$ glasses and liquids: A study by NMR and IR spectroscopy and MD simulations. *Chemical Geology*, 96(3-4), 333-349.

Rajamma, R., Labrincha, J. A., and Ferreira, V. M. (2012). Alkali activation of biomass fly ash–metakaolin blends. *Fuel*, 98, 265-271.

Rossi, A. D., Simão, L., Ribeiro, M. J., Hotza, D., and Moreira, R. F. P. M. (2020). Study of cure conditions effect on the properties of wood biomass fly ash geopolymers. *Journal of Materials Research and Technology*, 9(4), 7518-7528.

Ryu, G. S., Lee, Y. B., Koh, K. T., and Chung, Y. S. (2013). The mechanical properties of fly ash-based geopolymer concrete with alkaline activators. *Construction and building materials*, 47, 409-418.

Saeli, M., Senff, L., Tobaldi, D. M., Seabra, M. P., and Labrincha, J. A. (2019). Novel biomass fly ash-based geopolymeric mortars using lime slaker grits as aggregate for applications in construction: Influence of granulometry and binder/aggregate ratio. *Construction and Building Materials*, 227, 116643.

Seco, A., Ramírez, F., Miqueleiz, L., and García, B. (2011). Stabilization of expansive soils for use in construction. *Applied Clay Science*, 51(3), 348-352.

Sekhar, D. C., and Nayak, S. (2018). Utilization of granulated blast furnace slag and cement in the manufacture of compressed stabilized earth blocks. *Construction and Building Materials*, 166, 531-536.

Simão, L., Fernandes, E., Hotza, D., Ribeiro, M. J., Montedo, O. R. K., and Raupp-Pereira, F. (2021). Controlling efflorescence in geopolymers: A new approach. *Case Studies in Construction Materials*, 15, e00740.

Sitarz, M., Mozgawa, W., and Handke, M. (1997). Vibrational spectra of complex ring silicate anions—method of recognition. *Journal of molecular structure*, 404(1-2), 193-197.

SLS (Sri Lanka Standards). (2009), Specification for compressed stabilised earth blocks: part 1: requirements, *SLS 1328: 1*, Colombo, Sri Lanka.

Suwan, T. (2016). Development of self-cured geopolymer cement. *Doctoral dissertation*, Brunel University London.

Tang, L., Cong, S., Geng, L., Ling, X., and Gan, F. (2018). The effect of freeze-thaw cycling on the mechanical properties of expansive soils. *Cold Regions Science and Technology*, 145, 197-207.

Tay, J. H., and Show, K. Y. (1997). Resource recovery of sludge as a building and construction material—a future trend in sludge management. *Water Science and Technology*, 36(11), 259-266.

Tchakouté, H. K., Rüscher, C. H., Kong, S., Kamseu, E., and Leonelli, C. (2017). Thermal behavior of metakaolin-based geopolymer cements using sodium waterglass from rice husk ash and waste glass as alternative activators. *Waste and biomass valorization*, 8(3), 573-584.

Trujillo, N. B. (2016). Mix Design and Mechanical Characterization of Stabilized Compressed Earth Blocks and Assemblies for the Jemez Pueblo in New Mexico. *M.Sc. Engg thesis*, Department of Civil Engineering, University of New Mexico.

Uchino, T., Sakka, T., Hotta, K., and Iwasaki, M. (1989). Attenuated toatal reflectance Fourier-transform infrared spectra of a hydrated sodium soilicate glass. *Journal of the American Ceramic Society*, 72(11), 2173-2175.

Uchino, T., Sakka, T., and Iwasaki, M. (1991). Interpretation of hydrated states of sodium silicate glasses by infrared and Raman analysis. *Journal of the American Ceramic Society*, 74(2), 306-313.

Ukrainczyk, N., Vrbos, N., and Koenders, E. A. (2016). Reuse of woody biomass ash waste in cementitious materials. *Chemical and Biochemical Engineering Quarterly*, 30(2), 137-148.

Vempati, R. K., Rao, A., Hess, T. R., Cocke, D. L., and Lauer Jr, H. V. (1994). Fractionation and characterization of Texas lignite class 'F' fly ash by XRD, TGA, FTIR, and SFM. *Cement and concrete research*, 24(6), 1153-1164.

Wang, H., Li, H., and Yan, F. (2005). Synthesis and mechanical properties of metakaolinite-based geopolymer. *Colloids and Surfaces A: Physicochemical and Engineering Aspects*, 268(1-3), 1-6.

Wang, L., Kwok, J. S., Tsang, D. C., and Poon, C. S. (2015). Mixture design and treatment methods for recycling contaminated sediment. *Journal of hazardous materials*, 283, 623-632.

Wei, Y. L., Yang, J. C., Lin, Y. Y., Chuang, S. Y., and Wang, H. P. (2008). Recycling of harbor sediment as lightweight aggregate. *Marine Pollution Bulletin*, 57(6-12), 867-872.

Weng, C. H., Lin, D. F., and Chiang, P. C. (2003). Utilization of sludge as brick materials. *Advances in environmental research*, 7(3), 679-685.

Xu, Y., Yan, C., Xu, B., Ruan, X., and Wei, Z. (2014). The use of urban river sediments as a primary raw material in the production of highly insulating brick. *Ceramics international*, 40(6), 8833-8840.

Ye, N., Yang, J., Ke, X., Zhu, J., Li, Y., Xiang, C., Wang, H., Li, L., and Xiao, B. (2014). Synthesis and characterization of geopolymer from Bayer red mud with thermal pretreatment. *Journal of the American Ceramic Society*, 97(5), 1652-1660.

# APPENDIX A

# SEM IMAGES OF SOIL - SDA GEOPOLYMER MIXTURES AT DIFFERENT MAGNIFICATION

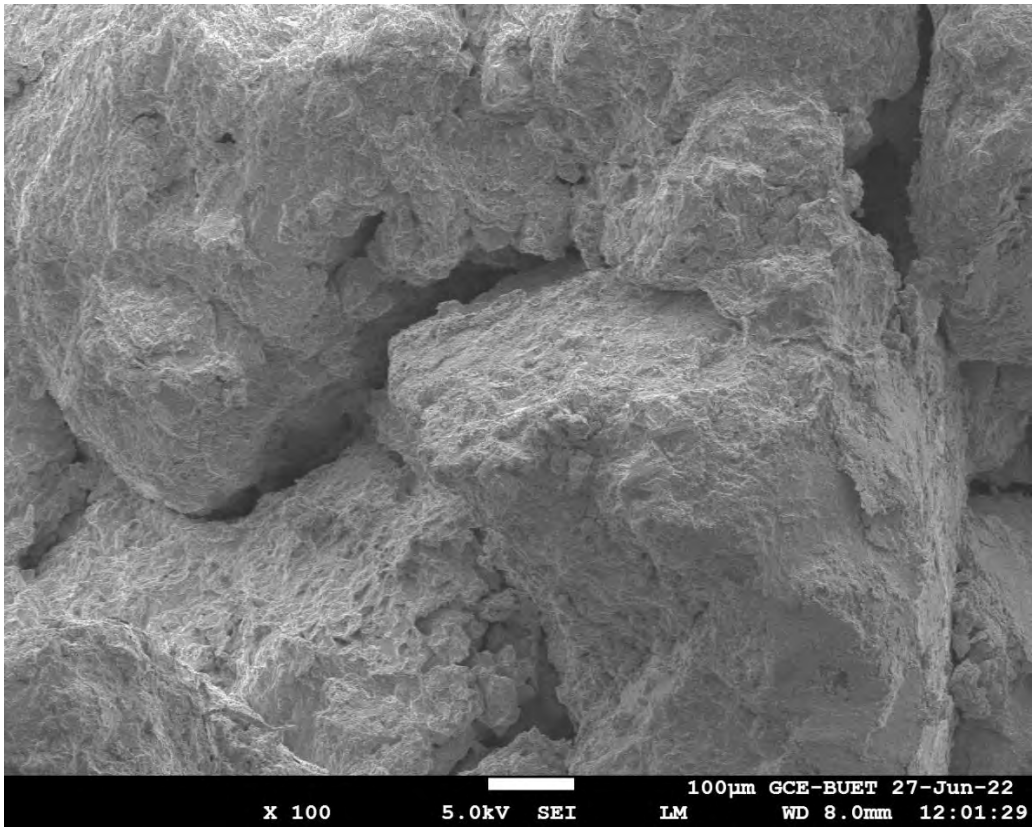
100µm GCE-BUET 27-Jun-22
X 100 5.0kV SEI LM WD 8.0mm 12:01:29

(a)

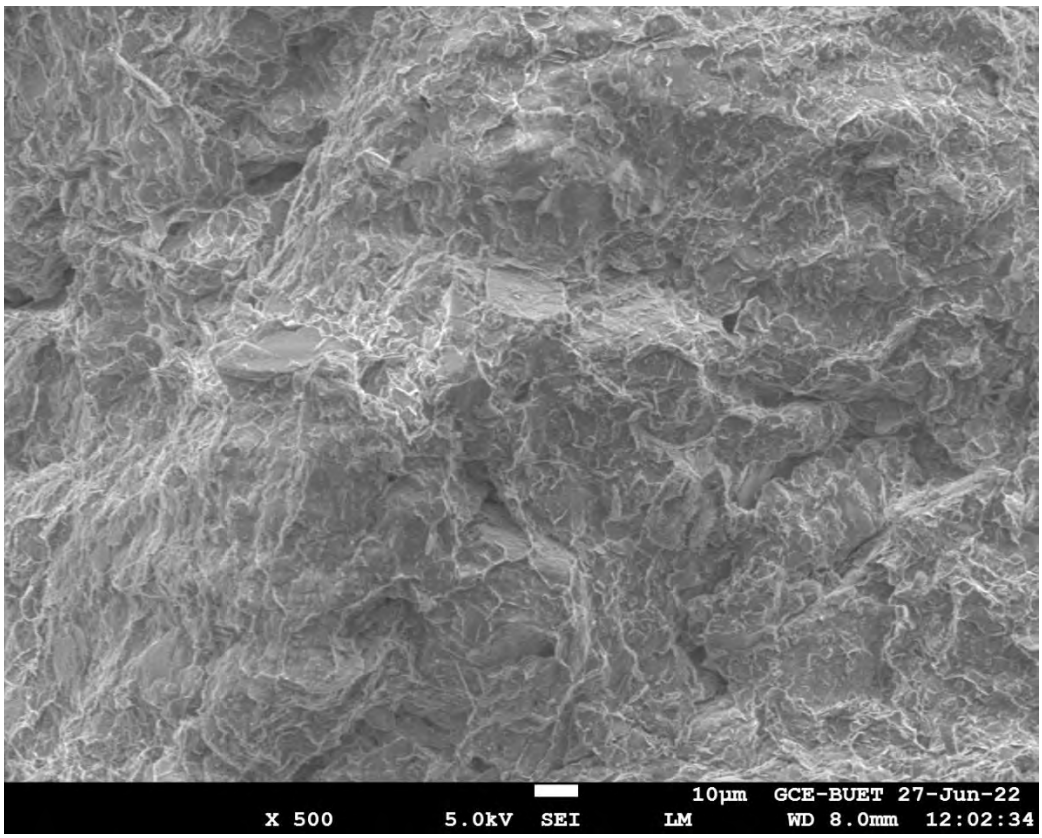
10µm GCE-BUET 27-Jun-22
X 500 5.0kV SEI LM WD 8.0mm 12:02:34

(b)

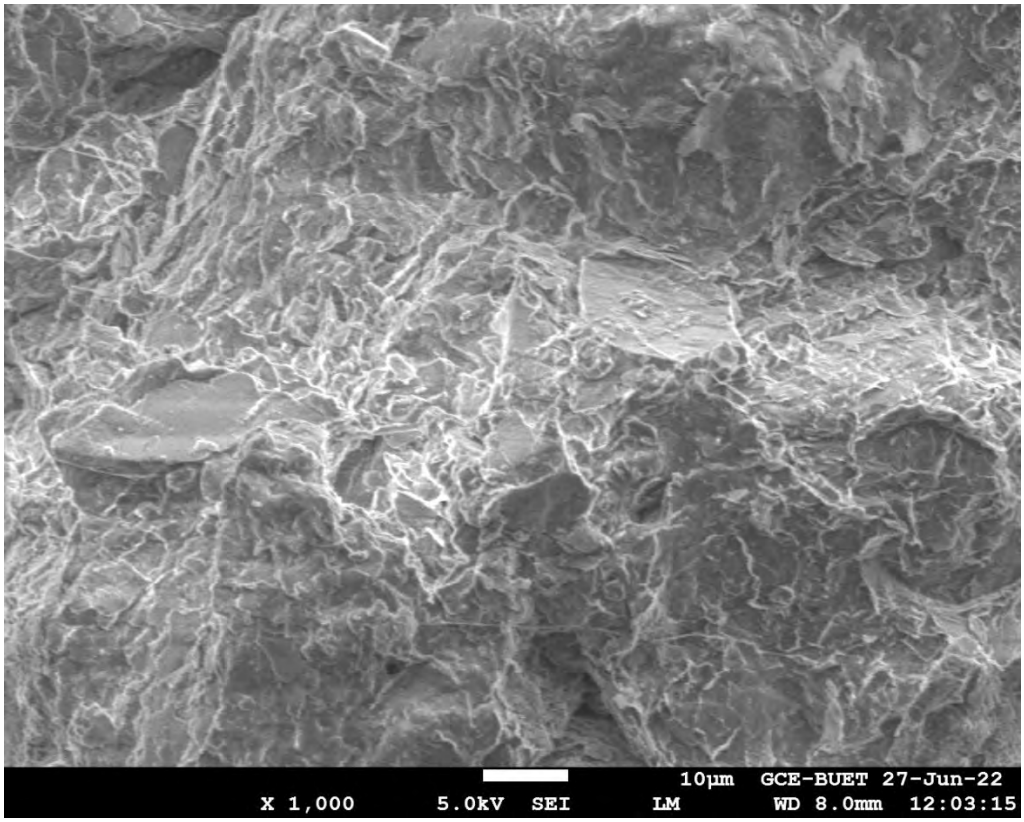
10µm GCE-BUET 27-Jun-22
X 1,000 5.0kV SEI LM WD 8.0mm 12:03:15

(c)

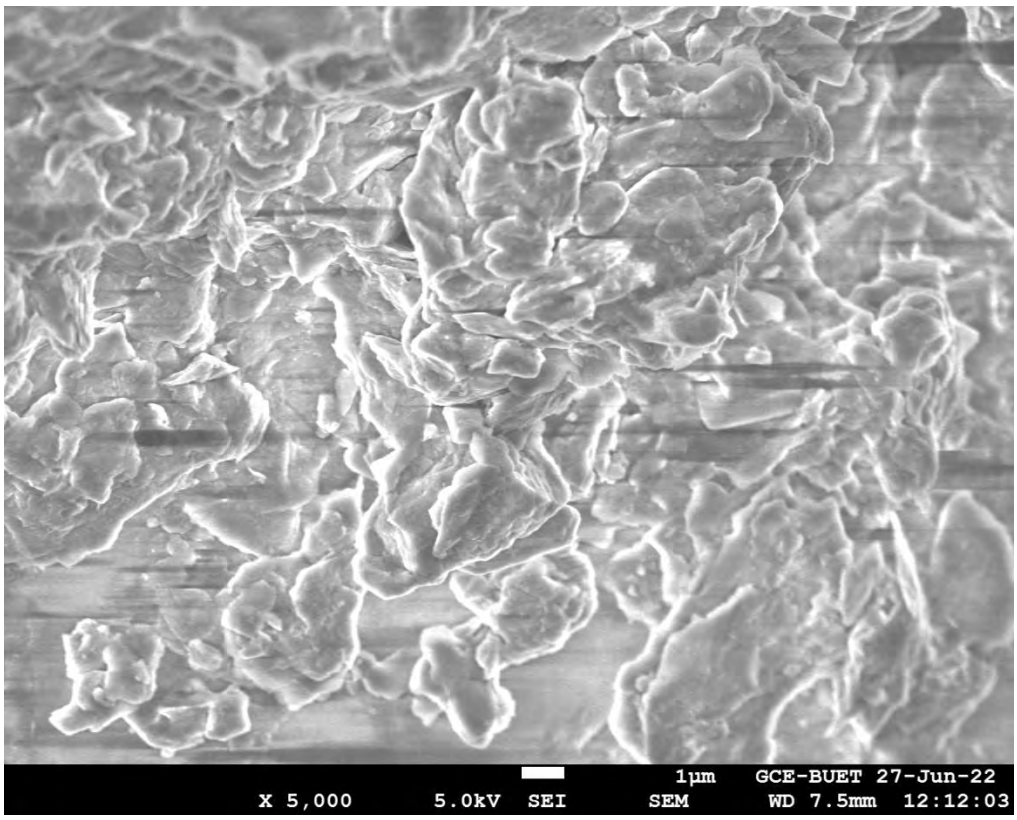
1µm GCE-BUET 27-Jun-22
X 5,000 5.0kV SEI SEM WD 7.5mm 12:12:03

(d)

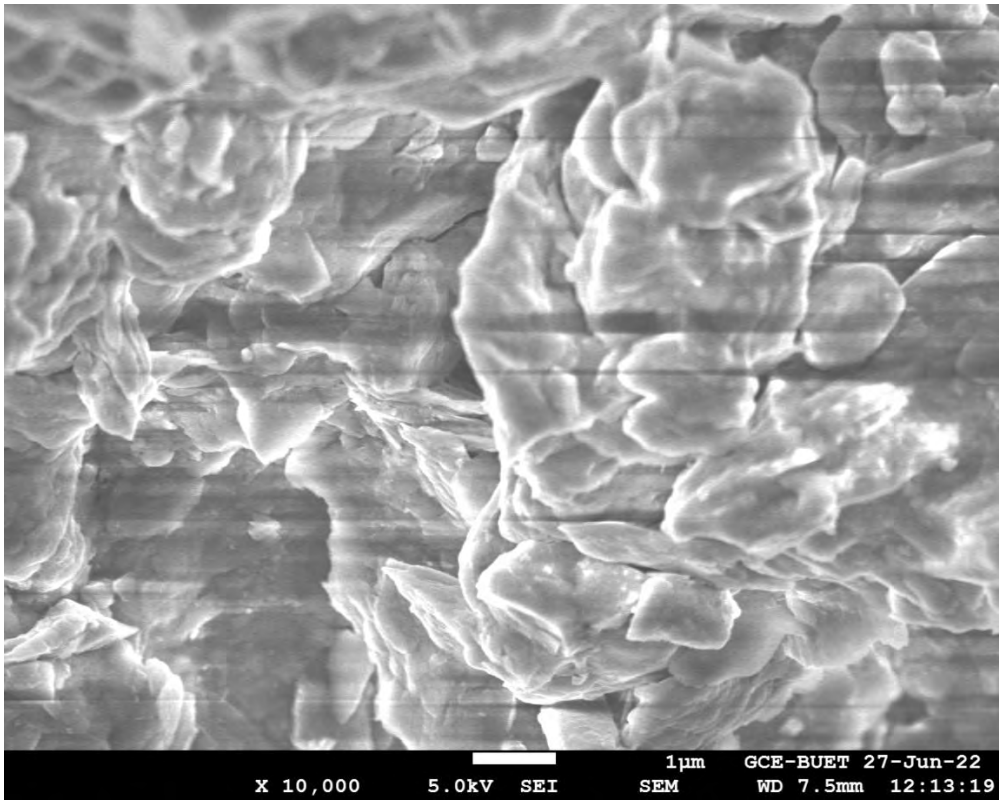


(e)

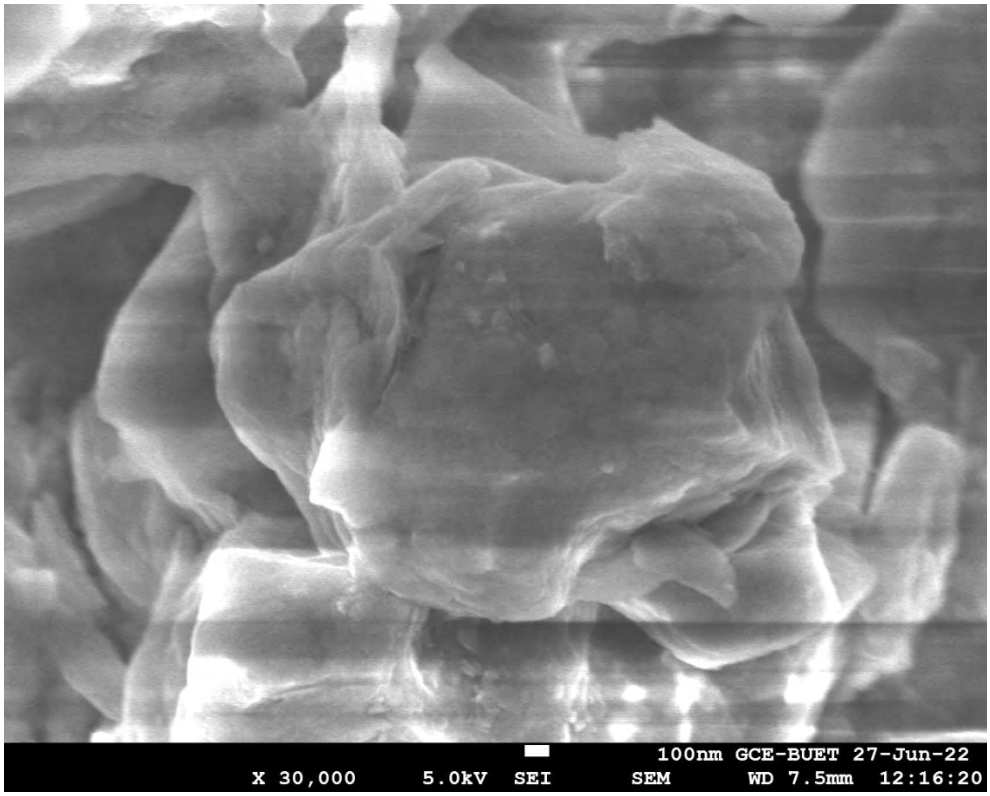


(f)

**Figure A.1:** SEM Images of soil sample compacted at OMC – (a) x 100, (b) x 500, (c) x 1000, (d) x 5000, (e) x 10000 and (f) x 30000

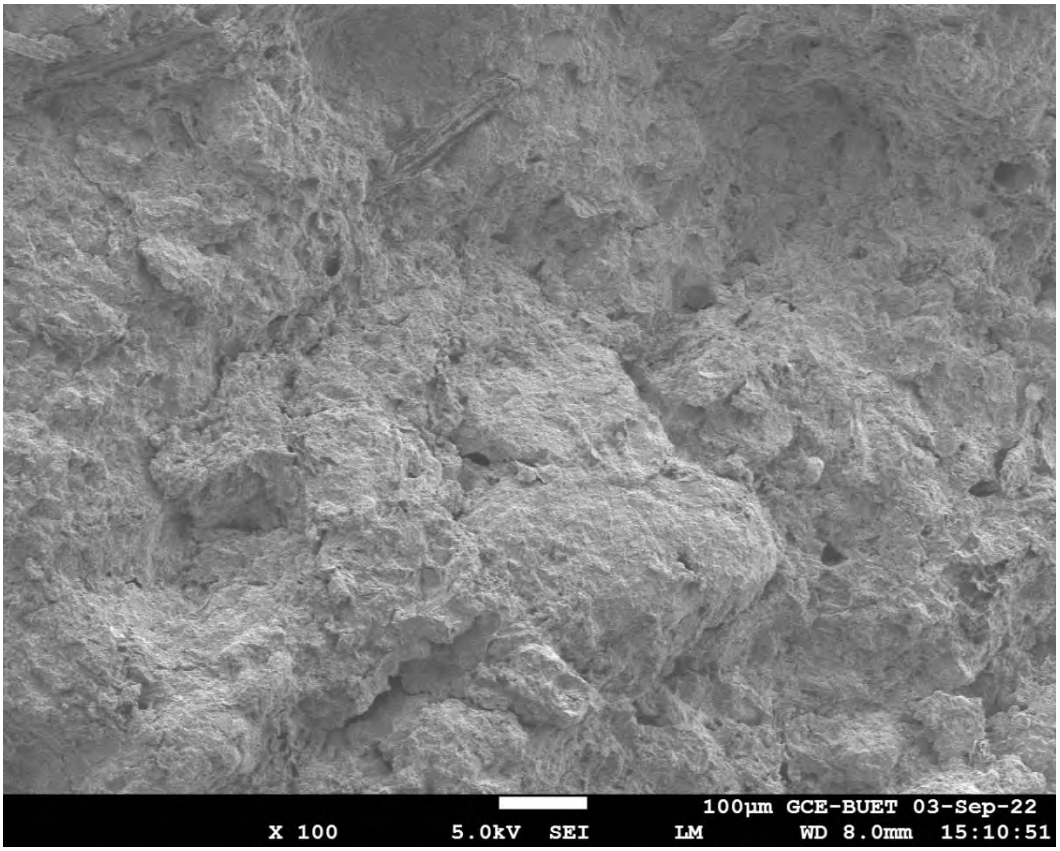
X 100 5.0kV SEI LM 100µm GCE-BUET 03-Sep-22 WD 8.0mm 15:10:51

(a)

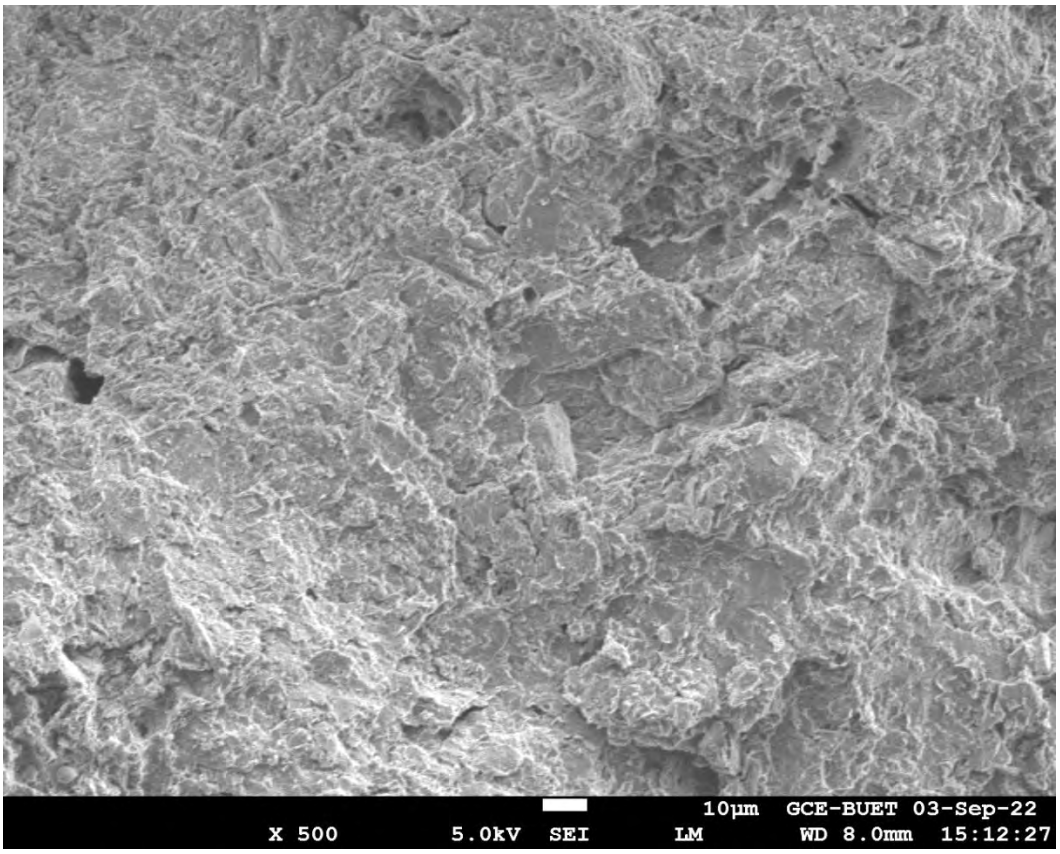
X 500 5.0kV SEI LM 10µm GCE-BUET 03-Sep-22 WD 8.0mm 15:12:27

(b)

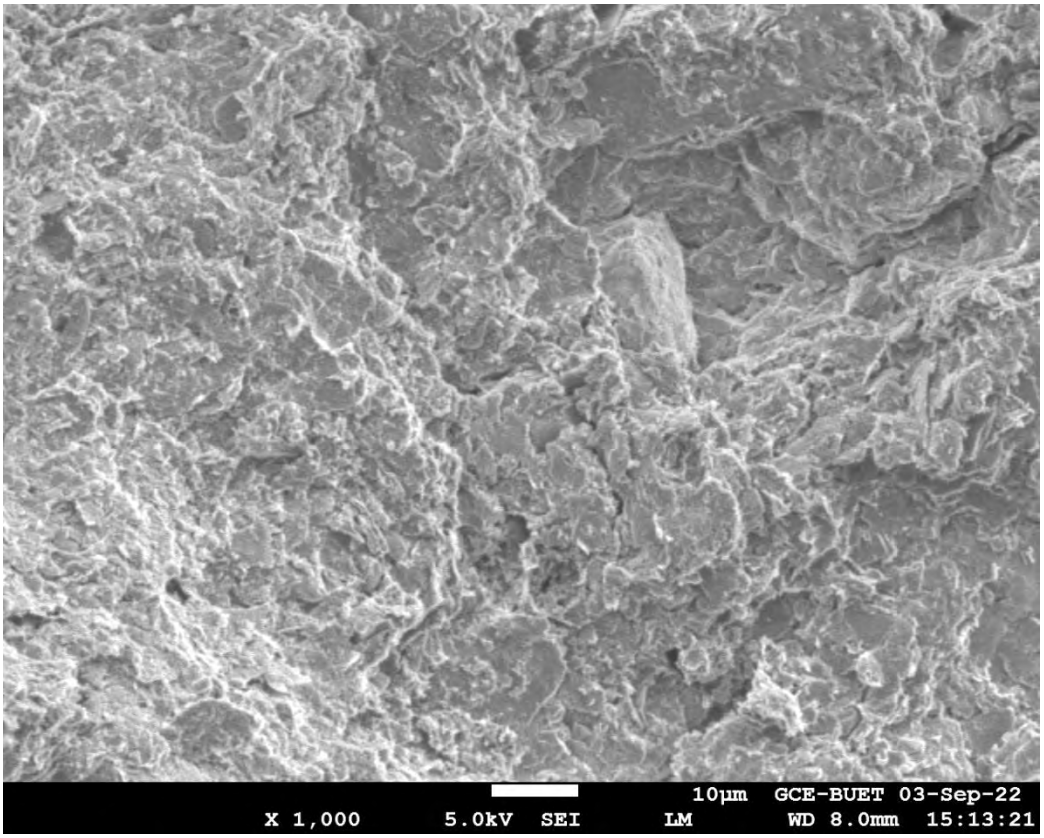
X 1,000 5.0kV SEI LM 10µm GCE-BUET 03-Sep-22 WD 8.0mm 15:13:21

(c)

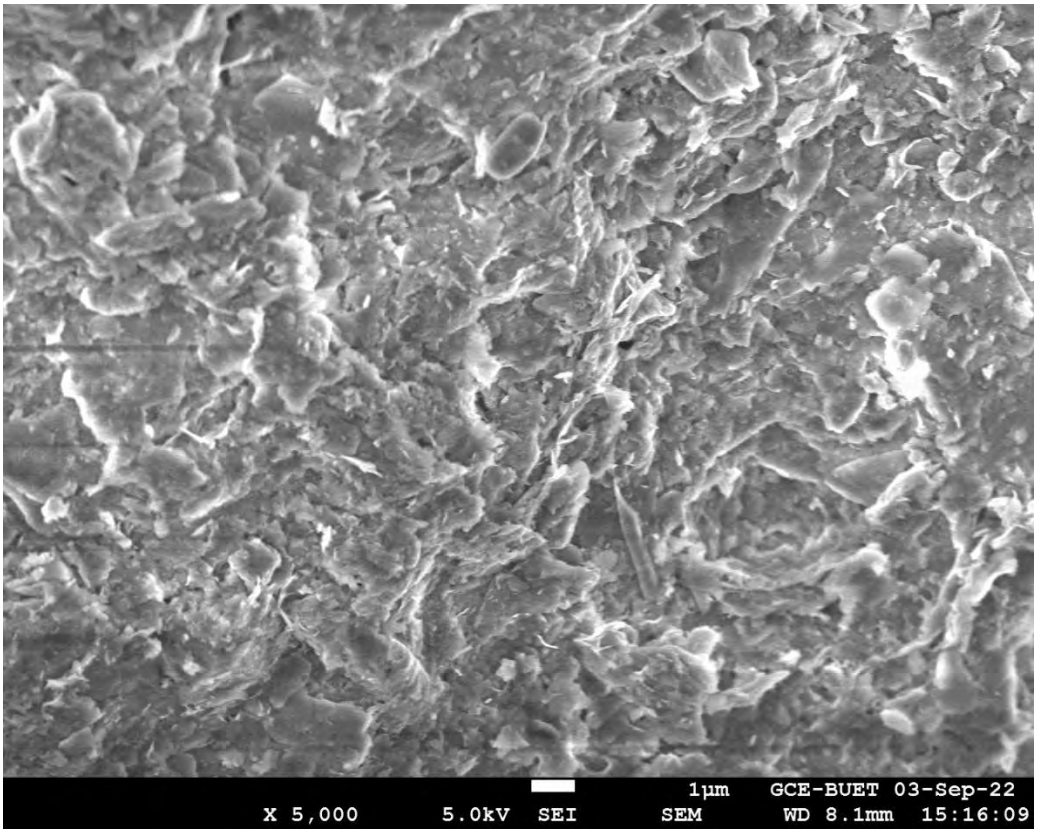
X 5,000 5.0kV SEI SEM 1µm GCE-BUET 03-Sep-22 WD 8.1mm 15:16:09

(d)

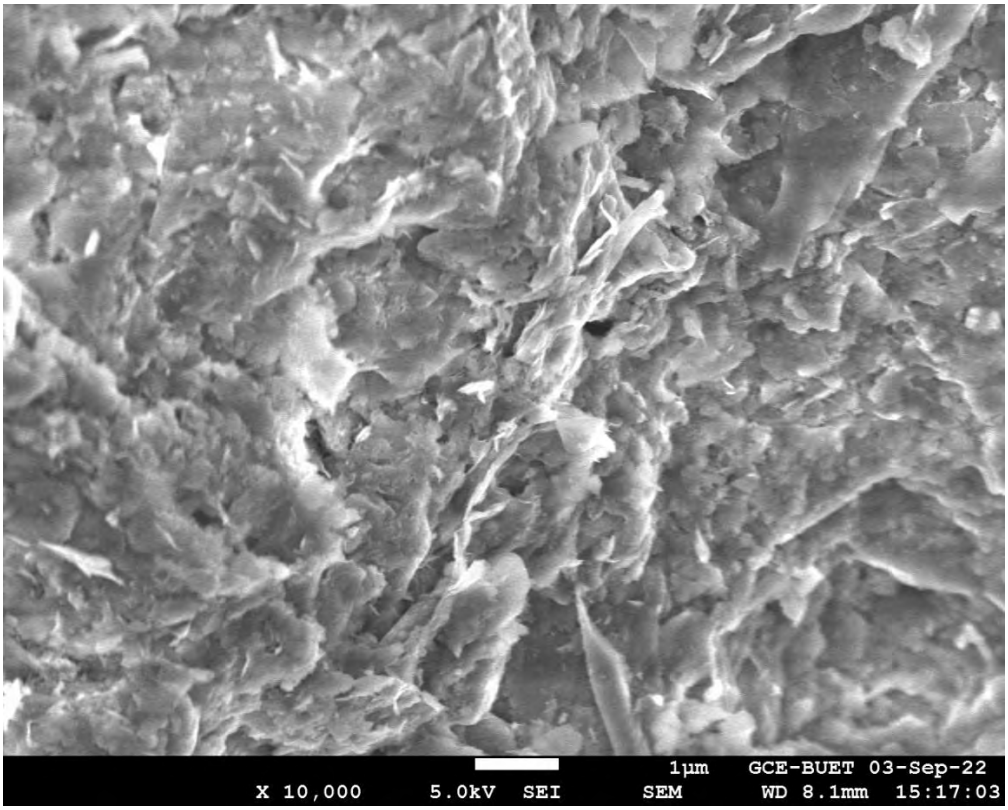


(e)

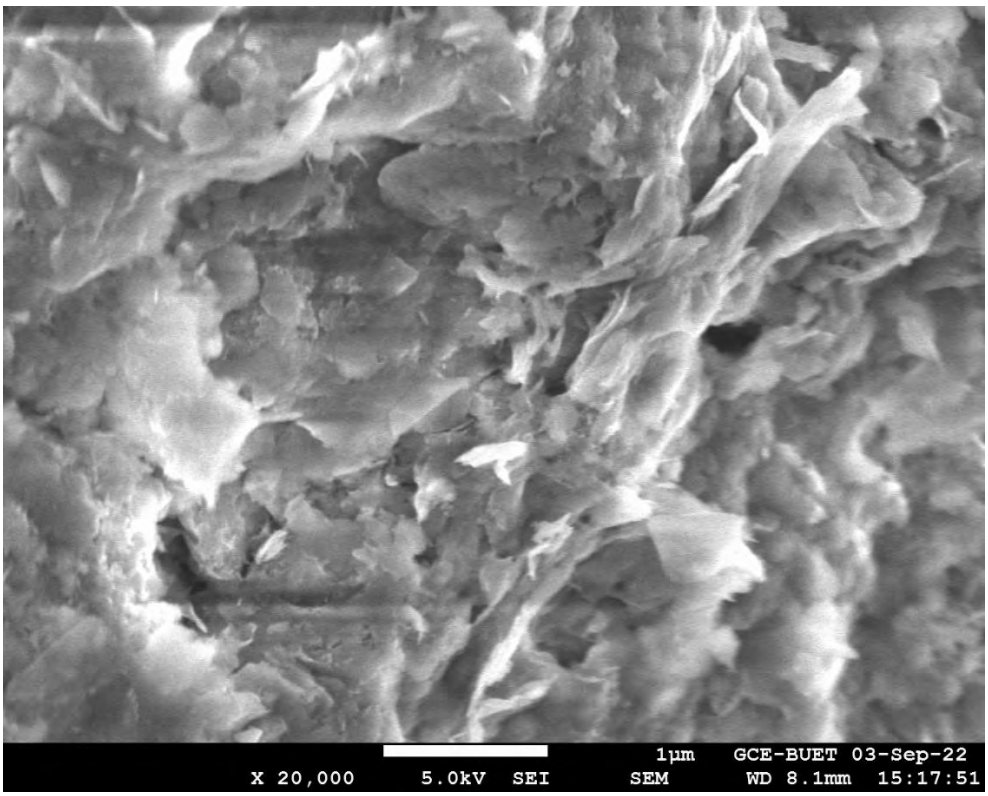


(f)

**Figure A.2:** SEM Images of sample having 5% SDA and A:B ratio 0.3 – (a) x 100, (b) x 500, (c) x 1000, (d) x 5000, (e) x 10000 and (f) x 20000

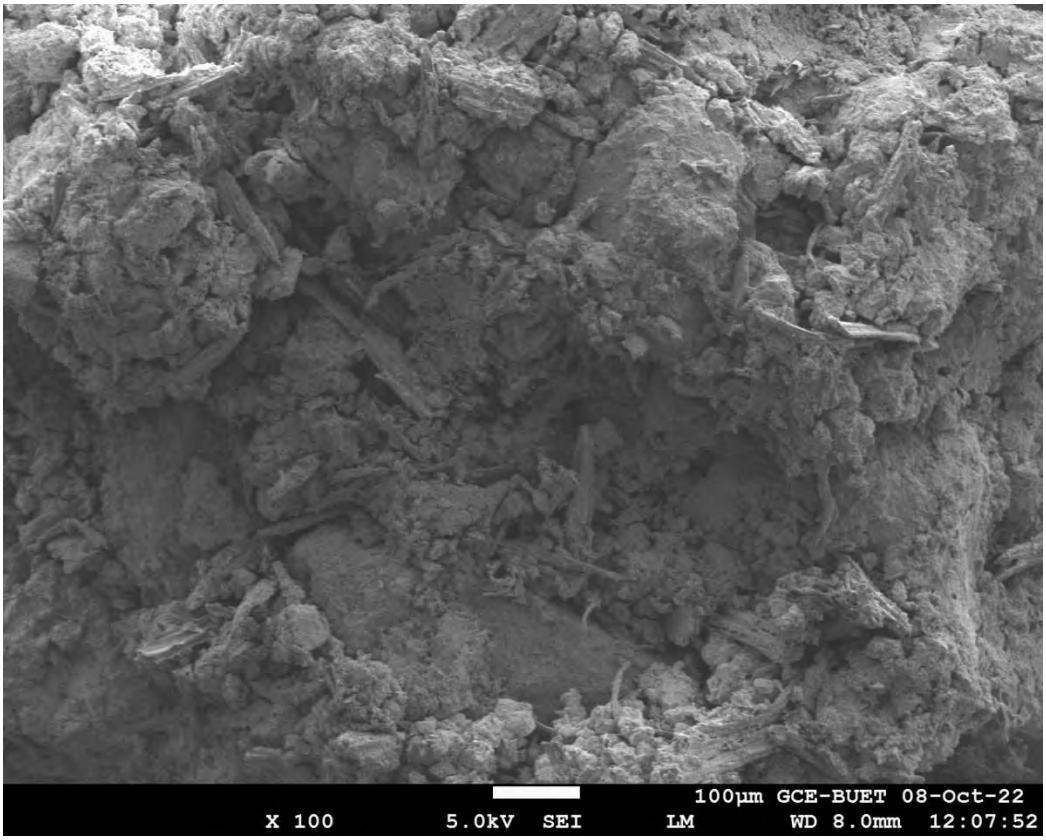
X 100 5.0kV SEI LM 100µm GCE-BUET 08-Oct-22 WD 8.0mm 12:07:52

(a)

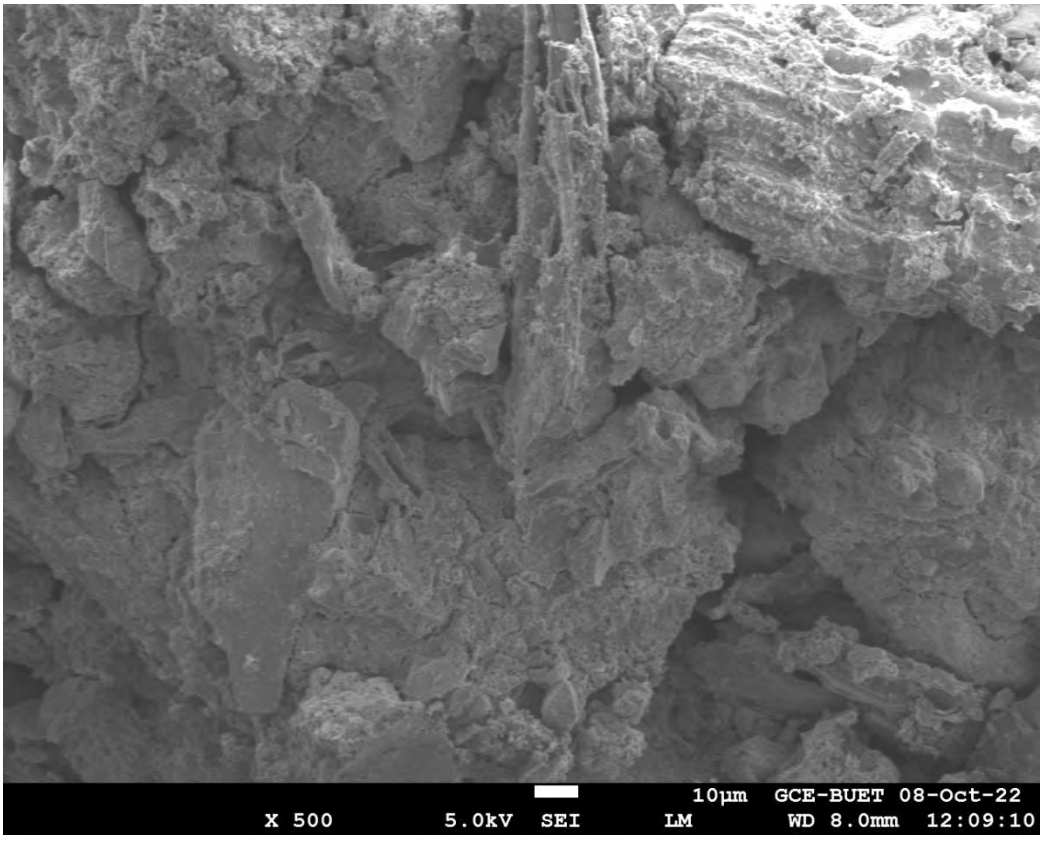
X 500 5.0kV SEI LM 10µm GCE-BUET 08-Oct-22 WD 8.0mm 12:09:10

(b)

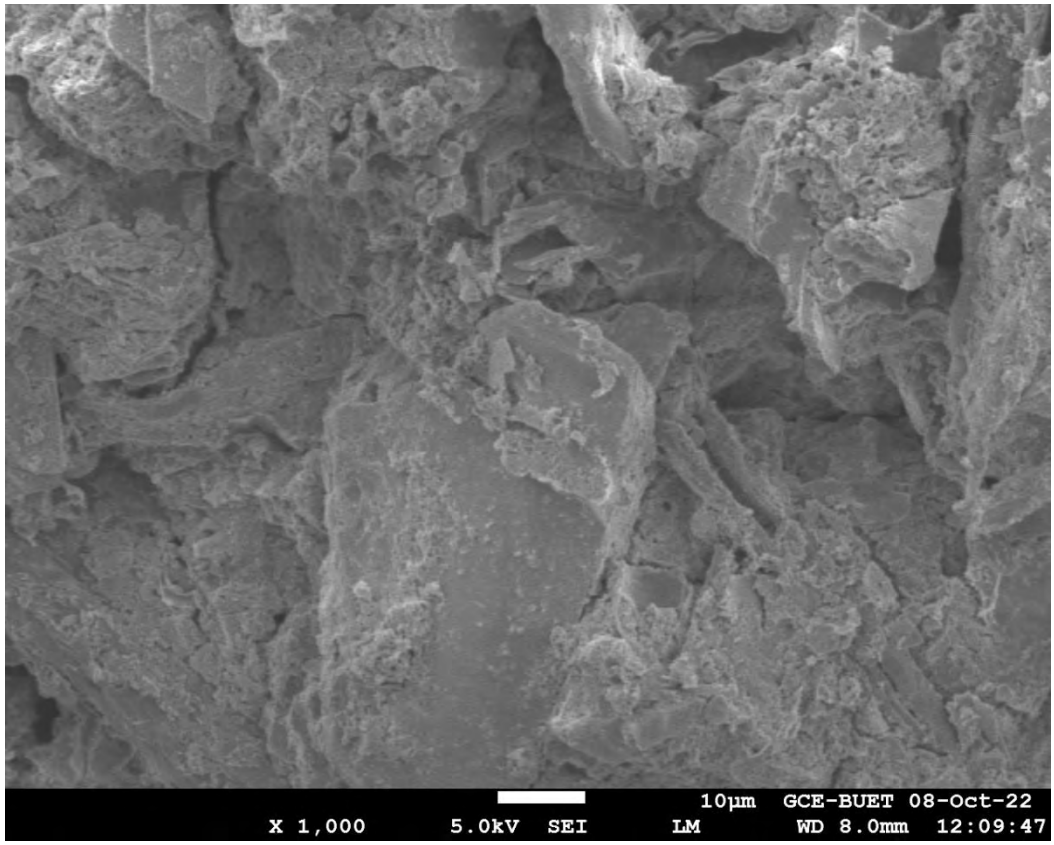
X 1,000 5.0kV SEI LM 10µm GCE-BUET 08-Oct-22 WD 8.0mm 12:09:47

(c)

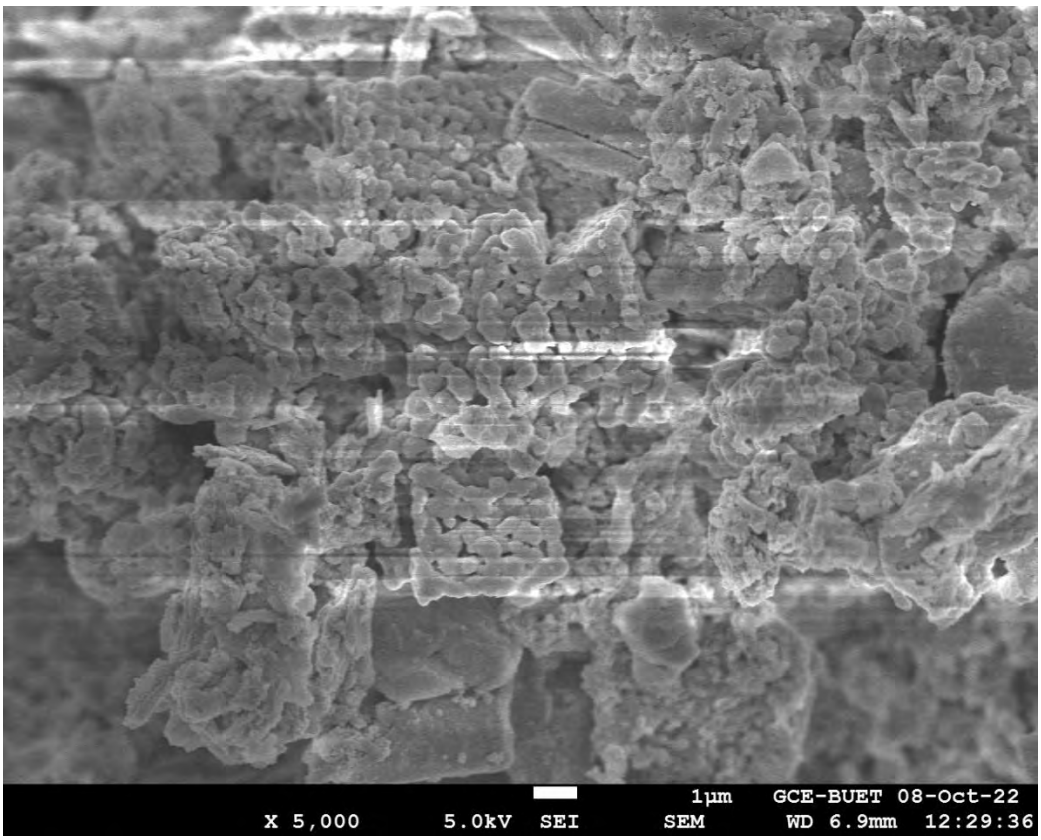
X 5,000 5.0kV SEI SEM 1µm GCE-BUET 08-Oct-22 WD 6.9mm 12:29:36

(d)

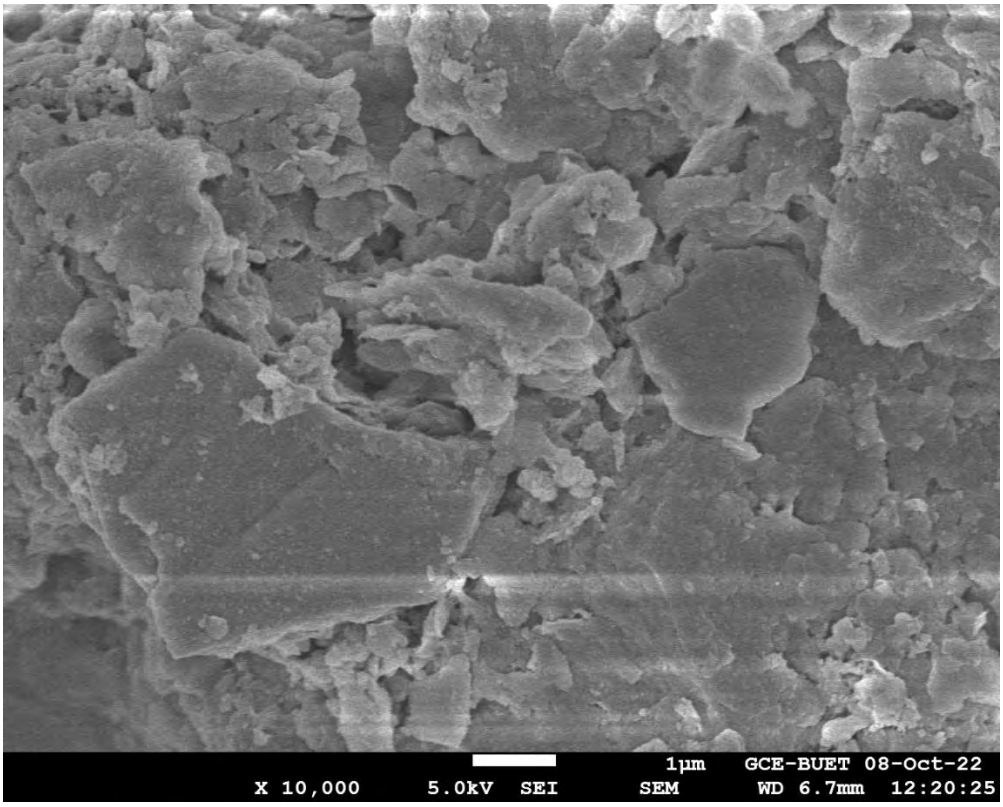


(e)

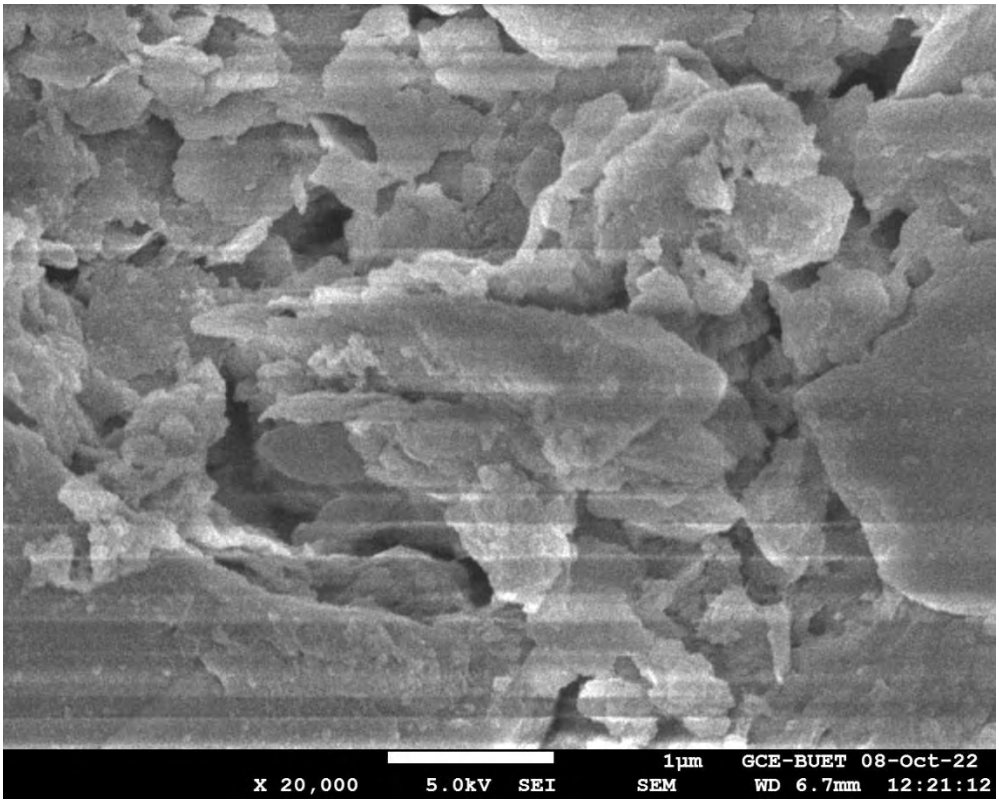


(f)

**Figure A.3:** SEM Images of sample having 15% SDA and A:B ratio 0.3 – (a) x 100, (b) x 500, (c) x 1000, (d) x 5000, (e) x 10000 and (f) x 20000

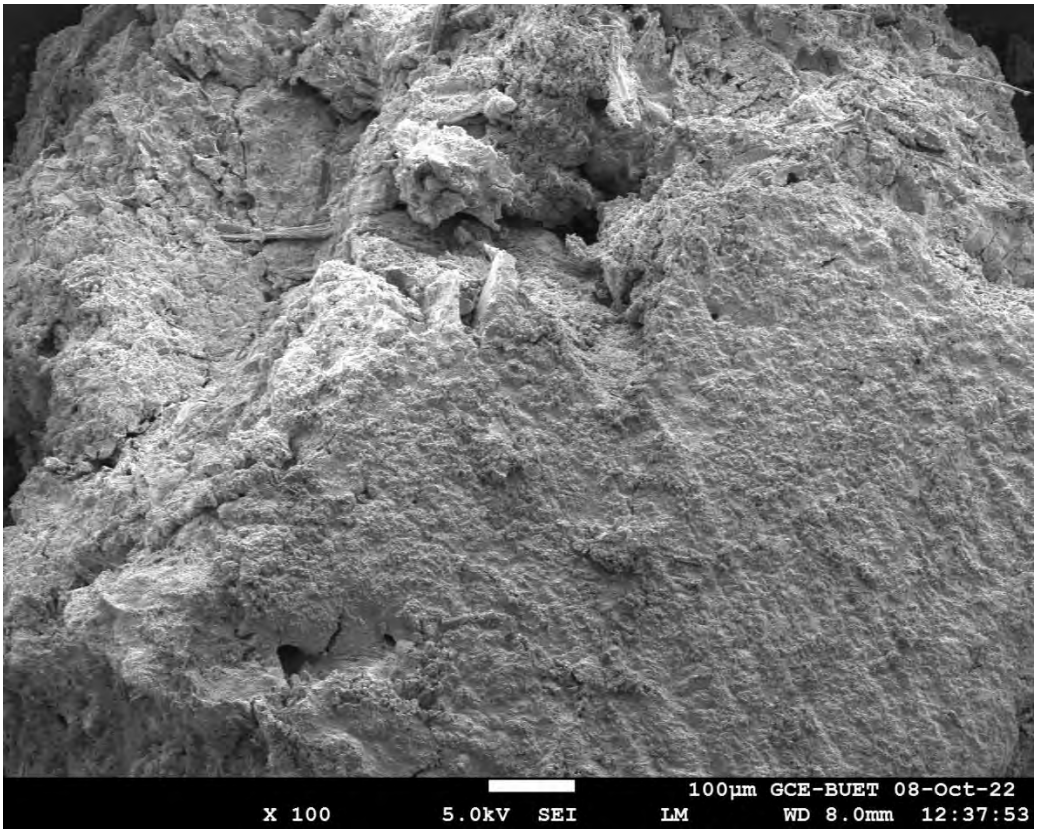
X 100 5.0kV SEI LM
100µm GCE-BUET 08-Oct-22
WD 8.0mm 12:37:53

(a)

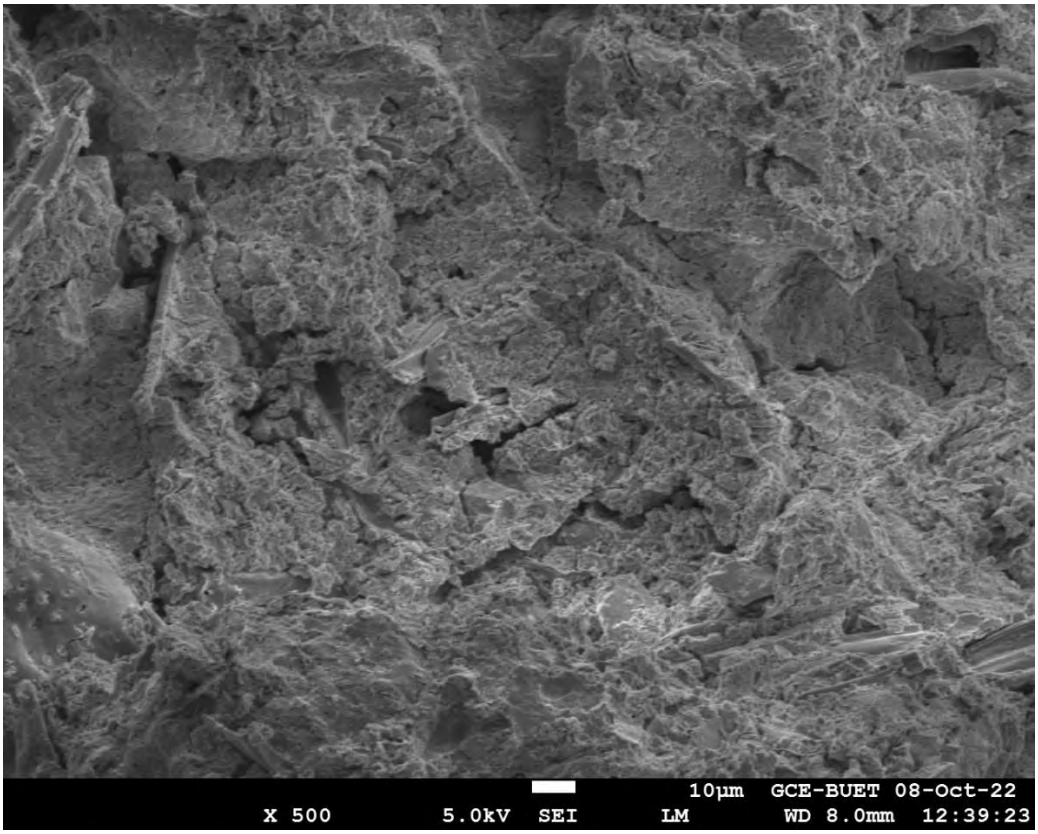
X 500 5.0kV SEI LM
10µm GCE-BUET 08-Oct-22
WD 8.0mm 12:39:23

(b)

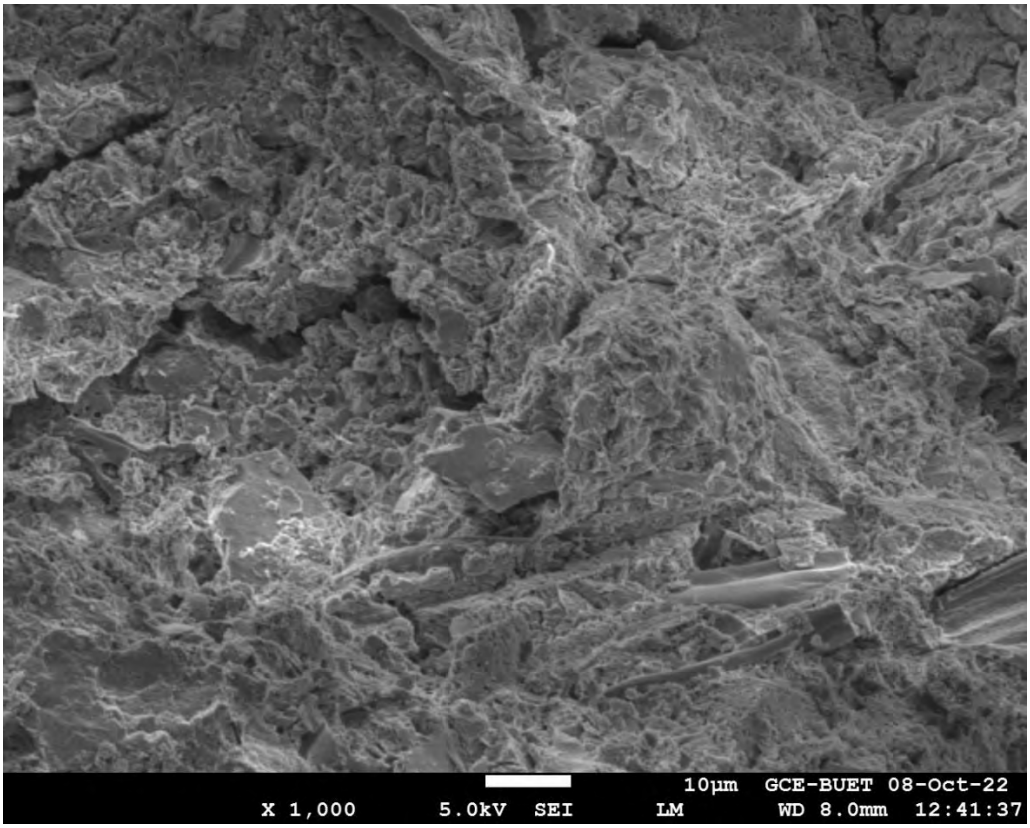
10µm GCE-BUET 08-Oct-22
X 1,000 5.0kV SEI LM WD 8.0mm 12:41:37

(c)

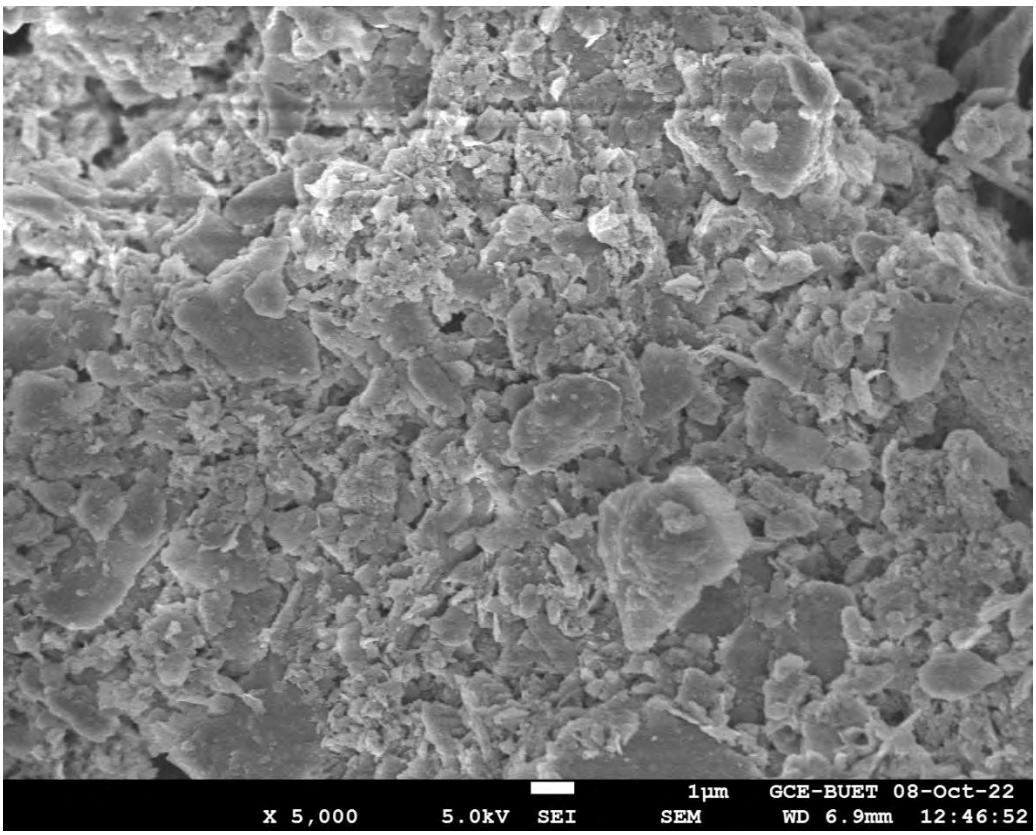
1µm GCE-BUET 08-Oct-22
X 5,000 5.0kV SEI SEM WD 6.9mm 12:46:52

(d)

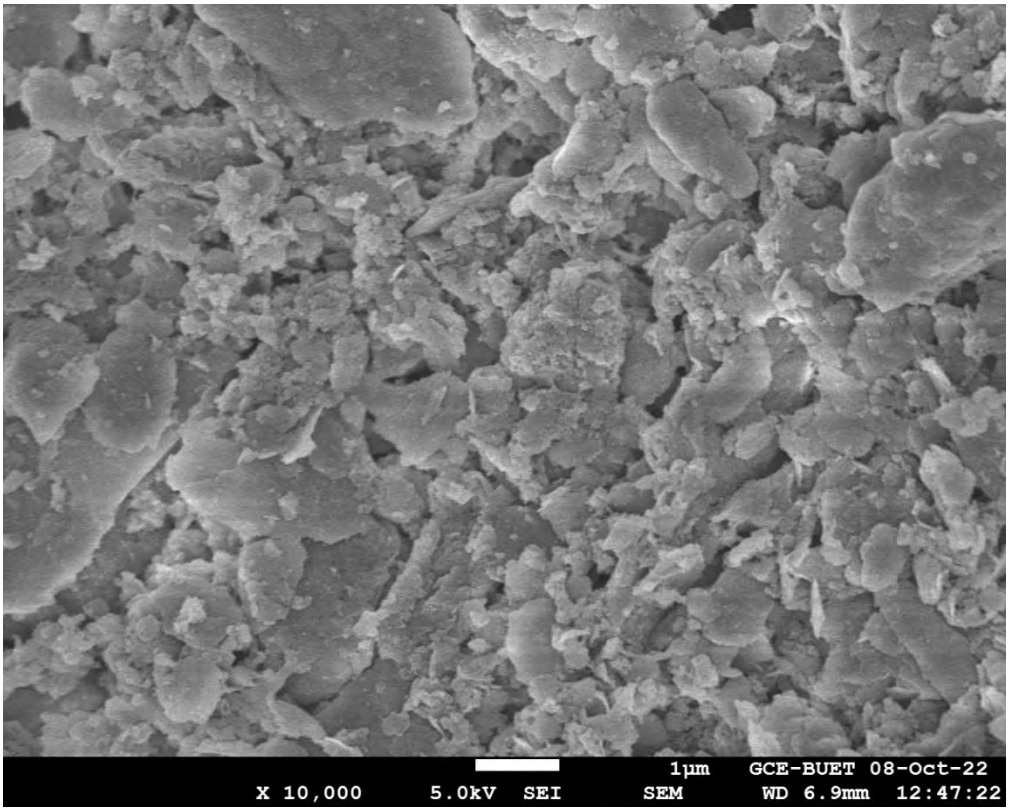


(e)

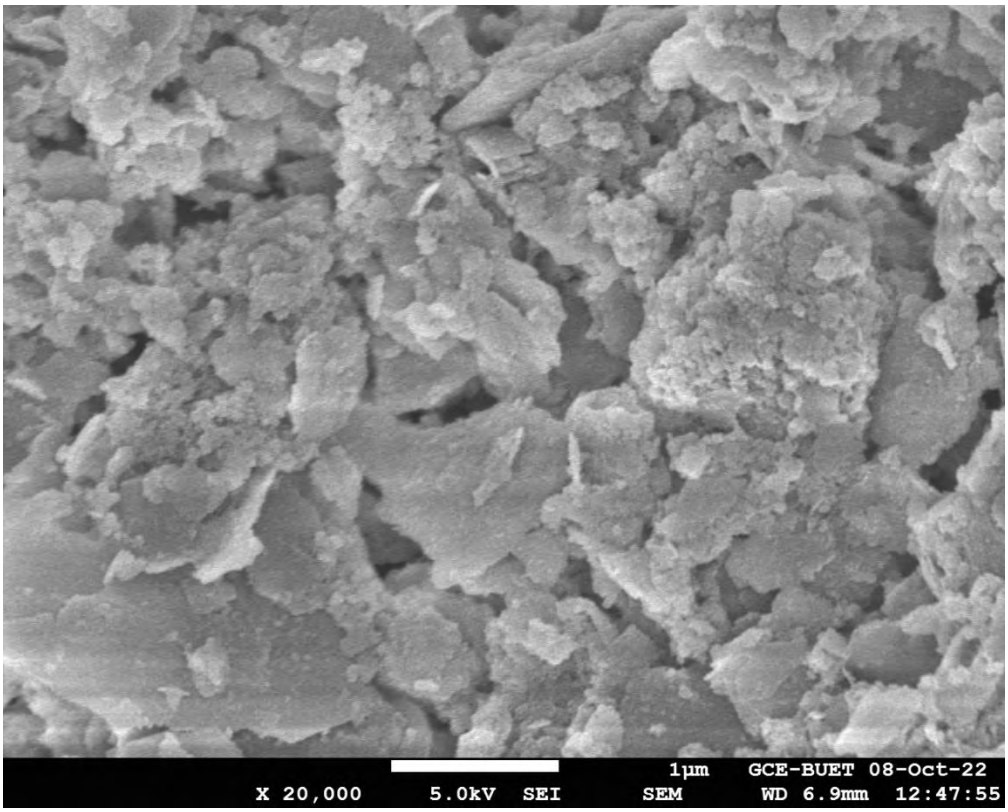


(f)

**Figure A.4:** SEM Images of sample having 15% SDA and A:B ratio 0.4 – (a) x 100, (b) x 500, (c) x 1000, (d) x 5000, (e) x 10000 and (f) x 20000

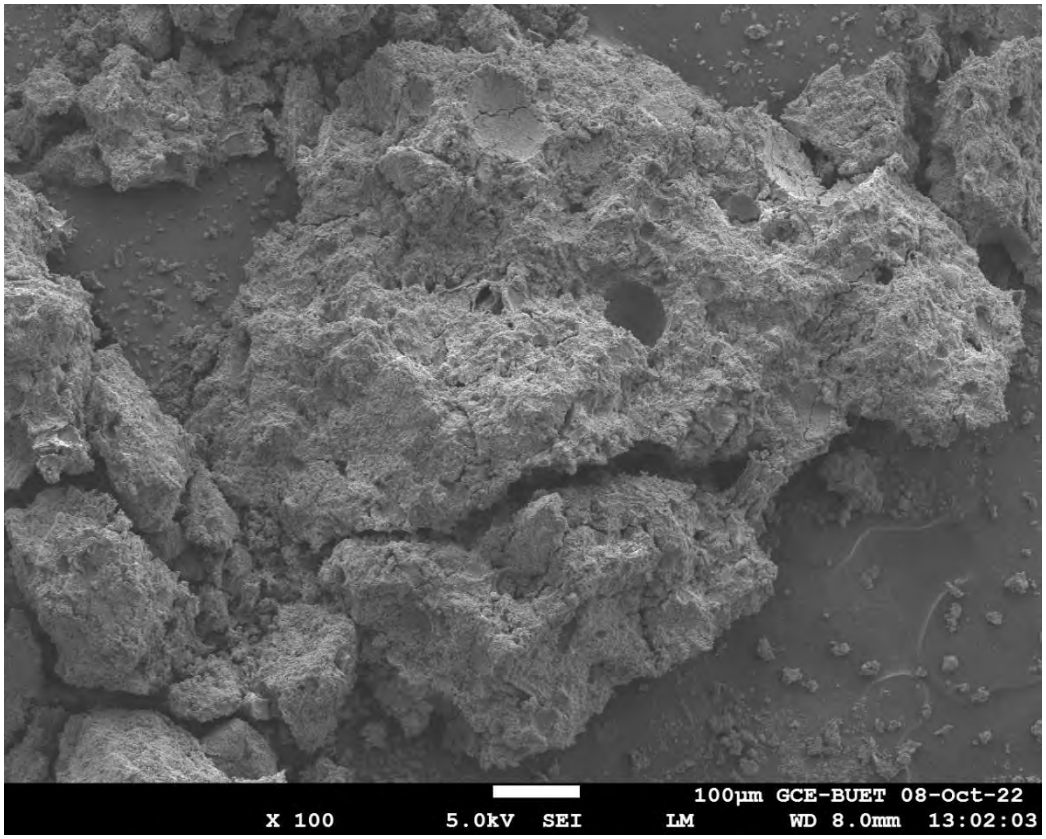
X 100 5.0kV SEI LM 100µm GCE-BUET 08-Oct-22 WD 8.0mm 13:02:03

(a)

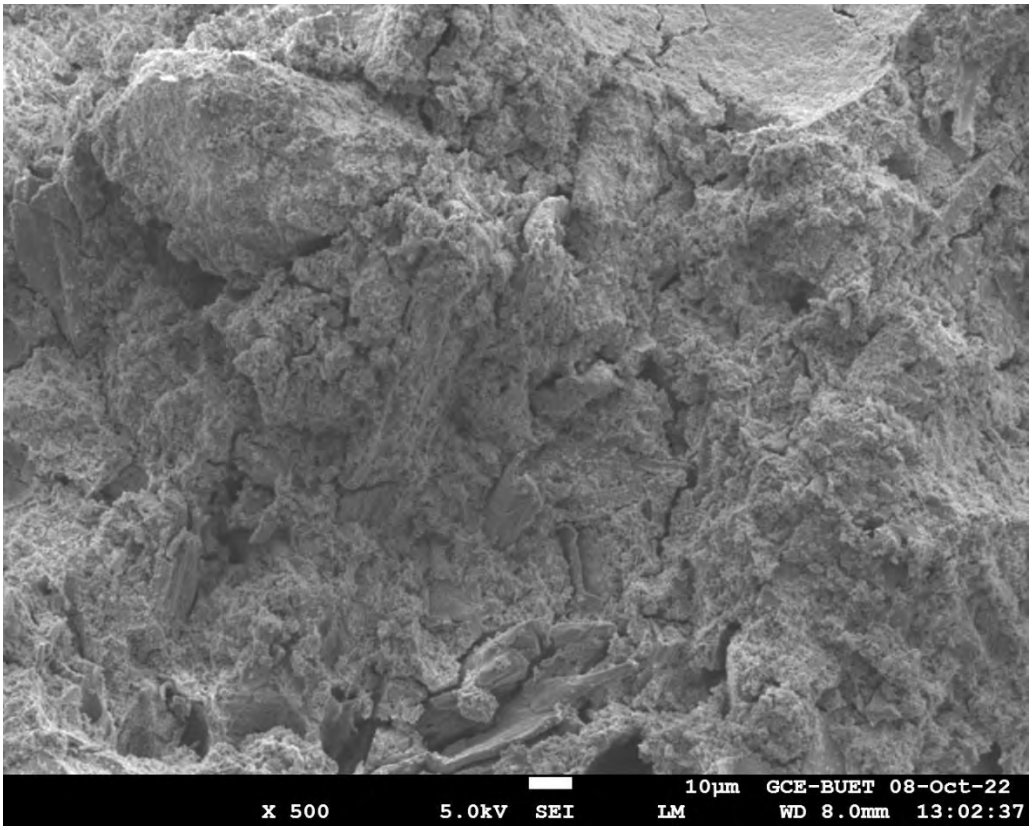
X 500 5.0kV SEI LM 10µm GCE-BUET 08-Oct-22 WD 8.0mm 13:02:37

(b)

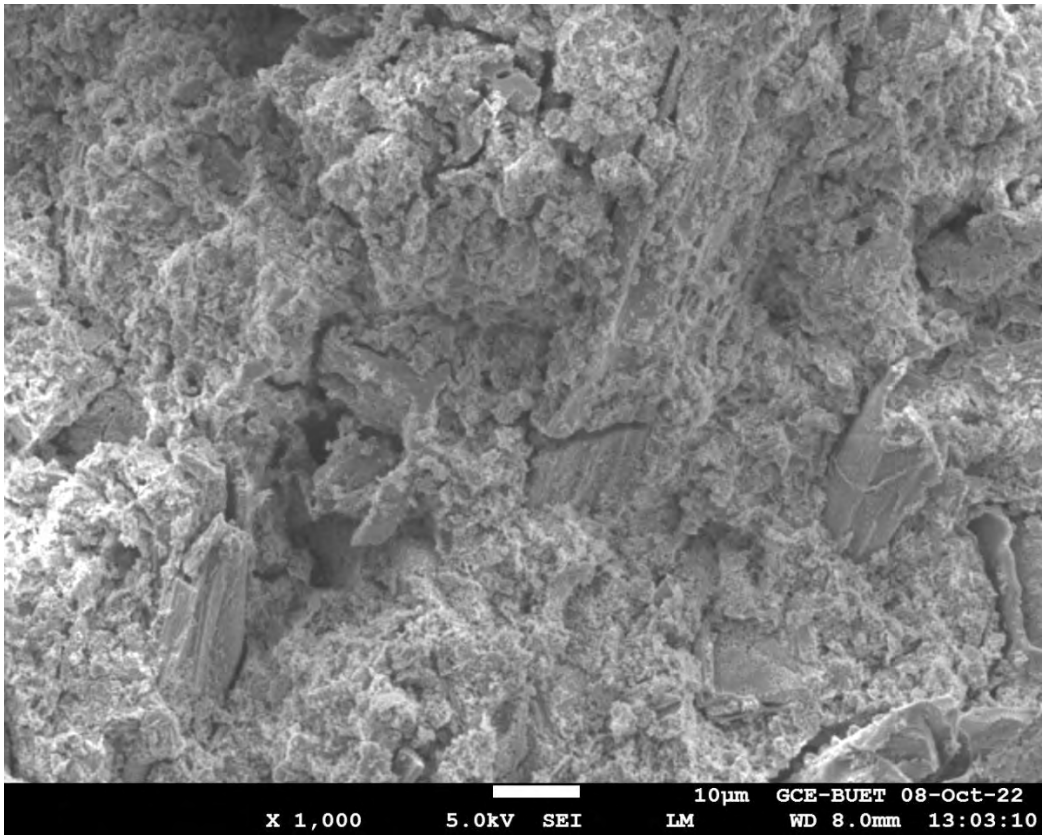
X 1,000 5.0kV SEI LM 10µm GCE-BUET 08-Oct-22 WD 8.0mm 13:03:10

(c)

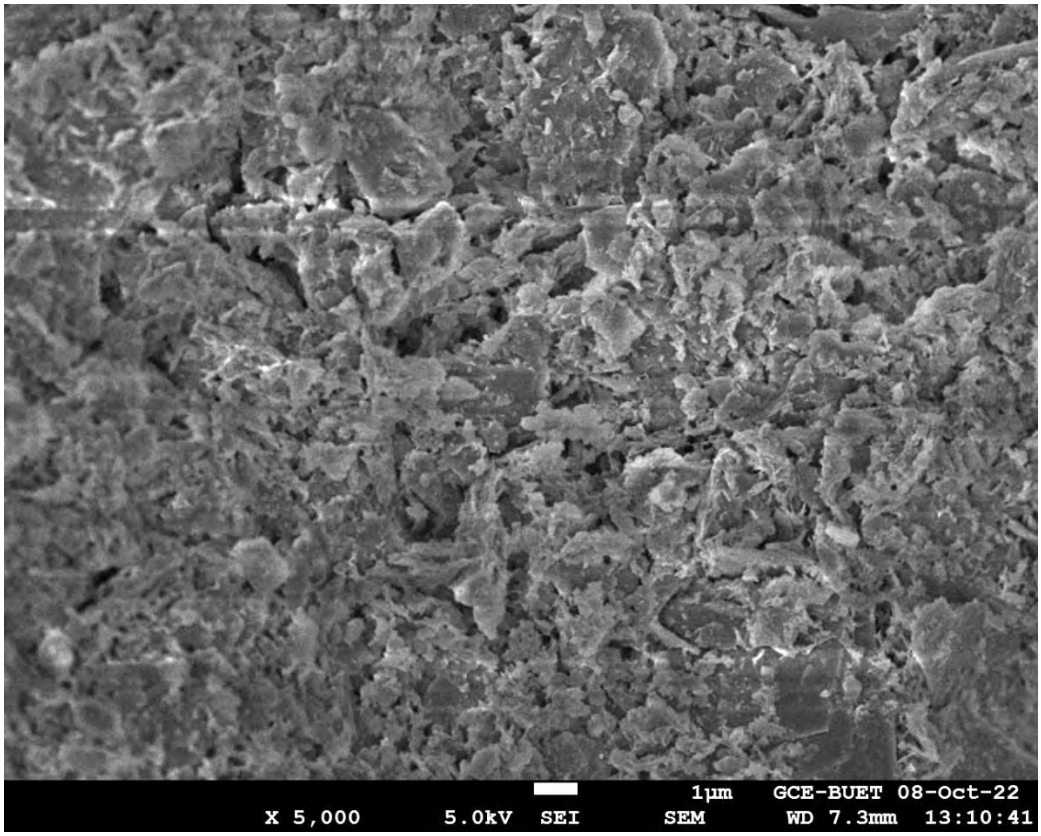
X 5,000 5.0kV SEI SEM 1µm GCE-BUET 08-Oct-22 WD 7.3mm 13:10:41

(d)

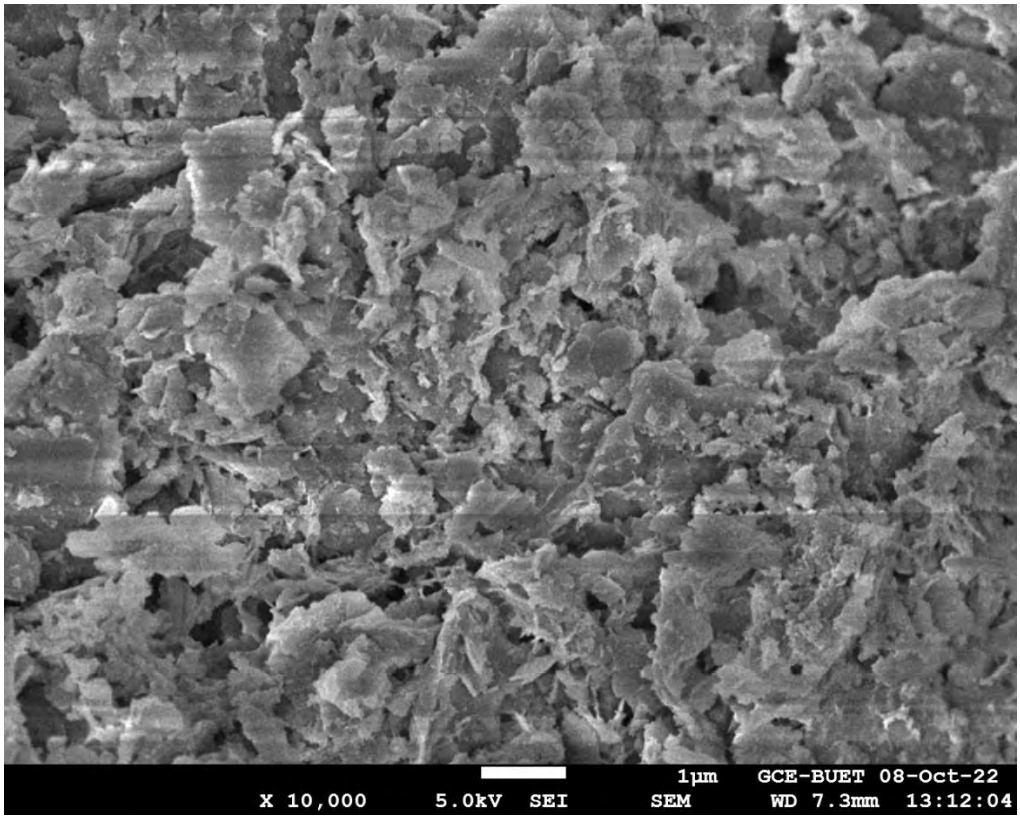


(e)

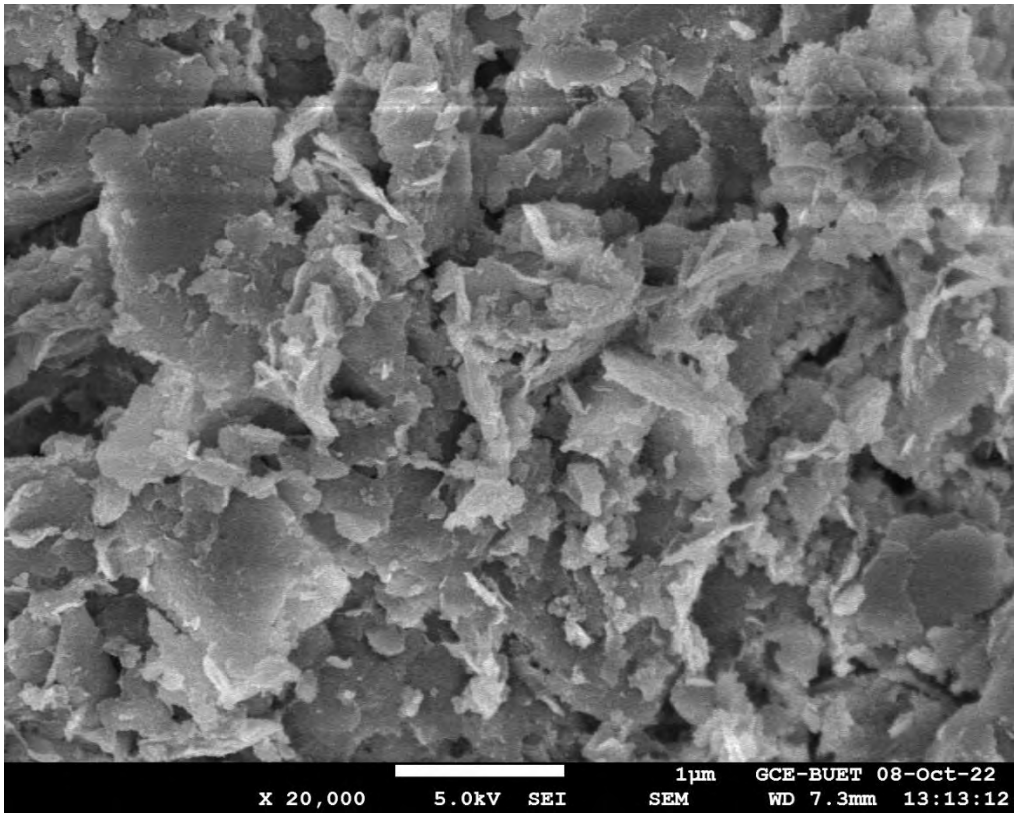


(f)

**Figure A.5:** SEM Images of sample having 15% SDA and A:B ratio 0.5 – (a) x 100, (b) x 500, (c) x 1000, (d) x 5000, (e) x 10000 and (f) x 20000